INFORMATION TO USERS

This manuscript has been reproduced from the microfilm master. UMI films the text directly from the original or copy submitted. Thus, some thesis and dissertation copies are in typewriter face, while others may be from any type of computer printer.

The quality of this reproduction is dependent upon the quality of the copy submitted. Broken or indistinct print, colored or poor quality illustrations and photographs, print bleedthrough, substandard margins, and improper alignment can adversely affect reproduction.

In the unlikely event that the author did not send UMI a complete manuscript and there are missing pages, these will be noted. Also, if unauthorized copyright material had to be removed, a note will indicate the deletion.

Oversize materials (e.g., maps, drawings, charts) are reproduced by sectioning the original, beginning at the upper left-hand corner and continuing from left to right in equal sections with small overlaps. Each original is also photographed in one exposure and is included in reduced form at the back of the book.

Photographs included in the original manuscript have been reproduced xerographically in this copy. Higher quality 6" x 9" black and white photographic prints are available for any photographs or illustrations appearing in this copy for an additional charge. Contact UMI directly to order.

U·M·I

University Microfilms International
A Bell & Howell Information Company
300 North Zeeb Road, Ann Arbor, MI 48106-1346, USA
313/761-4700 800/521-0600

Order Number 9119610

Kinetic studies of hypoxanthine/guanine phosphoribosyltransferase from yeast

Aybar-Batista, Diogenes, Ph.D.

City University of New York, 1991

U·M·I
300 N. Zeeb Rd.
Ann Arbor, MI 48106

KINETIC STUDIES OF HYPOXANTHINE/GUANINE PHOSPHORIBOSYLTRANSFERASE FROM YEAST

by

DIOGENES AYBAR-BATISTA

A dissertation submitted to the Graduate Faculty in Biochemistry in partial fulfillment of the requirements for the degree of Doctor of Philosophy, The City University of New York.

1991

This manuscript has been read and accepted for the Graduate Faculty in Biochemistry in satisfaction of the dissertation requirement for the degree of Doctor of Philosophy.

Date

Chair of Examining Commitee

7/18/90
Date

Executive Officer

Supervisory Commitee

The City University of New York

to

Donald L. Sloan
(in memoriam)

Abstract

KINETIC STUDIES OF HYPOXANTHINE/GUANINE PHOSPHORIBOSYLTRANSFERASE FROM YEAST

by

Diogenes Aybar-Batista

Advisers: Donald L. Sloan and Steven Meshnick

Hypoxanthine/guanine phosphoribosyltransferase (HGPRTase) from different sources has been studied extensively over the last twenty years. A new high performance liquid chromatographic (HPLC) procedure that improves the yield of HGPRTase has been developed. This salt-burst elution procedure permits the rapid and efficient partial purification of virtually any globular protein by suddenly exposing it to a high ionic strength medium. After determining by column chromatography the ionic strength required to elute a protein, the salt-burst procedure is designed. For HGPRTase purification, two elution buffers were used: a) 20mM Tris-HCl (pH 7.8) and b) 20 mM Tris-HCl (pH 7.8) plus 1M NaCl. The enzyme was eluted with a 25 sec burst of 30% buffer b. With this technique an average of 23-fold purification was achieved in a single step. Complete recovery of activity was observed.

A survey of phosphoribosyltransferase (PRTase) activities in yeast was accomplished using reversed-phase HPLC assay

procedures. The following bases were observed to be utilized during PRPP-dependent nucleotide synthesis: adenine, xanthine, hypoxanthine, guanine, uracil, orotate, nicotinamide, nicotinate and quinolinate. Gradient elution procedures have also been developed that allow the separation of PRTases assay components.

By utilizing the known equilibrium constants of Mg-PRPP complexes, a series of curves was developed which allow the determination of the concentrations of free PRPP, monomagnesium PRPP (Mg-PRPP) and dimagnesium PRPP (Mg_2-PRPP), at any pH ranging from 4.5 to 9.7 (at [$MgCl_2$] = 10mM). This permitted exploration of HGPRTase kinetics, taking into account the effect of pH on the substrate nature and concentration. This exploration was conducted at pH 4.5, 5.0, 5.5, 6.0, 6.5, 7.0, 7.5, 8.5 and 9.7. It was observed that HGPRTase changes its kinetic mechanism in going from a high to a low pH. At high and low pH values (pH $\geq$ 7.5 and pH = 4.5) the enzyme appears to follow an ordered bi-bi mechanism with a dead-end second substrate inhibition. But at intermediate pH values (5.0 $\leq$ pH $\geq$7.0) the enzyme shows kinetic patterns that are varying and difficult to interpret. A dead end inhibition by guanine (the second substrate) was observed at all pH values. This inhibition was found to be stronger at high pH. A kinetic mechanism that attempts to explain these results is proposed.

HGPRTase was shown to be reversibly inactivated by mercuric ion, but unaffected by the cysteine-specific modifying agent fosfomycin. Of the alternate substrates tested only xanthine

proved to be a substrate for HGPRTase. Adenine, caffeine and 3-methylxanthine showed no apparent product formation over a period of 12 hr. The inhibitory effect of these bases was also investigated, and the inhibition shows mixed characteristics for all of them. This effect was investigated further for caffeine at low (200 μM) and high (1000 μM) PRPP concentrations, showing a noncompetitive character at high PRPP concentration and uncomopetitive character at low PRPP concentration.

TABLE OF CONTENTS

TABLE OF CONTENTS

TABLE OF CONTENTS

LIST OF TABLES

LIST OF FIGURES

LIST OF FIGURES

LIST OF FIGURES

LIST OF FIGURES

LIST OF ABBREVIATIONS

CNDO	Complete Neglect of Differential Overlap
CNS	Central Nervous System
DTT	Dithiotreitol
HA	Hydroxyapatite
HGPGTase	Hypoxanthine/Guanine Phosphoribosyltransferase
HPLC	High Performance Liquid Chromatography
IR	Infrared Spectroscopy
NaMN	Nicotinate Mononucleotide
NaPRTase	Nicotinate Phosphoribosyltransferase
NmMN	Nicotinamide Mononucleotide
NmPRTase	Nicotinamide Phosphoribosyltransferase
NMR	Nuclear Magnetic Resonance
OPRTase	Orotate Phosphoribosyltransferase
QSAR	Quantitative Structure-Activity Relationship
PRPP	5-Phosphoribosyl-1-pyrophosphate
PRTase	Phosphoribosyltransferase
uv	Ultraviolet

Introduction

The Enzyme

Hypoxanthine-guanine phosphoribosyltransferase (EC 2.4.2.4), HGPRTase, catalyzes the formation of the purine nucleotides, GMP and IMP, from 5-phosphoribosyl-1-pyrophosphate (PRPP) and the appropriate purine base in the salvage pathway of purine metabolism. This enzyme is part of a collection of ten phosphoribosyl-transferases (PRTase) found in most organisms and is part of the biosynthetic pathway of purine, pyrimidine and pyridine nucleotides, and for the aromatic amino acids histidine and tryptophan (1). Their catalytic function involves cleavage of the pyrophosphate moiety in PRPP required by all the enzymes, with an accompanying inversion at C_1 of the ribofuranose ring during nucleotide formation. The resulting nucleoside monophosphate is specified by the particular PRTase substrate which is generally a purine, pyrimidine or pyridine base, and specifically includes hypoxanthine-guanine, orotate, adenine, quinolinate, glutamine or anthranilate. The enzymes involved in this pathway have been reviewed elsewhere (1, 2, 3). The fact that all of these enzymes require PRPP gives a clue of the metabolic importance of this substrate and its biosynthesis from ATP and ribose-5-phosphate by phosphoribosylpyrophosphate synthetase (EC 2.7.6.1) (4-10).

Relevance of the Study

The study of the activity and regulation of the PRTases is important for various reasons: 1) many genetic and metabolic diseases are caused by deficiencies in the activity or in the regulation of one or more enzymes of this group (9-21). 2) Since tumor tissue needs to reproduce at a very much higher rate than normal tissues (22,23), this set of enzymes involved in the biosynthesis of nucleotides (which are necessary for replication, redox processes and energy circulation), would be enhanced in activity and/or expression (22,23). Regulation of these enzymes could be a key issue in cancer growth control. The involvement of HGPRTase in the pathogenesis of Lesch-Nyhan syndrome (1-3,11,12,24), its role in the etiology of hereditary forms of gout (1,2,13,25) and its increasing use as a genetic marker in mammalian cell genetics (26-28), have all stimulated efforts toward the purification and characterization of this enzyme from a number of species: human parasites such as *Giardia lambia* (29) and *Schisotoma mansoni* (30), enteric bacteria (31), *E. coli* (32), mouse (33,34), hamster (34), baker's yeast (36-38), *Saccharomyces cerevisiae* (35), *Schizosaccharomyces pombe* (39), beef brain (40) and human (41-46). Particularly in humans there has been an extensive investigation of the structure, function and expression of HGPRTase in different tissues, with special attention to erythrocytes (42,44,47-52), brain (45,53,54), fibroblasts (55) and lymphoblasts (11, 56, 57), as well as its genetic variants (24,55-58), post-translational modifications leading to isozymes (47,48) and comparative studies for different human tissues (53).

The Human Enzyme

Human HGPRTase is a soluble cytoplasmic enzyme that is widely distributed in human tissues, expressed highest in brain (2,3,54), where it accounts for as much as 0.05% of the total soluble protein (54). The native enzyme is normally a tetramer of identical subunits (52,59). The enzyme subunit from erythrocytes has been sequenced. It consists of 217 amino acids with a molecular weight of 24,470 daltons (42). Under certain nonphysiologic conditions, the enzyme is converted to catalytically active dimers (59). HGPRTase in erythrocytes exhibits substantial electrophoretic heterogeneity, which is caused in part by post-translational modifications in its primary structure (47,60-62). Three major forms of the enzyme subunit have been defined by means of isoelectric techniques, and these findings suggest that there are at least two post-translational modifications (41,47,61,62), one of which appears to be the partial deamination of asparagine at position 106 (63). The instability of asparagine residues in proteins is a general phenomenon that is believed to trigger certain biologic processes (64). Studies by Johnson *et al.* (47) suggest that the modification of HGPRTase in erythroid cells is initiated in the reticulocyte and continues thoughout the lifetime of the erythrocyte. The modified isozymes differ from the parent molecule in the pH dependence of activity and in the relative utilization of the two purine base substrates, hypoxanthine and guanine (48). In contrast to the changes in the catalytic properties of the enzyme, the modifications have no effect on the heat stability or on the equilibrium between enzyme dimers and

tetramers (48). Human brain HGPRTase (native form) has been compared to that of erythrocyte (53). Only minor differences of amino acid composition were recognized between these two enzymes. The two enzymes were found tobe immunologically indistinct, which suggests that the first-order structure of the brain enzyme closely resembles that of the erythrocyte form, pointing to the possibility that the two enzymes are encoded by the same gene. In contrast, kinetic studies indicated that the brain enzyme has a higher affinity for PRPP than the erythrocyte enzyme, but lower affinity for hypoxanthine. This implies that the enzymes may differ in conformation (53). overall, thse observations indicate that the brain enzyme might be a post-translationally modified form tailored for the particular needs of the brain. Further evidence that the two enzymes are coded by the enzyme gene is that all HGPRTase deficiency syndromes always reflect impaired function of both brain and erythrocyte HGPRTase (2,3,11,13,24).

Medical Importance

In humans , deficiencies in HGPRTase are associated with two clinical syndromes: gout and the Lesch-Nyhan syndrome.

Gout is a ciinical disorder found mainly in males. The disease chiefly affects the joints and produces a characteristic type of acute and chronic arthritis, related to the presence of crystals of sodium urate. The cardinal biochemical feature is hyperuricemia. In primary gout, of which there are several biochemically distinct

forms, the hyperuricemia is attributable to an inborn error of metabolism, while in secondary gout, of which there are many varieties, the hyperuricemia occurs as a complication of an acquired disorder or of the use of certain drugs (2). There are two different groups of primary gout: Idiopathic primary gout, which is polygenic, and gout associated with specific enzyme defect, of which there are four types: 1) deficiency or absence of glucose-6-phosphatase, 2) feedback resistance of glutamine-PRPP-amidotransferase, 3) increased activity of glutathione reductase variant, and partial or total deficiency of HGPRTase. This latter is X linked (2). Of these, two are directly related to purine metabolism: glutamine-PRPP amidotransferase and HGPRTase.

Lesch-Nyhan syndrome is an inherited disorder generally associated with a virtually complete deficiency of HGPRTase (3), although it has been reported to occur in patients with only partial deficiency of the erythrocyte enzyme (5-10% remaining activity) and the fibroblast enzyme (30%) (12). The disease affects only males, it is characterized clinically by hyperuricemia, excessive production of uric acid and certain characteristic neurologic features, including self-mutilation, choreoathetosis, spasticity and mental retardation (3). It is not clear yet how the enzyme deficiency induces the syndrome. The concentration of hypoxanthine and xanthine in the cerebrospinal fluid is four times higher than that observed in healthy patients (65,66), and this has been associated with elevated purine biosynthesis in the brains of patients with Lesch-Nyhan (3). Although it has been suggested that

de novo purine nucleotide biosynthesis exists in the central nervous system (67), more recent work has shown that brain tissue is particularly dependent on the purine salvage pathways (1, and refs. therein). These findings and the fact that elevated concentrations of oxypurines in the cerebrospinal fluid could be the result of transport from plasma driven by a concentration gradient (68,69), contradict the above stated suggestion that the relatively high concentration of hypoxanthine and xanthine in the cerebrospinal fluid is due to elevated purine biosynthesis in the brain of patients with Lesch-Nyhan. It has been suggested that the syndrome could be related to the accumulation of toxic metabolites in the CNS (1, and refs. therein), but the CNS lacks xanthine oxydase, so hypoxanthine and guanine are not further oxidized to uric acid within this tissue (3). Furthermore the concentration of uric acid in the cerebrospinal fluid is consistently normal in patients with the syndrome (65), and the purines from the CNS can be degraded by the humoral system (65,68,69). This leaves one with the conclusion that the depletion of intermediates or cofactors necessary for normal CNS function in the absence of HGPRTase may be the cause of the syndrome (1, and refs. therein). Recently, a whole family of G-proteins have been found to play a crucial role in the transduction of hormonal and neurotransmitter signals across neuronal membranes (70-79). These enzymes require either GDP or GTP or both for their functioning. Since 1) the brain is dependent on the salvage pathways for the biosysthesis of purine nucleotides, and, 2) Lesch-Nyhan patients lack HGPRTase activity in the brain, the brains of these patients may be depleted of GMP, GDP and GTP,

which in turn would hamper the signal transduction systems which need G-proteins. Here is a plausible explanation of how HGPRTase deficiency is linked to the syndrome. A likely treatment would imply finding an effective transport system that would allow GMP, GDP, GTP or a combination of these to pass the blood-brain barrier.

General Features of HGPRTase

Because of the close similarities of the kinetic properties and requirements between HGPRTases from different species (1), it is possible to obtain valuable information from a model system that could later be applied to develop drugs for the treatment of the related human diseases. In our work we use as a model system the yeast enzyme because it can easily be purified in large quantities and is evolutionarily closer to the mammalian enzyme than the bacterial form. The following is a summary of the most common features of HGPRTases from different organisms.

The HGPRTases from different sources share several common features, e.g., the enzyme requires a divalent metal ion for catalysis. magnesium or manganese are the most effective cations, cobalt being also an activator, while other cations, such as barium, calcium and zinc are inhibitory (31,35-37,80,81). As with other PRTases a Mg^{+2}-PRPP complex is the active form of PRPP (36,80-85). In the human enzyme the imidazole portion of the purine ring is necessary for substrate binding, although imidazole alone is not bound (81). The amino acid residues involved in binding the substrates have been studied by chemical modification of the rat

liver and human erythrocyte enzymes (83,84). These HGPRTases are found to be inactivated by sulfhydryl and free amino-modifying reagents, but protected by Mg^{+2}-PRPP (83,84). The involvement of an amino group in binding PRPP was also suggested by the irreversible inactivation of the HGPRTases by periodate-oxidized PRPP and GMP (86-88).

Kinetic studies of the human and yeast enzymes established that PRPP is the first substrate to bind to HGPRTase (84,89,90). However, depending on the concentration of Mg^{+2}, a ping-pong type mechanism, involving a phosphoribosyl-enzyme, or an ordered sequential mechanism appear to be in operation (84). A hybrid mechanism has been suggested where the ordered addition of PRPP, then the purine, is followed by the random release of Mg^{+2}-nucleotide and Mg^{+2}-PPi complexes (85,91). The Michaelis constants for hypoxanthine, guanine and PRPP vary from 100 μM to 1.0 μM (1). The enzyme is active over a broad pH range with an alkaline optimum of 8.0 to 10.0 (31,35,81,92). The turnover number for HGPRTase ranges from 125 to 1435, depending on the source of the enzyme (1). While vertebrate HGPRTases are likely tetrameric (49,51,52,59,81,83,91), the enzyme from yeast has been reported to be a monomer of molecular weight of 51,000 daltons by Schmidt *et al.* (35). More recently, however, Sloan *et al.* (37) showed that the yeast HGPRTase is a dimer of identical subunits 26,000 daltons each and that the monomer may be catalytically active. While the mammalian enzyme is present as a

variety of isozymes (47,49,61-63), the HGPRTase from yeast displays only one isoelectric species (35,37).

The Substrates

One of the most striking features of HGPRTase is its apparently capriciously complex kinetic and self-regulatory properties. A closer look at the enzyme's "behavior" will reveal how intricately involved the chemical properties of its substrates are bestowing upon the enzyme such strange kinetic properties.

First Substrate

The first substrate to bind to HGPRTase is 5-phosphoribosyl-α-1-pyrophosphate (PRPP) (84,89,90). The concentration of PRPP in erythrocytes is in the range of 4.0-11.6 μM, while in fibroblasts it is 5.0-13 μM (143,144). The importance of this molecule is self- evident when one realizes that at least 10 different enzymes (the PRTase family) compete for this one substrate, enzymes that catalyze the synthesis of cofactors for the energy and electron flow, as well as building blocks for vital macromolecules (1). This makes PRPP play a central role in the regulation of the metabolic rate as a whole. Bagnara *et al.* (5) reported that when *E. coli* is fed with purine bases, all purine nucleotide precursors depleted the intracellular content of PRPP. It has also been shown that in bacteria, when the growth rate was limited by the carbon source available in the growth medium, the intracellular nucleotide content is proportional to the growth rate, while the intracellular content of PRPP showed a similar, though stronger, dependence,

suggesting that at lower growth rates the availability of PRPP could become limiting for nucleotide biosynthesis (4). In mammals the role of PRPP is even more crucial and complex. It has been shown that PRPP plays a determinant role in metabolic cooperation between communication-competent cells in a neighborhood (7). PRPP is freely exchangeable between these cells, so that the intracellular activity of HGPRTase in one cell can be regulated by changes of the levels of its substrates in another cell through metabolic cooperation (7). The pool size of PRPP has also been linked to the hyperuricemic syndromes described above (6,9,10), due to the superactivity of PRPP synthetase, the increased pool of PRPP accelerates the *de novo* biosynthesis of purine nucleotides, which in turn leads to higher levels of uric acid in defective HGPRTase patients. The study of the kinetic competition of a group of PRTases for the common substrate PRPP *in vitro* has been attempted in our laboratory (8). This work is discussed in detail in this thesis.

The most important aspect of the first substrate of HGPRTase is that in solution many different species of PRPP exist, complexed to divalent metal ions and/or protons in different proportions. The proportions at which these different complexes exist depend on the total concentration of each ionic species, on the pH and on the ionic strength of the medium (80,82,85,93). Not all these species are substrates for the enzyme. Today it is well known that a magnesium-PRPP complex is the actual substrate (36,80-85,94), even though there is still controversy as to whether Mg_2-PRPP

(80,85,94) or Mg-PRPP (36) is the actual substrate. We believe that evidence indicates that they are both substrates, but one is preferred over the other under certain conditions and *vice versa* as suggested earlier by Ali and Sloan (36) (see "Discussion"). The stability constants of the PRPP complexes present in solution in the presence of Na^+, K^+, Mg^{+2} and H^+, have been measured (81-85,93,95,96), and can be used to calculate the concentration of each species at different pH values and different total concentrations of PRPP and $MgCl_2$. This would allow us to determine the true Km value for the actual Mg-PRPP substrate, because now we can know the concentration of the true substrate under the working conditions (see "Materials and Methods").

The facts that a magnesium ion-PRPP complex is the real substrate for HGPRTase and that PRPP can easily complex with divalent metal ions leads to the conclusion that divalent metal ions could appear to be inhibitors of this enzyme if the metal-PRPP complex in question is nonproductive, either because this complex cannot bind to the active site (in which case we would say that PRPP has been sequestered by the metal ion) or because after binding, the geometry (and perhaps the electronics) of the complex is not adequate for catalysis. This inhibitory effect has been observed for calcium, zinc and barium (31,35-37,80,81), although zinc has been reported to be an activator at concentrations below 100 μM (37b). This could be of physiological importance, because Ca^{+2} and Zn^{+2} also have biological functions and could be at relatively high concentrations in certain tissues.

Second Substrate

Guanine and hypoxanthine are both possible second substrates for HGPRTase. The concentration of oxypurines in the human plasma is 10-40 μM (145), in which hypoxanthine is 3-20 μM (146) while guanine is 6-30 μM (136). The appparent K_m of guanine for human erythrocyte HGPRTase is $5.0x10^{-6}$, while that of hypoxanthine is $1.7x10^{-5}$ (147), thus the affinity of human erythrocyte HGPRTase for guanine is more than 3 times stronger than for hypoxanthine. In yeast the affinity of HGPRTase for guanine is almost three times than for hypoxanthine while the V_{max} is almost five times faster for guanine than for hypoxanthine (89). These facts indicate that of these two purines guanine is preferred by HGPRTase as substrate, *in vitro* as well as *in vivo*.

A number of investigators have shown that guanine and its derivatives have physical and chemical properties that set them apart from other nucleic acid components. These involve "stickiness", a tendency to aggregate, adsorb and bind, to be insoluble and to form gels and viscous solutions (97). Guanine solubility in water at 20 °C is one part in 200,000 (98). One of the properties responsible for these phenomena is undoubtedly hydrogen bonding. Guanine has the most complex structure of any of the common heterocycles of nucleic acids, and offers the largest number of intermolecular hydrogen bonding possibilities (97), and this is the main reason why it is so difficult to work with guanine solutions. In order to have an accurate measurment of the actual concentration of guanine solutions, they should be carefully

prepared fresh and very dilute (see "Materials and Methods"). Otherwise replicability will be unattainable, and in some cases no enzyme activity will be apparent or the kinetics will show complicated patterns that will not allow one to calculate an accurate initial velocity (laboratory experience).

Cations are electrophilic species and are attracted to the various electron-rich sites in guanine and its derivatives. It is well known that heavy metals like mercury, silver and barium complex and form salts with guanine and other heterocycles (97,99). In studies of mercuric ions with guanine, it was demonstrated that the ionization of the 1-proton is affected, but the amino group is not involved (100). Others have shown that it also binds to N-7 of guanosine and, when high concentrations of mercury are used, a displacement of a proton from the amino group is observed (101). This behavior of divalent heavy metal ions may expain, in part, the bell-shaped curve of the activation of HGPRTase by divalent metal ions reported by Sloan *et al.* (36). It may also be the reason why heavy metal ions inhibit the enzyme (31,35-37,80,81), as has been suggested by Ali and Sloan for the case of zinc (37b).

Another crucially important chemical property of guanine and xanthines is their multiple tautomerism. There are three different types of tautomerism that can be cosidered for purine derivatives: 1) Prototropic tautomerism, corresponding to the displacement of the protons among the four available ring nitrogens, 2) the amine-

imine tautomerism, liable to occur in amino purines like adenine and guanine (see Figure 1), and 3) the lactam-lactim tautomerism of the hydroxypurines like xanthine, hypoxathine and guanine derivatives (see Figure 2) (102).

It is very important to know the relative stability of the different tautomeric forms in solutions of the naturally occuring purines, in order to establish their role in the molecular biology and biochemistry of cells and, consequently, to design drugs suitable for the treatment of related diseases. The *a priori* examination of the problem (of which tautomeric form is more stable under particular conditions) requires the consideration of several factors determining the free energy of transformation of the compound from one tautomeric form to the other and consequently the equilibrium constant of this transition (103).

First, during a change in tautomeric form the system of σ bonds of the molecule is reorganized. Second, the structure of the π-electron system in conjugated molecules is modified and consequently, so is their resonance energy. Third, the solubilizing power of the molecule is altered if the tautomeric equilibrium is examined in solution, the most important situation

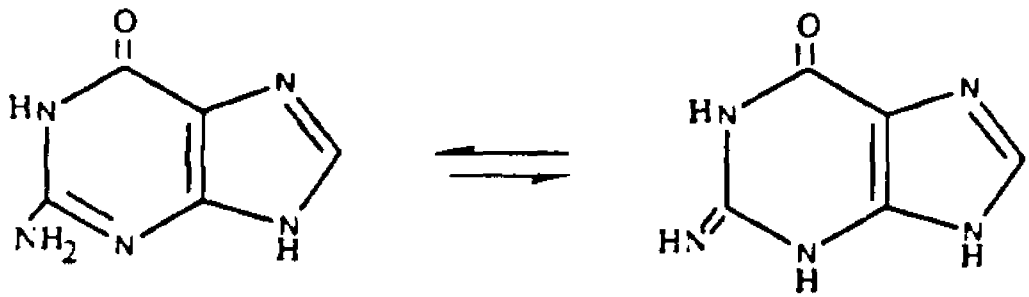

Fig. 1. Amine-imine tautomerism of aminopurines.

Fig. 2. Lactam-lactim tautomerism of hydroxypurines.

for the investigation of chemical and biochemical problems. Fourth and finally, during transformation of the compound from one tautomeric form to another, the system of intramolecular hydrogen bond is modified. The combined action of these factors determines the relative stability of the different tautomeric forms at the particular conditions concerned (102,103).

The most general features of the compound and of the solvent affecting the rate of interconversion and the equilibrium constant of the process can be summarized as follows:

The rate of interconversion of two tautomers is greatest when both of the alternative atoms to which the mobile proton can be attached are heteroatoms, in this case isolation of the separate isomers is usually impossible. If one of the alternate atoms involved in the tautomerization is carbon, the rate of interconversion is somewhat slower, but still fast. When both of the atoms involved are carbon, however, interconversion is comparatively slow and requires a catalyst (104).

The proportion of any one tautomer present in an equilibrium mixture can change if a change in environment alters the relative stability of the isomers, by preferentially stabilizing one of them. If one isomer is more polar than the other, it will be preferentially stabilized in media with high dielectric constants (104). This effect has been clearly demonstrated for 7-methyl-guanine and guanine, in which the rate of exchange of the N-7 proton with

deuterium are accelerated with increasing concentration of a large number of buffers with widely different pK values (105). Specific interaction with the solvent, in particular hydrogen bonding with the solvent acting as the hydrogen donor or acceptor or both, often preferentially stabilizes one of the isomers (102,104). Temperature can also affect the equilibrium mixture of tautomers (106), as does the pH, but it has been reported that the guanine keto-enol tautomerization constant is not appreciably affected (97).

Purine tautomerism is very complicated to study because of the variety of possibilities that it presents. Of the common nucleic acid components guanine has the largest number of tautomeric forms. There are twenty ways in which four tautomeric protons can be distributed among three of the six sites available (indicated by (*) in Figure 3) (97).

There is abundant evidence, obtained with a large variety of techniques, such as infrared spectroscopy (107,108,124), Raman spectroscopy (109), u.v. spectroscopy (110), NMR (107,111,112), measurement of ionization constants (97,106,113) and X-ray crystallography (102,114-116), that the amine and lactam forms are the common tautomeric forms of the majority of biological purines. Besides experimental techniques, a variety of theoretical calculation techniques have been used to determine the more stable tautomeric forms of purines and their derivatives (102,103,117).

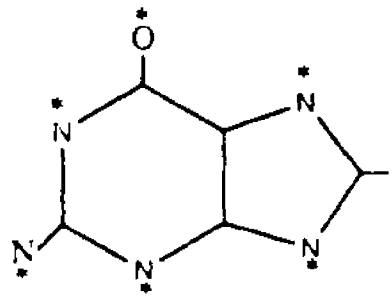

Fig. 3. Distribution of tautomeric protons in the guanine skeleton. Four protons may be distributed in six different locations indicated by (*).

Pullman and Pullman (102) reported a summary of the quantum mechanical methods applied to investigate theoretically the probable stability, the total energy states, the electric charge at each atom and the dipole moment of the different tautomeric forms of purine derivatives. Each of these parameters was calculated using the different methods described and then used to predict the relative stability of the tautomers. A similar treatment , but more generalized, is presented by Kochetkov *et al.* (103). Using a variety of quantum mechanical methods, Olaru *et al.* (117) applied QSAR (Quantitative Structure-Activity Relationships) calculations to determine the electronic structure of purine derivatives known to inhibit PRTases and determined their relationship to their function.

The use of uv-spectroscopy for the study of tautomeric equilibria of purine bases gives only minimal information because the spectra of the stabilized tautomeric forms differ only very slightly from each other. Infrared spectroscopy, NMR and proton dissociation and exchange studies have proved to be effective. In guanine for example, the IR spectra of the crystalline state show bands corresponding to $-NH_2$, indicating that the amino form is favored, which has been confirmed by NMR studies (102). Another piece of evidence that indicates that the amino group is very stable and hence is tautomerically favored, is the fact that in 1-methyl-guanine the dissociation to an anion has a pK_{2a} of 10.5, while no dissociation to an anion is observed in 1,7 or 1,9-dimethyl-guanine

(4). This implies that the proton on the amino group of guanine does not have acidic properties, i.e., it is not readily exchangeable. Another important controversy has been pointed out by Pullman and Pullman (102). They have defined how the use of uv-spectroscopy for interpreting tautomeric equilibrium of purines could be misleading: Unambiguous infrared spectroscopic evidences clearly show that the three isomeric forms 2-, 6- and 8-hydroxypurines exist essentially, both in the solid state and in solution, in the keto form, as they all present the characteristic C=O stretching vibration (near 1670 cm^{-1} in the 2- and 6-hydroxypurines, and near 1740 cm^{-1} in the 8-hydroxypurines) and shows no band that could be attributed to an O-H group. This was specifically demonstrated for guanine in which the C=O frequency is at 1665 cm^{-1} (97,107,118,119). Yet, Fujita *et al.* (120), by using uv-spectra, concluded that the lactim form of guanine should be about 12 kcal/mole more stable than its lactam form, which led them to propose that the predominant form of guanine in the gaseous state could be the lactim form, in contradiction with the data obtained by IR-spectroscopy.

The next tautomeric puzzle for hypoxanthine and guanine is how two protons distribute in the four ring nitrogen atoms, presenting four possibilities (see Figure 4). The N(3)H tautomers of hypoxanthine (first column, Figure 4) have been predicted, by CNDO calculations, to be about 8-14 kcal/mole less stable than the corresponding N(1)H tautomers (second column, Figure 4), the N(3)H-N(7)H tautomer being more stable than the N(3)H-N(9)H one

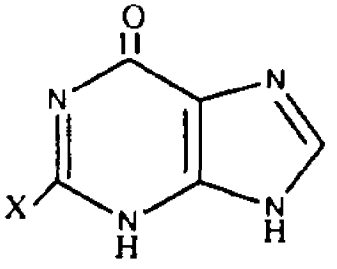

N(3)H-N(9)H

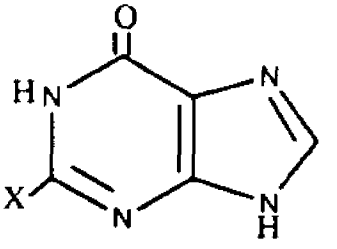

N(1)H-N(9)H

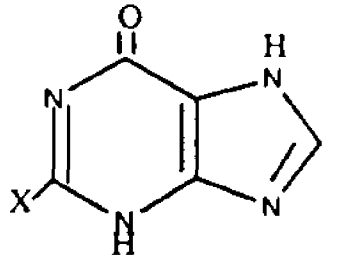

N(3)H-N(7)H

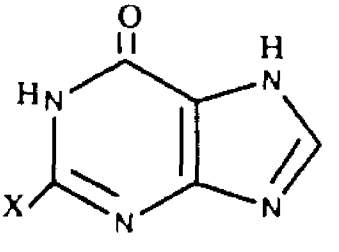

N(1)H-N(7)H

Fig. 4. Distribution of two protons between the four ring nitrogen atoms of hypoxanthine (x = H) and guanine (x = NH_2).

by about 6 kcal/mole (102). The majority of purine compouds exist preferentially as derivatives of the N(9)H form, but the xanthine structures exist essentially as derivatives of its N(7)H form, which appears as probably its predominant form (102). Large number of physicochemical studies and CNDO/2 calculations support the N(9)H-amine form of adenine as the most stable form of adenine (102,113).

The amine group of guanine affects the distribution of the tautomeric protons among the four ring nitrogens, thus, making it differ from hypoxanthine. This is important to note because both guanine and hypoxanthine are substrates for HGPRTase, while xanthine and adenine are not (see "Results", "Inhibition and Alternate Substrates").

Most of the work done to determine the relative stability of the N(1)H or N(3) tautomer of guanine leads to confusing results (102,105,121,122), but most studies agree that the N(1)H is more stable. In uncharged guanine derivatives in which the 1-position bears a hydrogen, this proton generally dissociates with a pK_{2a} in the range of 8.8-10 (97). A great variety of guanine derivatives (with the exception of 7,9-dimethylguanine) accept protons in acidic solutions to form a cation with pK_{1a}'s in the range 2-3.5. The assumption has usually been made that this involves the addition of another proton at some point in the guanine molecule, rather than a full rearangement of all tautomeric protons, and the key question being where does the proton go (97)? Evidence shows

that guanine derivatives protonate on the imidazole ring depending on the tautomer in question (97,106), but there is still controversy as to the mechanism for this protonation. The latest evidence published suggests an involvement of N(3) (105), which implies that somehow this protonation may require the rearrangement of the electronic distribution of the π-system of the rings.

Quantum mechanical calculations predict that the N(7)H and the N(9)H tautomers of guanine have, within 1 kcal/mole, identical stabilities, with perhaps a slight advantage for the N(7)H form (102). These results are supported by data obtained from uv-spectroscopy (97) and studies of the ionization constants of substituted guanines (97,106). The compound 7-methylguanine is slightly more basic than 9-methylguanine (guanine, pK_{1a} = 3.0, pK_{2a} = 9.3, 7-methylguanine, pK_{1a} = 3.5, pK_{2a} = 10.0, 9-methylguanine, pK_{1a} = 2.9, pK_{2a} = 9.8) (97), and if one assumes that 7-methylguanine accepts a proton on the N(9) in acid and *vice versa*, then one may conclude that the N(7)H tautomer predominates slightly over the N(9)H (97).

All this allows the conclusion that guanine exists in solution as a mixture of about equal proportions of only two of the twenty different tautomeric forms in which it can exist, that is: [N(1)H-N(7)] <=> [N(1)H-N(9)] (see Figure 5). These two species will be called T(7) and T(9) respectively during subsequent discussions.

N(1)H-N(9)H

T(9)

N(1)H-N(7)H

T(7)

Fig. 5. Interconversion between the two most abudant tautomeric forms of guanine.

It is interesting to note that whenever the biological importance of guanine tautomerism has been discussed in the literature, all attention has been focused on the effect on the structure of the nucleic acids, while the effect on the metabolism and salvage of guanine is not even mentioned (97,102,103,107,123). Since any enzyme acting on GMP has to "distinguish" between guanine and GMP, the sp^2-sp^3 states of N(7) and N(9) ought to be important for the recognition. Otherwise, guanine would be an inhibitor of most of the GMP utilizing enzymes. GMP is [N(7)-sp^2]-[N(9)-sp^3]. Since guanine is a mixture of T(7) (which is [N(7)-sp3]-[N(9)-sp2]) and T(9) (which is [N(7)-sp2]-[N(9)-sp3]), it is reasonable to assume that T(9) would inhibit such an enzyme. This would have far reaching implications in metabolic regulation and the necessity to salvage (clean up) guanine from the medium to stop it from interfering with other paths and metabolic functions (see above, "The Enzyme"). Moreover the nucleophilicity of nitrogen depends on its hybridization state, which together with the geometry implies that two different mechanisms (geometrically and electronically speaking) are required for the T(7) and the T(9) forms of guanine to accept a group at N(9) to form a nucleotide (see Figure 6 and Figure 7). As could be deduced from these mechanisms water must accept the guanine proton directly or indirectly, because otherwise the enzyme would be inactivated (which means that under certain conditions an isotope effect should be observed).

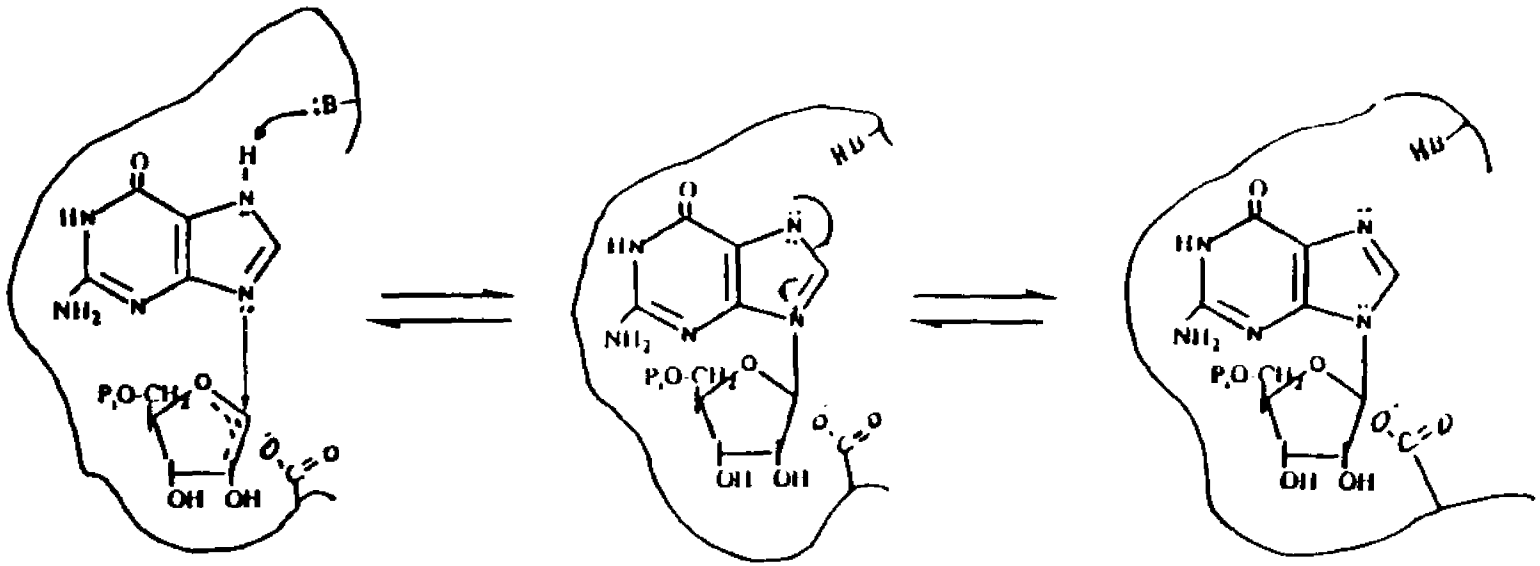

Fig. 6. Hypothetical mechanism of the enzymatic addition of the T-7 tautomer of guanine to the "activated" sugar ring of PRPP after the displacement of the pyrophosphate moiety.

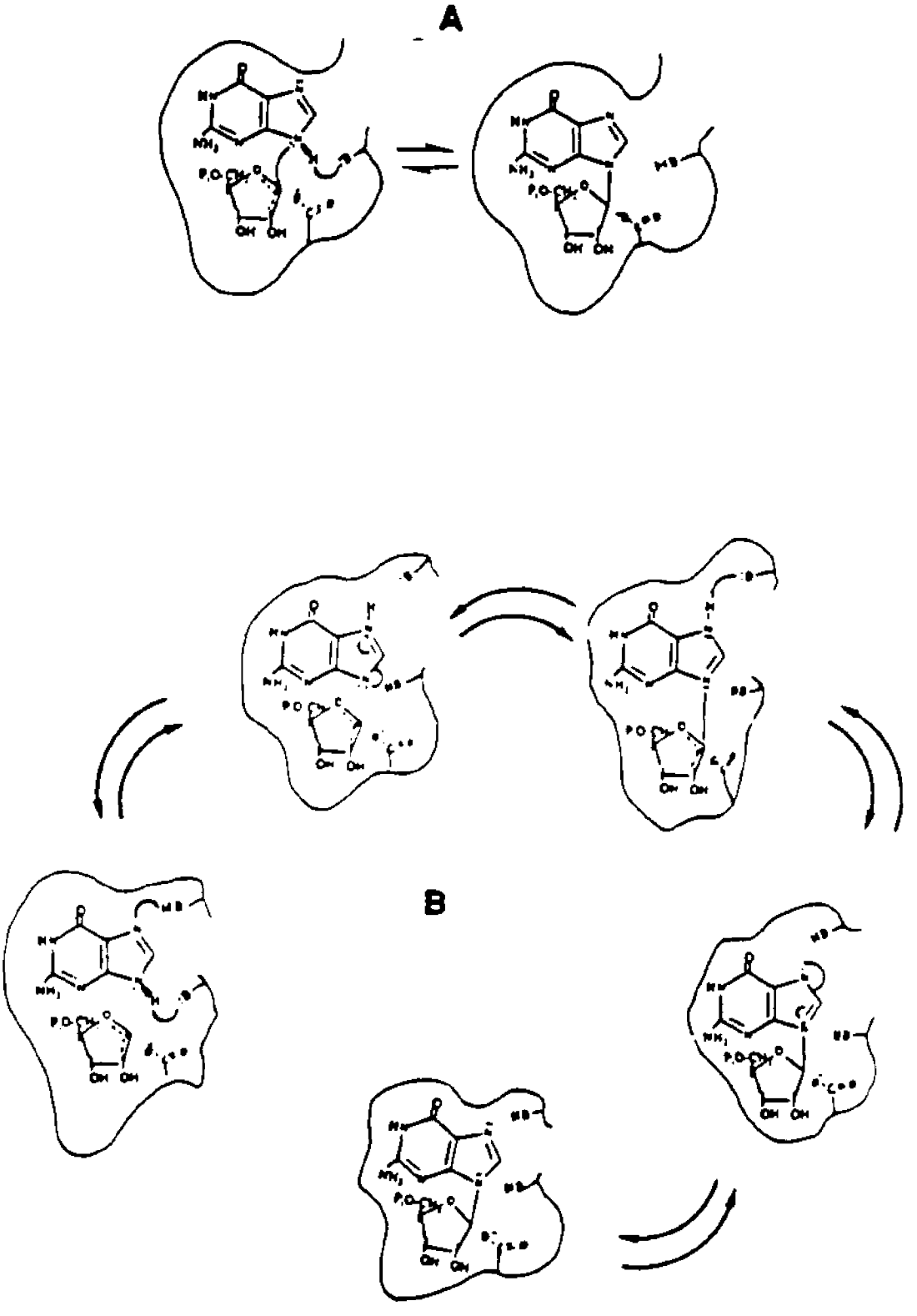

Fig. 7. Hypothetical mechanism for the enzymatic addition of the T-9 tautomer of guanine to the "activated" sugar ring of PRPP. **a.** Direct mechanism. **b.** Tautomerisation mediated mechanism

It is very doubtful that the enzyme would use both forms of guanine as substrate, because there is only one active site and three very different geometries and mechanisms for the two tautomers, so either T(7) or T(9) is the preferred substrate, but not both. If T(7) is the substrate, T(9) would probabily act as a competitive inhibitor of T(7) and GMP, both in the foward and reverse reactions, because it might have affinity for both the T(7) and the GMP binding sites (see "Results and Discussion"). If T(9) is the substrate, T(7) would probabily be a competitive inhibitor of T(9). The fact that N(9) is the acceptor of the phosphoribosyl group makes T(7) the best candidate to be a substrate. There are several other reasons to suspect that T(7) is the preferred substrate. If T(9) is accepted as substrate, the enzyme would have to either tautomerize to T(7) (see Figure 7-b) or probably would have an active site too compacted for guanine to donate a proton and accept the phosphoribosyl group simultaneously, since the unshared pair of electrons and the proton on N(9) are only 109° apart (see Figure 7-a). Even if the mechanism followed is the tautomerization of T(9) to T(7), T(7) would be a preferred substrate, because it would be just like an intermediate in the mechanism. The enzyme would bind it preferentially and would have a much larger turnover number because: 1) energy has to be spent to convert T(9) to T(7) (see above) and 2) the mechanism is shorter by two steps, the other steps being the same as for T(9), so even if T(9) can be a substrate it will have an inhibitory effect on the enzyme in the presence of T(7) because it would slow down the reaction rate.

Materials and Methods

Materials

Baker's Yeast (Budweiser brand) was obtained from Valente Yeast, Inc., Flushing, NY. PRPP (tetrasodium salt), hypoxanthine, guanine, adenine, xanthine, 3-methylxanthine, caffeine, fosfomycin, GMP, IMP, UMP, nicotinamide, quinolinic acid, nicotinamide nucleotide (NMN or N_mMN), ATP (sodium salt), nicotinate (free acid), nicotinate nucleotide (NaNM), ADP (sodium salt), pyridoxal phosphate (sodium salt), sodium acetate, Tris-HCl, Bis-Tris-propane, POPSO and monoethanolamine were supplied by Sigma Chemical Co.. The chloride salts of magnesium and mercury were from Baker Analytical Reagents. TSK Fractogel-DEAE 650S was obtained from Toyosoda Mfg., whereas HA Sepharose-4B was purchased from Pharmacia. A prepacked monoQ HR 5/5 (0.5x5 cm) anion exchange column was also obtained from Pharmacia. The protein determination reagents were obtained from Bio-Rad Laboratories. All other reagents were analytical grade. Distilled water was further purified and deionized (to a conductivity reading of 18) with a Gelman Water-I Purifier.

Experimental Procedure

Salt-Burst procedure for Protein Purification Chromatography.

A Pharmacia FPLC System containing a Frac-100 fraction collector, UV-1 optical and control units, a REC-481

single channel recorder, two P-500 pumps, an LCC-500 controller and a RA-120 chromatographic rack was employed in these studies.

Enzyme Preparation and Assay:

HGPRTase was isolated initially from 10 lb of baker's yeast according to the published procedure of Ali and Sloan (36). The purification was halted after the ammonium sulfate fractionation and this sample was dialyzed against 20mM Tris-HCl buffer pH 7.8 (in a volume ratio 1:100, twice). Afterward the sample was concentrated in a pressurized Amicon Ultrafiltration Cell model 8050 with a Diaflo-Ultrafilter membrane PM10. This concentrated suspension was employed in the salt burst procedure. A spectrophotometric assay procedure (described below) was employed to monitor the position of HGPRTase in the FPLC elution profile. The Bio-Rad microassay procedure (125) was employed for protein concentration determinations.

Preparation of the TSK DEAE-650S Column:

The TSK gel material was suspended (for about four hours) repeatedly in 1 mM sodium azide until the supernatant remained clear. Prior to the packing of the column the gel was suspended in an equal volume of 100 mM potasium chloride, degassed under vacuum and treated with ultrasound for 2-3 minutes (three times) and degassed again. The slurry was placed in the column and

equilibrated with 4 liters of 20 mM Tris-HCl buffer (pH 7.8). After several elutions of the yeast protein extract this column was regenerated with 1 liter of 1 M sodium hydroxide followed by 1 liter of 500 mM Tris-HCl (pH 7.8), and thereafter equilibrated as described above.

Linear and Step Gradient Ion exchange Chromatography:

A small (10 ml) Mono Q column packed with a suitable quaternary amine was used. The column was equilibrated at pH = $pI_{(protein)}$ + 1 (pH 7.8). Small samples (4 to 5 100 µl samples) were eluted successively through the column, with a linear salt gradient employing buffer B (20 mM Tris-HCl containing 1M sodium chloride, pH 7.8), and with gradient steepness as a variable (see Figure 8a). In every case the enzyme activity was located within the elution profile. After the best relative concentration of buffer B was determined (the value at which the enzyme activity is eluted), various step-gradients were applied just below that concentration of B, until optimal gradient step heights [%B-2] and step widths [SL-2] were established (see Figure 8b) The procedure was then scaled up by packing a large 250 ml column with a 1-10 g binding capacity for proteins (see above). Starting with 1 ml injections of the protein suspension, SL-1 and SL-2 were optimized, taking into account the void volume (vv) of the column and the size of the injection (see Figure 8c). The latter affects BW-1 and BW-2 (Figure 9 shows typical elution

profiles for the different salt gradients used in this study, these hypothetical profiles are guides to identify the parameters involved in the procedure), %B-1 and %B-2 remain the same as in the small column. The same procedure can be used to optimize larger injections (10 ml or more), but starting with larger SL-1 and SL-2.

Salt-Burst Ion Exchange Chromatography:

This procedure is a variation of a step gradient elution, where an appropriate buffer concentration is only briefly introduced onto the column to elute a particular protein. As shown in Figure 9a, the procedure involves an initial establishment of a salt concentration in the buffer that will elute most of the proteins but will not elute the protein to be purified (see "Results" and "Discussion"). Thereafter the salt concentration that will elute the required protein is established with a salt pulse (Figure 9c) followed by a separating low salt period (SL-2 in Figure 9c) and thereafter by the elution of all other proteins with high salt. Three step length must be determined (Figure 9b and 9c): SL-1, the time necessary to elute initially most of the proteins; SL-2, the time between the elution of the required protein and the washing of the column with high salt and the pulse width PW, the time period of the salt-burst that results in maximal purification. For HGPRTase two buffers were employed: 20

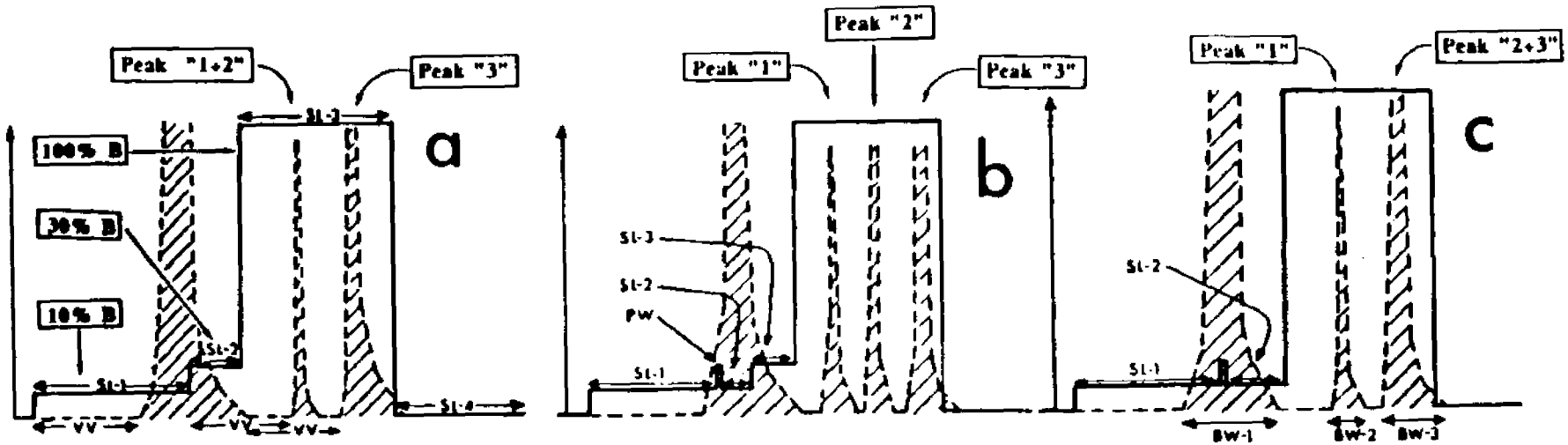

Fig. 9. Typical elution profiles for an HGPRTase preparation from yeast. In this Figure the percent of Buffer B in the mobile phase is indicated by the solid line. The absorbance of the eluate at 254 nm is indicated by the diagonal lines and the various time settings within the elution are indicated as: SL, step length; PW, salt burst length; VV, net void volume for each absorbance region. **a.** A typical step gradient profile. **b.** A typical step/burst gradient combination profile. **c.** A typical salt burst gradient profile. SL = step length (ml), PW = burst pulse width (ml), VV = void volume (ml), BW = peak base width (ml).

mM Tris-HCl (pH 7.8, buffer A) and 20 mM Tris-HCl containing 1M sodium chloride (pH 7.8, buffer B). Two programs were written to automate the protein injections and the salt burst elutions (Table I).

Multiple Enzyme Competition for PRPP

Enzyme Purification:

HGPRTase, OPRTase, and N_aPRTase were purified from baker's yeast to apparent electrophoretic homogeneity through the use of published procedures (89,126,127). N_mPRTase was purified partially from a yeast extract using $(NH_4)_2SO_4$ fractionation, whereas other phosphoribosyltransferases were examined by making use of this extract.

Enzyme Assay Procedures:

Measurements of the initial velocities of HGPRTase, OPRTase, and N_aPRTase catalyzed reactions were accomplished using modifications by Hanna and Sloan (128), and by Ali and Sloan (89) of the method described by Flaks (129). The complete assay mixture consisted of 0.1 ml hypoxanthine (100 μM), 0.1 ml orotate (100 μM), 0.1 ml ATP (100 μM), 0.1 ml nicotinate (100 μM), 0.2 ml PRPP (100 μM, 40 μM or 20 μM), 0.1 ml of 10 mM $MgCl_2$ and 0.5 ml 0f 20 mM triethanolamine buffer (pH 8.0) in a final volume of 1.2 ml. The mixture was placed in a 38°C water bath and the reaction was initiated by the addition of approximately 0.01 μg

TABLE I

Description of the Programs used to Automate the Injection and Elution of Hypoxanthine/Guanine Phosphoribosyltransferase through a TSK DEAE 650s Ion Exchange Column on the Pharmacia FPLC.

Elution Volume	Function	Value	Description
Injection Program			
0	loop time	10	enzyme injection time
0	valve position	1.2	loop selection
0	ml/min	5	rate of flow
1	valve position	1.1	load signal
1	ml/min	12	flow increase
6	loop end	-	injection complete
Gradient Program			
0	conc. % of B	0	conc. of Buffer B
injected			
0	clear	-	-
0	monitor	1	uv unit activated
0	level %	5	threshold level
0	integrate	1	integrator activated
0	port set	6	fraction collector zeroed
0	cm/min	0.05	recorder speed
0	loop	1	number of loop
injections			
0	method	3	injection program on
0	conc. % of B	10	Buffer B conc. after
injection			
0	ml/min	12	flow rate
100	ml/mark	20	computer recorder on
200	port set	6.1	fraction collector on
200	% B	10	10% step ends (200 ml)
200	% B	30	start burst
205	% B	30	burst ends (5 ml)
205	% B	10	second 10% step begins
250	% B	10	10% step ends (50 ml)
250	% B	100	100% step begins
430	% B	100	100% step ends
460	port set	6	-
511	integrate	0	-
650	conc. % of B	0	wash of column
650	end of loop	-	-

HGPRTase, 0.3 μg OPRTase and 0.7 μg N_aPRTase. Aliquots of this solution were removed at appropiate time intervals. The reaction occuring in each of this aliquots was terminated by heating in a boiling water bath for 2 minutes. The samples were then clarified first by centrifugation and then by filtration through a 0.45 μm HA Millipore filter prior to HPLC injection. The HPLC elution profiles were employed to determine the time course of the reaction as described previously (89,128). Variations on this basic assay mixture were employed in which appropriate bases were excluded or included. These changes are described in the Figure legends. During the survey for PRTase activities in yeast 100 μl yeast protein extract was employed (see legend in Figure 14).

High Performance Liquid Chromatography:

A Waters HPLC instrument equipped with a model 6000A and a M-45 solvent delivery system, model 600 solvent programer, model U6K sample injector, model 440 absorbance detector, and a Houston Omniscribe chart recorder was used in the assay procedure. A single 3.9 mm X 30 cm Waters mBondapak C_{18} column (equilibrated with 15 mM $NH_4H_2PO_4$, pH 6.0) was placed on line with the solvent delivery system at a flow rate of 1.2 ml/min. Two gradient systems were used for this studies. 1) A 20 minute linear gradient ranging from 0% to 100% 25 mM $NH_4H_2PO_4$, pH 6.0, was used to separate the bases and the nucleotides. 2) The μ-Bondapak C18 column was first

equilibrated with 25 mM $NH_4H_2PO_4$ buffer, pH 6.0. Thereafter a linear gradient of zero to 10% methanol/water solution was employed to separate the bases and nucleotides within a 20 minute period. 10 µl samples from solutions containing the three enzymes and substrates were injected using a Hamilton 801 microliter syringe. Nucleotides and bases in the eluent were detected at 254 nm with a 0.1 absorbance setting. All of the solvents used in the chromatographic procedures were eluted by a vacuum filtration trough a 0.45 µm HA Millipore filter.

Kinetics and pH Study

Enzyme Assay Procedures:

For any kinetic study with enzymes, the most important experimental factor is to determine the conditions to obtain initial velocity values as accurately as possible. Two factors are involved in affecting this accuracy: kinetic factors intrinsic to the enzyme, substrate and medium, and factors inherent in the detection method. In this study after many trials it has been concluded that the spectrophotometric assay best fitted the necessary requirements for the following reasons: 1) The use of the HPLC method (described above) required heating to stop the reaction at different times. This introduced error because yeast HGPRTase is heat-stable (see below). This might allow the appearance of relatively high levels of product at time zero, produced during the heating of the reaction mixture to

stop the reaction, thus masking the actual initial rate (laboratory observations). 2) Since the stoichiometry of the chromophores involved in the reaction is known, it is very easy to demonstrate that the rate of appearance of the chromophoric product is directly related to the rate of change of the total absorbance (see eq. I) and is independent of any constant chromophore. Thus, for a single substrate-chromophore and single product-chromophore spectrophotometry is suitable. 3) A procedure involving spectrophotometric assay allows a continuous monitoring and recording of the absorbance with very little delay, which allows the determination of the absorbance as a linear function of time.

eq. I $$dC_p/dt = [1/(\varepsilon_p - \varepsilon_s)]\ dA_t/dt$$

C_p = concentration of the product chromophore

ε_p = extinction coefficient of the product

ε_s = extinction coefficient of the substrate

A_t = total absorbance

Assays were carried out so that at least one minute of linear rate was observed in the time dependence of absorbance for the determination of the initial velocity. Enzyme and substrate concentrations were varied until this condition was achieved. Studies of the range of concentrations of

guanine and PRPP were conducted at each pH. It was necessary to use a different set of guanine and PRPP concentrations because the variation of the kinetic parameters with pH restricted the working range of concentrations for accurate initial velocities.

Since the experiments were conducted in different batches, the activity of the enzyme used was slightly different for each batch. The rate at [PRPP] = 200 μM and [G] = 20 μM (pH 7.5) was taken as the standard and all batches were normalized to this standard. The standardization procedure was as follows: For every batch HGPRTase was diluted with stabilizing buffer (50 mM Tris-HCl, 10 mM $MgCl_2$, 1 mM DTT, 15% glycerol, pH 7.5) to have an activity close to that of the first batch, then the rate was measured at [PRPP] = 200 μM and [G] = 20 μM (pH 7.5) 3-4 times, averaged and called **[v]**. For every batch a factor was then calculated as follows: f = $[v]/[v]_o$, where $[v]_o$ is the averaged velocity at [PRPP] = 200 μM and [G] = 20 μM (pH 7.5) for the first batch, then the actual 1/v ($1/v_a$) was obtained by multiplying the measured 1/v by the factor f.

The reaction mixture contained : Buffer 600 μl (different buffers over the pH range), MgCl2 (0.1 M) 100 μl, PRPP (varying concentrations) 100 μl, guanine (varying concentrations) 100 μl, and enzyme solution 100 μl. The reactants were added as follows : First all reagents but

guanine are added to the cuvette and placed in the spectrophotometer for about three minutes until a base line is established. This allows for both the enzyme to come to equilibrium with the medium so that there is no non-steady state region in the initial velocity curve due to changes in the microenvironment of the enzyme, and the reaction mixture to warm up to room temperature. 2) Then guanine is added and the cell placed back into the spectrophotometer and the change in absorbance with time is recorded at λ= 257.5 nm (for GMP). The absorbance ranges used during the assays were 0-0.1 and 0-0.05 absorbance units, depending on the range of substrate concentration used. The solutions of guanine added to the reaction mixture were prepared at the moment of use by diluting a stock solution (2 mM) with deionized water (the stock solution was prepared new every two days and stored at room temperature and alkaline medium). The PRPP solution was prepared in the same manner, but diluted with 50 mM Tris-HCl buffer (pH 7.5), and the stock solution was prepared in deionized water and stored at -76°C.

Buffer Selection for pH Range:

The pH study was conducted in the pH range 4.5-9.7. No experiment could be performed at pH values above 9.7 because at those pH values Mg^{+2} precipitated as $Mg(OH)_2$. Several buffers were tested for a variety of ranges of pH. Most of the buffers tested presented one of two

TABLE II

Buffers selected for the pH study and pH range in which they were used

pH Range	Buffer
4.5-5.0	Acetate-Na
5.5-6.5	Bis-tris-propane
7.0-8.6	Tris-HCl
9.7	Monoethanolamine

problems: 1) they absorbed at the wavelength of observation (257.5 nm) or 2) they trapped Mg^{+2} inhibiting the enzyme activity. The buffers shown in Table II were chosen because they produced the least interference. All buffers were used at a concentration of 50 mM except monoethanolamine which was 1% v/v.

Determination of the Effective Concentration of Substrates:

The concentrations of T-7 and T-9 at each guanine concentration were estimated from the published approximate values of the $\Delta G°$ for the interconversion between the two tautomeric forms, $\Delta G° \sim 1$ Kcal/mole => $1/k_t \sim 0.2$ (see "Introduction" and 97, 102, 106).

The concentrations of the monomagnesium and dimagnesium complexes of PRPP at every pH and for every total concentration of PRPP, at a fixed concentration of $MgCl_2$ (all experiments were conducted at 10 mM $MgCl_2$), were calculated by solving the system of simultaneous equations resulting from the equilibrium between the different species of PRPP that exist in solution under the experimental conditions (see Table III). The values of the equilibrium constants were obtained from previous publications (30). The system of equations was solved for the concentrations of each of the species shown in Table III in terms of pH and the total concentratio of PRPP. The following variables were

TABLE III

Association Constants and Conservation Equations for the Different Magnesium-PRPP Complexes Formed in Solution

Equilibrium	Association (*) constant (M^{-1})
$H^+ + PRPP^{-5} \Leftrightarrow HPRPP^{-4}$	$4.8X10^6$
$H^+ + HPRPP^{-4} \Leftrightarrow H_2PRPP^{-3}$	$7.4X10^5$
$H^+ + Mg\text{-}PRPP^{-3} \Leftrightarrow Mg\text{-}HPRPP^{-2}$	$1.7X10^6$
$H^+ + Mg\text{-}HPRPP^{-2} \Leftrightarrow Mg\text{-}H_2PRPP^{-1}$	$6.0X10^3$
$Mg^{+2} + PRPP^{-5} \Leftrightarrow Mg\text{-}PRPP^{-3}$	$1.7X10^3$
$Mg^{+2} + Mg\text{-}PRPP^{-3} \Leftrightarrow Mg_2\text{-}PRPP^{-1}$	4.7X10

Conservation equations:

$$[PRPP_{tot}] = [PRPP^{-5}] + [HPRPP^{-4}] + [H_2PRPP^{-3}] + [Mg\text{-}PRPP^{-3}] + [Mg\text{-}HPRPP^{-2}] + [Mg\text{-}H_2PRPP^{-1}] + [Mg_2\text{-}PRPP^{-1}]$$

$$[Mg_{tot}] = [Mg\text{-}PRPP^{-3}] + [Mg\text{-}HPRPP^{-2}] + [Mg\text{-}H_2PRPP^{-1}] + 2X[Mg_2\text{-}PRPP^{-1}] + [Mg^{+2}]$$

* The values of the equilibrium constants were obtained from reference 30.

then defined: $[PRPP] = [PRPP^{-5}] + [HPRPP^{-4}] + [H_2PRPP^{-3}]$ (concentration of uncomplexed PRPP), $[Mg\text{-}PRPP] = [Mg\text{-}PRPP^{-3}] + [Mg\text{-}HPRPP^{-2}] + [Mg\text{-}H_2PRPP^{-1}]$ (concentration of monomagnesium PRPP complex), and $[Mg_2\text{-}PRPP^{-1}]$ (concentration of dimagnesium PRPP complex). The system of equations was solved analytically with the help of the computer program Mathematica from Macintosh. Each of the variables was plotted against pH at various total concentrations of PRPP (Figures 19-21). These graphs were used to determine the concentration of each species at every working condition and the dependence between the concentrations of the various complexes at different pH values (see Figures 22, 23 and 41).

The solubility product (K_{sp}) of $Mg(OH)_2$ is $1.1 \times 10^{-11}\ M^3$, while the association constant for the formation of $MgOH^{+1}$ is $3.8 \times 10^2\ M^{-1}$ (137), which allows us to determine the fraction of magnesium associated with OH^{-1} at every pH in the absence of any other anion, as can be appreciated in Figure 24, at all pH values below 9.5 practically all the magnesium exists as a free ion, which indicates that for that pH range OH^- is not competing for Mg^{+2} with any of the PRPP anions. Furthermore when the solubility product is used to calculate the pH at which a 10 mM solution of magnesium precipitates as $Mg(OH)_2$ in the absence of other anions, a value of 9.52 is obtained. With the presence of a competing anion $Mg(OH)_2$

precipitates at a higher pH. Thus this set of curves can be safely used for the pH range and Mg^{+2} concentrations used.

Alternate Substrates and Inhibitors

Enzyme Assay Procedures:

The HPLC assay procedure was used for the alternate substrate study. The spectrophotometric assay procedure was used for the inhibition and the enzyme temperature stability studies. Unless indicated otherwise, a standard reaction mixture to test for activity was composed as the following: 600 µl Tris-HCl 50 mM (pH 7.5), 100 µl guanine 1 mM, 100 µl PRPP 10 mM, 100 µl $MgCl_2$ 10 mM and 100 µl enzyme solution.

Enzyme Temperature Stability:

The ammonium sulfate fraction of the crude extract was tested for thermal stability of HGPRTase as follows: to each 100 ml of the enzyme suspension, 15% glycerol and 1mM DTT was added. The mixture was placed in a water bath at the appropriate temperature for five minutes, after which time it was quickly placed in an ice bath to cool, the denatured protein was removed by centrifugation at 16,000 rpm for 30 minutes and the supernatant tested for HGPRTase activity. Four temperatures were tested (50°C, 60°C, 70°C and 80°C).

Pure HGPRTase was tested as follows: 15 µl of the stock solution was placed in one ml of deionized water (or diluting buffer, see below), the mixture was incubated at room temperature, aliquots of 100 µl were taken at various intervals and the activity monitored. The experiment was done first for one hour and then continued for twelve hours.

Inactivation by Mercuric Ion:

Three experiments were conducted to test the effect of Hg^{+2} on HGPRTase : 0.1 ml of concentrated enzyme suspension was added to 0.1 ml $HgCl_2$ (pH 5.0) 100 mM, then incubated for 30 minutes at room temperature. After this time 0.1 ml of this mixture was diluted with 4.9 ml diluting buffer (50 mM Tris-HCl, 10 mM $MgCl_2$, 15% glycerol and 1 mM DTT, pH 7.5), then tested for activity. Two control experiments were run: a) an untreated-uninhibited control of 0.1 ml HGPRTase which was treated in the same way as above but with 0.1 ml acetate buffer (50 mM, pH 5) instead of $HgCl_2$, and tested in the regular reaction mixture. b) an untreated-inhibited control in which control a) was tested for activity in the presence of 100 µl $HgCl_2$ (pH 5.0, 1 mM) and 500 µl Tris-HCl.

The time dependence of the inactivation of HGPRTase by Hg^{+2} was studied at different Hg^{+2} concentrations. 0.1 ml HGPRTase was combined with 0.1 ml $HgCl_2$ of the appropriate conentration and incubated at room temperature, aliquots of

10 ml were removed at various times and placed into 1 ml diluting buffer (see above), then 100 µl of this mixture was added to the reaction mixture and the activity monitored. The two control experiments described above were also conducted for this experiment.

The reversibility of HGPRTase inactivation by Hg^{+2} was tested as follows: 15 µl HGPRTase was combined with a mixture containing 900 µl Tris-HCl (50 mM, pH 7.5) and 100 µl $HgCl_2$ (10 mM), then incubated for 30 minutes at room temperature, then placed in a flow dialysis chamber (at 4 °C) and dialysed against 100 mM mercaptoethanol (flow rate 1 ml/min), and at time intervals 100 µl aliquots were taken for activity assay. Two control tests were run: a) 15 ml HGPRTase, incubated with 1.0 ml 50 mMTris-HCl (pH 7.5), and then treated in the same way as above. b) 15 µl HGPRTase, incubated with 900 µl 50 mMTris-HCl (pH 7.5), and 100 µl 100 mM mercaptoethanol then treated as above.

Fosfomycin Effect on HGPRTase:

HGPRTase was incubated at room temperature in a mixture containing 50 mM Tris-HCl (pH 7.5) and fosfomycin (0.77 mM or 5 mM), aliquots were taken at intervals and assayed for activity. A control experiment was performed under the same conditions hut in the absence of fosfomycin.

Alternate Substrate Study:

HGPRTase (activity = 0.1 ml 1mM guanine utilized/min) was mixed with 1 ml reaction mixture containing 600 µl 50 mM Tris-HCl (pH 7.5), 100 µl of the appropriate base (1 mM, adenine, xanthine, 3-methylxanthine and caffeine: 1-3-7-trimethylxanthine), 100 µl PRPP, 10 mM, 100 µl $MgCl_2$, 10 mM, the mixture was incubated for 12 hours at room temperature and then 10 µl aliquot was injected onto the column. A control experiment was run in the absence of the enzyme.

Inhibition Studies:

A kinetic study over varying concentrations of guanine and of the inhibitor for fixed concentrations of PRPP was run. The reaction mixture consisted of 100 µl inhibiting base (varying concentrations), 100 µl guanine (varying concentrations),100 µl PRPP (high 10 mM, low 2 mM), 100 µl $MgCl_2$ (100 mM), 100 µl enzyme solution and 500 µl 50 mM Tris-HCl (pH 7.5), the mixture was placed in a cuvette and the reaction course followed spectrophotometrically.

Results

Salt-Burst Procedure

There are many steps that may be followed to establish the salt-burst procedure for the purification of any particular protein. The following procedure has been employed in our laboratory to purify HGPRTase from a yeast protein extract. The small mono-Q column was equilibrated at a buffer pH value equal to the pI of the protein plus 1 (pH 7.8 for HGPRTase). A series of elutions (100 µl protein sample injections) were then run using a linear gradient of buffer B with gradient of varying steepness, a typical example of which is shown in Figure 8a. In each case the enzyme activity was monitored for each fraction and plotted on an elution profile, so that the % concentration of buffer B at which the enzyme begins to elute (taking into account the void volume of the column) can be determined. From this experiment the best % concentration of buffer B to elute HGPRTase was determined. Thereafter a new series of elutions were performed in which step gradients were applied just below the concentration determined for buffer B, a typical example of which can be seen in Figure 8b. Several parameters were determined with this experiment, including optimal gradient heights and step widths, as well as the lag time before the elution steps. Two sets of parameters are crucial, the pre-elution step height and width (this step elutes proteins that would have otherwise co-eluted with HGPRTase activity), and elution step height and width. These parameters were optimized so

that a maximum amount of protein was pre-eluted before the eluting step.

As shown in Figures 8c and 8d, the next step is to scale up the elution volume by packing a 250 ml TSK column (with 10g protein binding capacity). Since the protein extract was highly concentrated (see "Materials and Methods"), direct injection of 10 ml of this suspension produced an apparent saturation below the binding capacity of the column (early saturation effect) due to the high ionic strength of the suspension (see "Discussion"). This problem was circumvented by designing a program to automatically dilute the protein suspension during injection (see Table I). This procedure allowed the attainment of the column binding capacity. As shown in Figure 9, the step lengths (SL-1 and SL-2) can be optimized on this new column from these experiments, taking into account the new void volume and the injection volume (sample plus diluting buffer). The buffer concentrations required to elute HGPRTase are (as expected) the same as those employed in the small scale experiments. The final task is to convert the conditions of the step-gradient into those for a salt-burst procedure (Figure 8e). The elution profiles can be better understood if the void volume of the column is taken into account: for every change in the gradient profile (entering the column) a change in the elution profile will be observed after a volume of buffer equal to the void volume of the column has been eluted. This can be better seen in Figure 9a. This goal may be achieved by dividing SL-2 (Figure 9a) into a salt pulse and a step, separated by

a low percentage of buffer B. This procedure splits the activity peak into two peaks (Figure 9b). Most of the activity will appear in the first peak following the salt burst. Then PW and SL-2 are optimized. Once PW and SL-2 are optimized, the second step (SL-3, Figure 9b) is eliminated by initiating the washing elution (100% buffer B) right after SL-2 (Figure 9c).

When the step-gradient procedure (Figure 8d) was changed into a "burst + step" gradient (Figure 10a), the activity peak (peak **1+2**, Figure 8d) eluted in two separate peaks (peaks **1** and **2**, Figure 10a), one of which displayed no activity. All the activity eluted in peak **1**. The specific activity of this activity peak is substantially increased (Figure 10 and Table IV). The distance between peaks **2** and **3** can be increased by increasing SL-2 (Figure 10a and 10b). By eliminating the 30% B step (SL-2 = 0) the last two non-activity peaks (**2** and **3**, Figure 10b) collapsed into a single one (peak **2+3**, Figure 10c), and a minimum total elution volume was achieved.

The pulse width (PW) was optimized by starting with a large PW value, diminishing this value until most of the nonactive protein is transferred from peak **1** to peak **2+3** (see Figure 11). The position of elution of the activity peak was also easily optimized, since it can be transfered to any exact position by simply displaceing the salt burst the desired volume in the desired direction (Figure 12), this was achieved by changing the values of SL-1 and SL-2. When the volume of SL-1 was decreased the activity peak was shifted towards the non-active region to the left

TABLE IV

HGPRTase Activity Before and After Purification by Various Preparative Ion Exchange HPLC Procedures.

Experiment	Volume (ml)	Total protein (mg)	Total Activity (units)*	Specific activity (units/mg prot)	% Yield	Purification (fold)
Step						
Injected	7	502	1514.9	3.02	--	--
Eluted	80	45	2129.2	47.3	140	15.7
Step/Burst						
Injected	7	504	1501.3	2.98	--	--
Eluted	50	34.0	1883.0	55.4	125	18.6
Burst						
Injected	7	490	1470.0	3.0	--	--
Eluted	50	43.5	1953.2	56.6	133	18.9

* Nanomoles GMP/Min

TABLE IVb

Purification Summary of HGPRTase Via Hydroxyapatite Ion Exchange Chromatography

Procedure	Protein (mg)	Total • Activity	Specific & Activity	% Yield	Purification
Autolysis	27,300	44,550	1.65	100	——
$MnCl_2$ +	17,472	14,677	0.84	32.8	0.5
$(NH_4)_2SO_4$	10,710	27,739	2.59	61.5	1.6
Heat Treat.	6,720	23,318	3.47	50.2	2.1
Hyd. Apat.	203.7	3,219	15.8	7.1	9.6
GMP Af. Chrom.	4.6	3,059	665	6.73	403.5

• **namoles GMP/min**

& **nanomoles GMP/min x mg prot**

\+ **The high concentration of Mn^{+2} inhibits HGPRTase**

TABLE IVC

GMP-Sepharose Affinity Chromatography of a Concentrated pool of Burst and Burst/Step Eluents

Procedure	Protein (mg)	Total • Activity	Specific & Activity	% Yield	Purification (fold)
Burst Pool	440	24,550	55.8	——	——
GMP-Aff.	36.4	23,150	636	94.3	11.4

• **nanomoles GMP/min**

& **nanomoles GMP/min x mg prot**

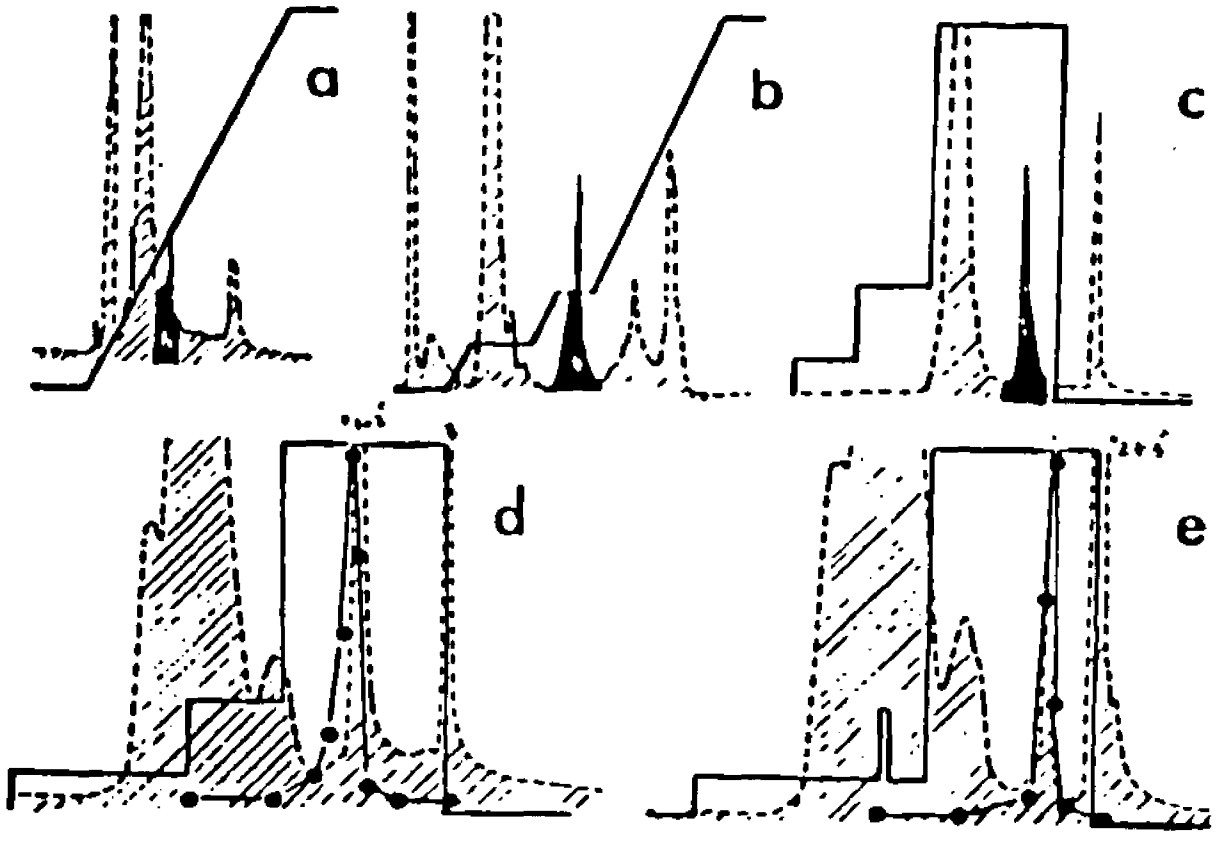

Fig. 8. Chromatographic steps that were followed to establish the most effective salt burst procedure for the purification of HGPRTase from yeast. Each figure represents a series of experiments, of which only a representative case is presented. a. A small sample of protein extract (100 µl) was eluted through a monoQ HR 5/5 column and eluted with a linear gradient with Buffers A and B (various gradient steepnesses were tested). HGPRTase activity is defined by the darkened area. b. The application of step gradients on the monoQ column containing 100µl protein extratact to optimize the eluting concentration of Buffer B and to define the step lengths (SL) for these step gradients. HGPRTase is again defined by the darkened area. c. The application of step gradients on the 250 ml TSK DEAE 650s column containing 1ml protein extract. Enzymatic activity is defined by the darkened peak. d. Repeat of the experiment defined in "c" except that 10 ml of protein extract (placed on the column in successive 1ml volumes) was eluted by the step gradient. HGPRTase activity is defined by the solid circles (peak "1+2" eluting after 30% B step, peak 3 eluting after 100% B step). e. Application of the information obtained from the other elutions ("a-d") to elute 10 ml of protein extract from the 250 ml column through the salt burst gradient elution (peak 1 eluting after the salt burst, peak "2+3" eluting after the 100% B step). In d and e HGPRTase activity is indicated by dark circles. The conditions for these elutions are described in "Materials and Methods".

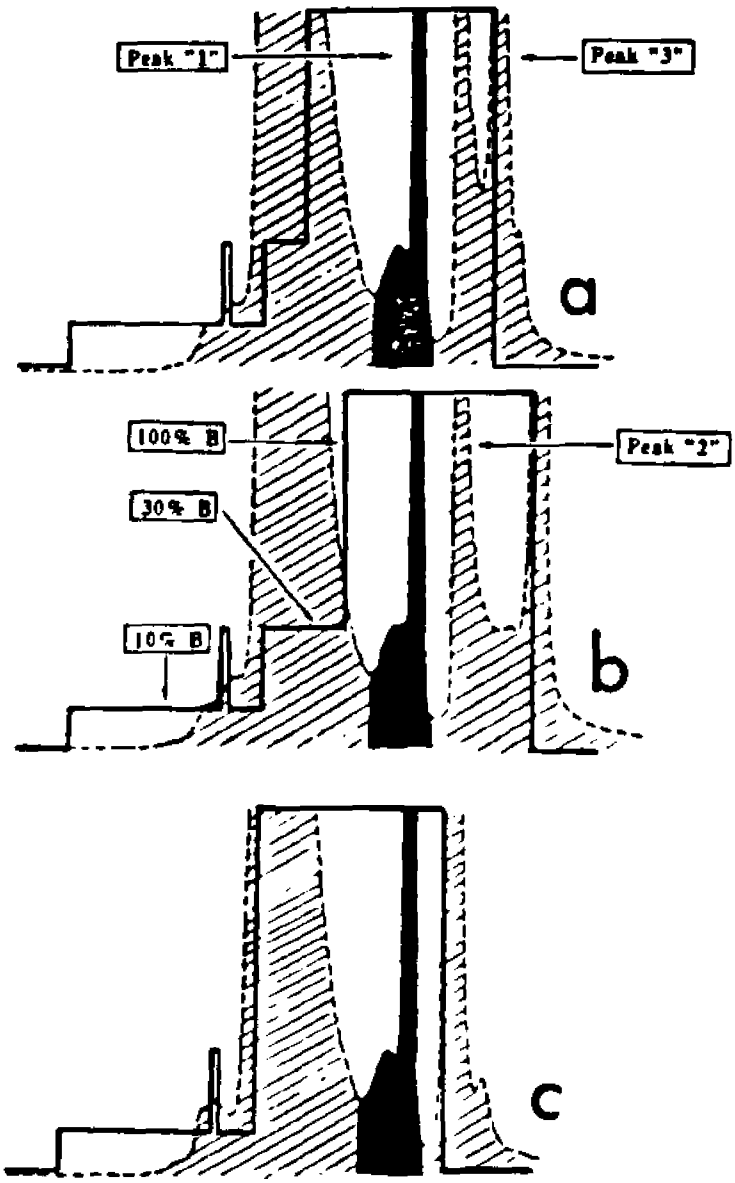

Fig. 10. Improvement of the HGPRTase purification yield in going from a step-gradient to a burst-gradient procedure. **a.** When the step-gradient (Fig. 8d) is changed into a "burst + step" gradien, the protein that elutes in the "active" peak (peak "1+2", Fig. 8d) elutes now in two separate peaks (peaks 1 and 2), the activity was found in peak 1 **b.** Separation of the generated inactive peak 2 via 30% B step followed by the 100% B elution. **c.** The peaks 2 and 3 are merged into a single peak ("2+3") by initiating the elution with 100% B right after SL-2, which saves buffer and time. % buffer B (solid lines), absorbance at 254 nm (dashed lines), HGPRTase activity (darkened area). In all cases 10 ml of protein extract were injected. The conditions for these elutions are described in "Materials and Methods".

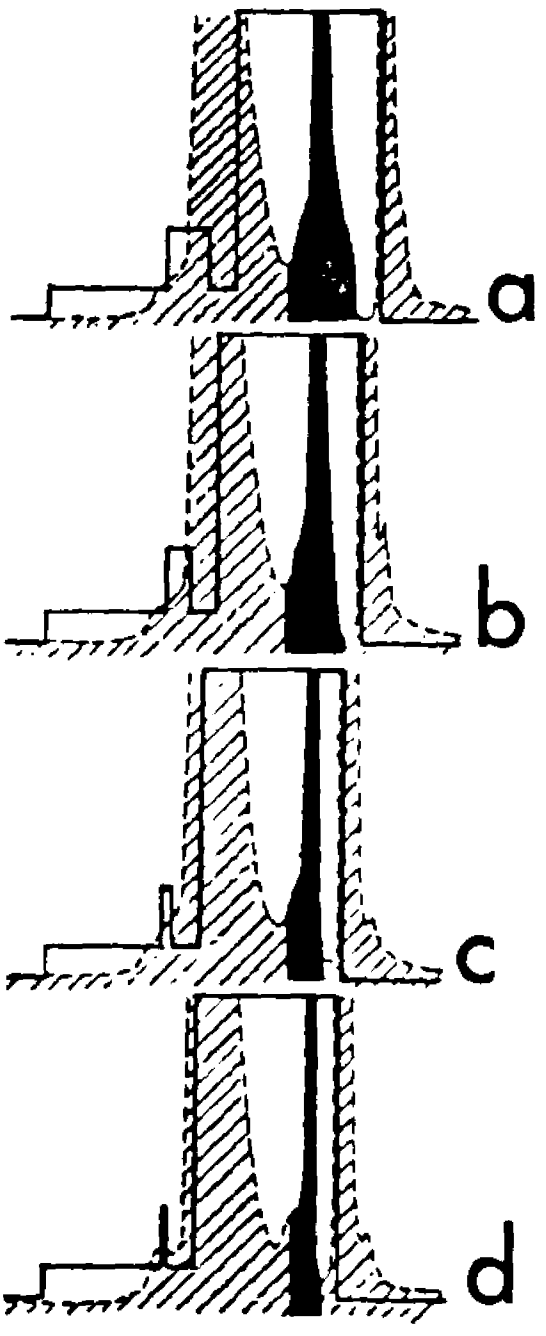

Fig. 11. Optimization of the pulse width (PW) during a salt burst gradient elution of 10 ml samples of protein extract. The PW volumes that were employed were: 50 ml (**a**), 30 ml (**b**), 10 ml (**c**) and 5 ml (**d**). % buffer B (solid lines), absorbance at 254 nm (dashed lines), HGPRTase activity (darkened area). Peak numbering the same as in Figure 10c. In all cases 10 ml of protein extract were injected. The conditions for these elutions are described in "Materials and Methods".

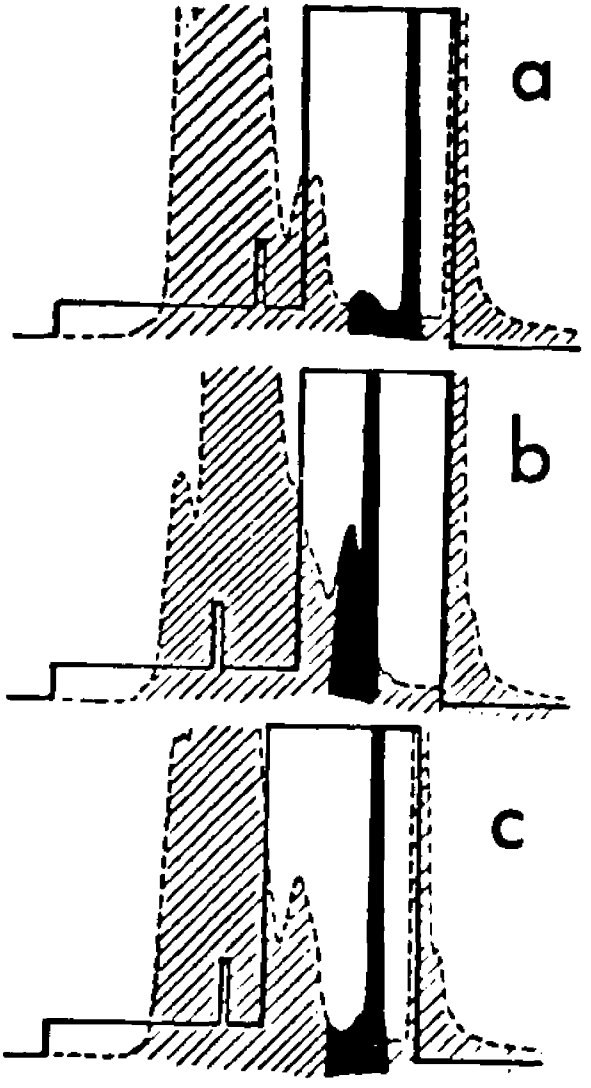

Fig. 12. Optimization of the position of the "active" peak in the salt-burst elution procedure. The relative position of the salt-burst in the elution profile can be changed by changing the values of SL-1 and SL-2, and the relative position of the "active" peak will change accordingly. When the volume of SL-1 (ml) is decreased, the "active" peak is shifted is shifted towards the "non active" region to the left. When SL-2 is decreased by certain volume the active peak is shifted towards the "non active" region to the right. **a.** SL-1 = 150 ml, SL-2 = 20 ml. **b.** SL-1 = 130 ml, SL-2 = 40 ml. **c.** SL-1 = 140 ml, SL-2 = 20 ml. % buffer B (solid lines), absorbance at 254 nm (dashed lines), HGPRTase activity (darkened area). In all cases 10 ml of protein extract were injected. The conditions for these elutions are described in "Materials and Methods".

(Figure 12a and 12b). When SL-2 was decreased the activity peak shifted towards the non activity peak to the right (Figure 12a and 12c). By altering these two parameters a minimum overlap between the non active eluates and the active HGPRTase region was achieved (Figure 12c).

The salt-burst chromatographic procedure makes use of non-equilibrium ion exchange dynamics of the elution in a fast flow rate environment. This can be seen in Figure 13. The elution profile of HGPRTase activity and of protein in the activity peak are out of phase in the step gradient. The activity elutes right at the beginning of the peak (Fig. 13a), while for the salt-burst procedure these profiles are in phase (Figure 13b). A very interesting phenomenon can be observed in Figure 13: the last peak in the step gradient elution contains practically no protein (Figure 13a), while having high absorbance at 254 nm, indicating that this peak may be comprised mainly of nucleotides and flavins. These may inhibit the enzyme and their absence may explain the gain in total activity observed when the collected total activity is compared to the total activity injected (see Table IV). Another observation is that inactive protein was transfered from peak **1** to peak **2+3** when the step is converted to a burst (Figure 13b). When The active eluents of several runs of the burst procedure were pooled together in a pressurized Amicon Ultrafiltration Cell and applied to a sepharose affinity chromatography column 94% of the activity was recovered (Table IVc).

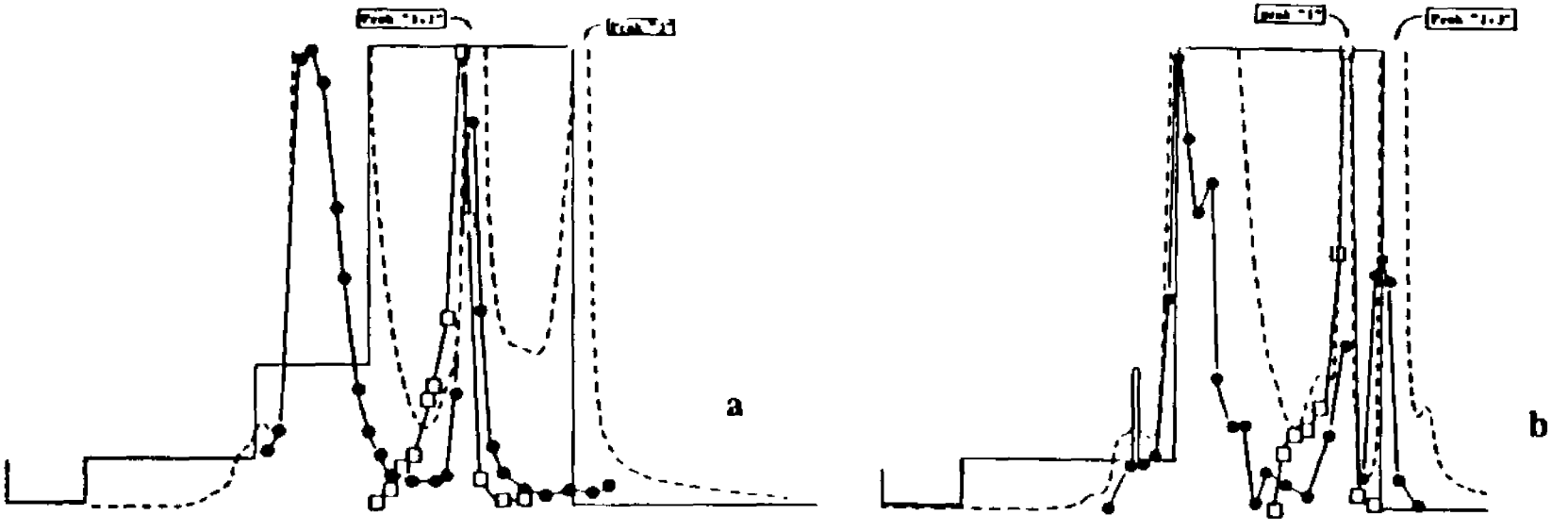

Fig. 13. Behavior of the protein and HGPRTase activity profiles during step and salt-burst gradient procedures. **a.** Step gradient procedure. **b.** Salt-burst gradient procedure. % buffer B (solid line), absorbance at 254 nm (dashed line), protein concentration, mg/ml, (solid circles), relative HGPRTase activity (squares). In all cases 10 ml of protein extract were injected. The conditions for these elutions are described in "Materials and Methods".

Multiple Enzyme Competition For PRPP

Survey of Phosphoribosyltransferase Activities in Yeast

The use of reversed-phase HPLC and isocratic elutions with 10% methanol, allowed us to monitor most of the ten known phosphoribosyltransferase activities in protein extracts from yeast. Both PRPP-dependent orotate and uracil utilizations were observed although OPM synthesis predominated under these conditions and the ability of this extract to sythesize UMP directly from uracil was lost over time. The UPRTase activity in yeast and its instability have been observed previously (130).

As shown in Figure 14, $N_aPRTase$ as well as $N_mPRTase$ and QPRTase activities were all observed. These three activities were monitored by including ATP in each of the assay solutions (Figure 14). Interestingly, very little QPRTase activity was observed under these conditions, whereas considerable concentrations of NMN and NaMN were synthesized. During this survey of pyridine nucleotide production a PRPP-independent nicotinamide-to-nicotinate transition was detected (Figure 14b).

The PRPP-dependent utilizations of several purine bases were characterized. Whereas hypoxanthine, guanine and xanthine are presumed to be substrates for HGPRTase (see "Alternate Substrates"), AMP production has been observed to occur through the use of a separate enzyme (APRTase) in yeast (39). In this survey the PRPP-dependent synthesis of IMP, GMP, XMP, and AMP

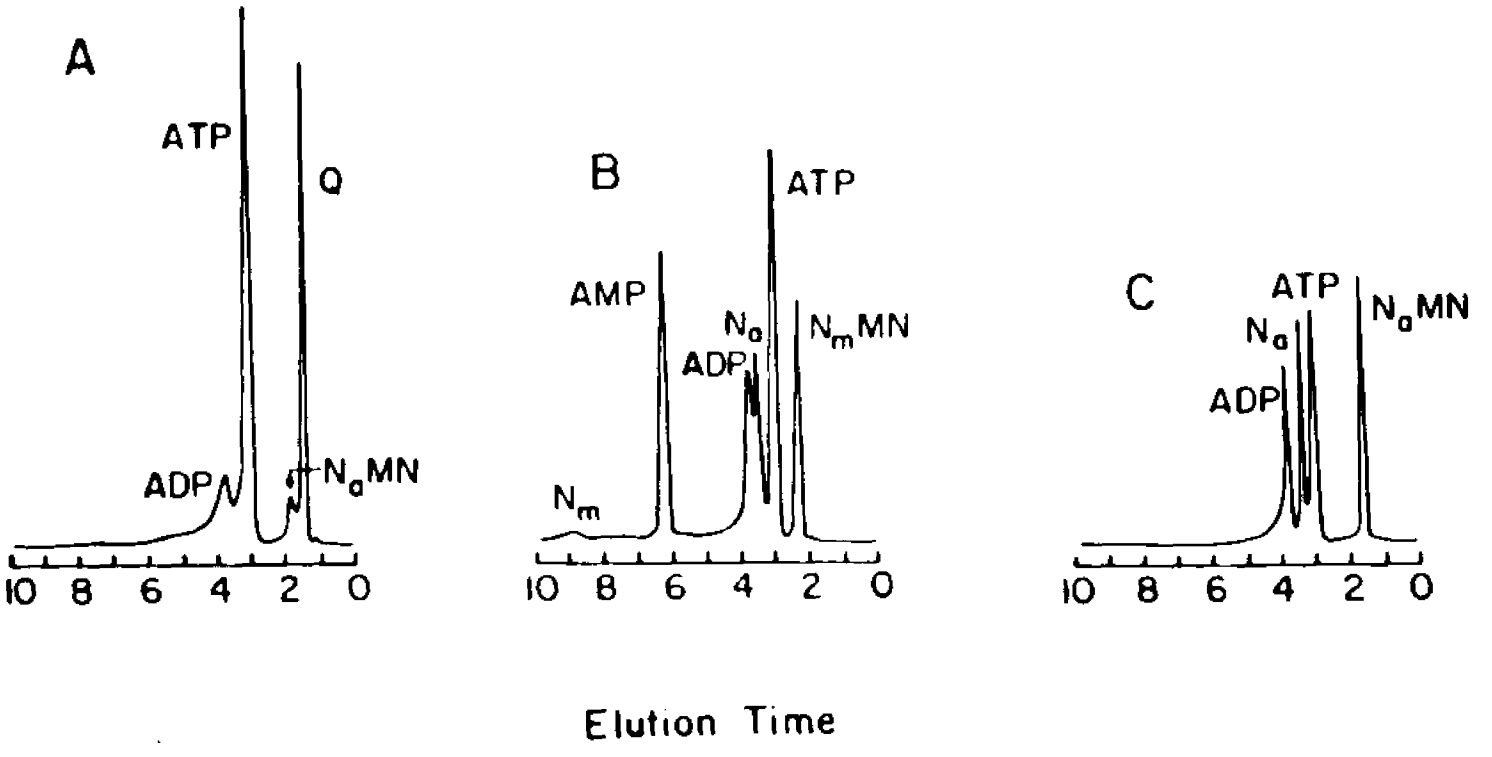

Fig. 14. HPLC assay procedures for the pyridine phosphoribosyltransferase (PRTase) activities. The concentrations of the assay components in the incubation mixture were: 50 mM Tris/phosphate buffer (pH 8.0), 1 mM $MgCl_2$, 1 mM ATP (when appropiate), 1 mM PRPP, 1 mM nicotinamide, nicotinate or quinolinate, 100 µl protein extrac. The final solution volume was 0.5 ml. **a.** HPLC elution profile after incubation of the extract with quinolinate. **b.** This profile after incubation with nicotinamide. **c.** This profile after incubation with nicotinate. Elution conditions are as described in "Materials and Methods".

were all observed, although relatively small concentrations of XMP and AMP were produced under the conditions of the assay.

Thus, 3 pyridine-, 4 purine- and 2 pyrimidine nucleotide synthetic reactions were detected in yeast during this survey.

Competition for PRPP by More than one PRTase

The HGPRTase-catalyzed reaction has been characterized as being reversible but favoring phosphoribosyltransfer (131). In contrast the OPRTase-catalyzed reaction has been characterized as reversible but favoring PRPP formation (127), and the N_aPRTase-catalyzed reaction is irreversible, primarily because of its concomitant ATPase activity (126). In addition these three enzymes have very different specific activities as pure enzymes (1300, 80, and 4.4 units/mg for HGPRTase, OPRTase and N_aPRTase respectively). In view of these dissimilarities, it is pertinent to ask how PRPP might be allocated among these three enzymatic reactions. Both the initial velocity and time dependence measurements had to be accomplished. The concentrations of the different enzymes were chosen so that their total activities were relatively equal.

A competition between HGPRTase and OPRTase was examined first. Listed in Table V are the initial velocities of these enzyme-catalyzed reactions, where the enzymes appear in the incubation solutions together and separately. The OPRTase concentrations were chosen relatively high in order to compensate for the high

TABLE V

Effects of the Presence of HGPRTase Assay Components on OPRTase and HGPRTase Activities Respectivelly

	Experiment	OPRTase Initial Activity (μmoles OMP/min) [μM PRPP]			HGPRTase Initial Activity (μmoles IMP/min) [μM PRPP]		
		100	40	20	100	40	20
pH 8	+ OPRTase - HGPRTase 100 μM orotate	23	17	12			
	+ OPRTase + HGPRTase 100 μM orotate	24	14	7			
	- OPRTase + HGPRTase 100 μM hypox.				36	29	19
	+ OPRTase + HGPRTase 100 μM hypox.				30	--	15
	+ OPRTase + HGPRTase 100 μM orotate 100 μM hypox.	24	8	3	29	20	15
pH 6	+ OPRTase + HGPRTase 100 μM orotate 100 μM hypox.	13	6	1	28	22	11

specific activity of HGPRTase. As shown in Table V, at lower PRPP concentration the presence of OPRTase alone has no effect on the HGPRTase-catalyzed synthesis of IMP, whereas the presence of HGPRTase alone inhibits the initial rate of OMP synthesis. Moreover, in the presence of the complete HGPRTase assay mixture, OMP synthesis is significantly inhibited whereas IMP synthesis is only slightly affected by the presence of all of the OPRTase assay components.

The time-dependent effects of one PRTase assay solution on another is illustrated in Figures 15a and 15b. As expected the major effect of the OPRTase assay solution is to slow the rate of IMP synthesis after 10 min of incubation. However, the effect of HGPRTase assay components is to reverse the synthesis of OMP until a new reduced equilibrium concentration is reached.

The competition between OPRTase and HGPRTase was repeated in the presence of 1/2 of the OPRTase and 1/5 of the HGPRTase concentrations utilized previously (Table VI, Figures 15a and 15b). As shown by the initial velocity values (Table VI), the effect of the addition of nicotinate is to inhibit OMP synthesis both in the presence and absence of ATP. Finally, the effect of the addition of the complete N_aPRTase assay solution has no effect on the initial velocity of IMP synthesis, but OMP synthesis is apparently activated. This apparent activation is in fact due to an OPRTase contaminant in the N_aPRTase preparation. These two enzymes copurify until the final steps of N_aPRTase isolation

TABLE VI

Effects of the Presence of N_aPRTase Assay Components on OPRTase and HGPRTase Activities
The PRPP concentration in All Experiments is 100 μM

Experiment	Initial Velocities		
	OPRTase (μmoles OMP/min)	HGPRTase (μmoles IMP/min)	N_aPRTase (μmoles NaMN/min)
1) + OPRTase + HGPRTase 100 μM orotate	11.6	4.3	--
2) + OPRTase + HGPRTase 100 μM orotate 100 μM hypox. 100 μM nicotinate	8.5	4.0	--
3) + OPRTase + HGPRTase 100 μM orotate 100 μM hypox. 100 μM ATP	11.0	8.0	--
4) + OPRTase + HGPRTase 100 μM orotate 100 μM hypox. 100 μM nicotinate 100 μM ATP	8.5	7.5	--
5) + OPRTase + HGPRTase + N_aPRTase 100 μM orotate 100 μM hypox. 100 μM nicotinate 100 μM ATP	27.5	7.5	2.8

The time-dependent effect of the three enzyme assay solutions on one another is illustrated in Figures 15c and 15d. The relatively slow synthesis of NaMN (and ADP) is linear and unaffected by the addition of the assay components of the other two enzymes. The effects of the OPRTase and N_aPRTase assay components on IMP synthesis is slight over a 10 min period (Figure 15d). However, the presence of the N_aPRTase assay solution eventually reverses IMP synthesis towards a new equilibrium concentration. This effect is shown in Figure 16 where the HPLC assay procedure and the component separation are also illustrated. Moreover, the effect of presence of N_aPRTase and HGPRTase assay solutions on OMP synthesis is to reverse this synthesis completely. As shown in Figure 15c and 16, all of the orotate that was added initially is present again after 30 min. Thus OPRTase, which catalyses the fastest rate of nucleotide synthesis initially, ultimately loses the competition for PRPP to the irreversible N_aPRTase-catalyzed reaction. Presumably, IMP synthesis would be reversed as well over a longer period of time under these assay conditions.

Kinetics And pH Study

Substrate Inhibition

In the course of studying the range of substrate concentrations for the pH study a dead end substrate inhibition of HGPRTase by guanine was observed. Since the effect was very

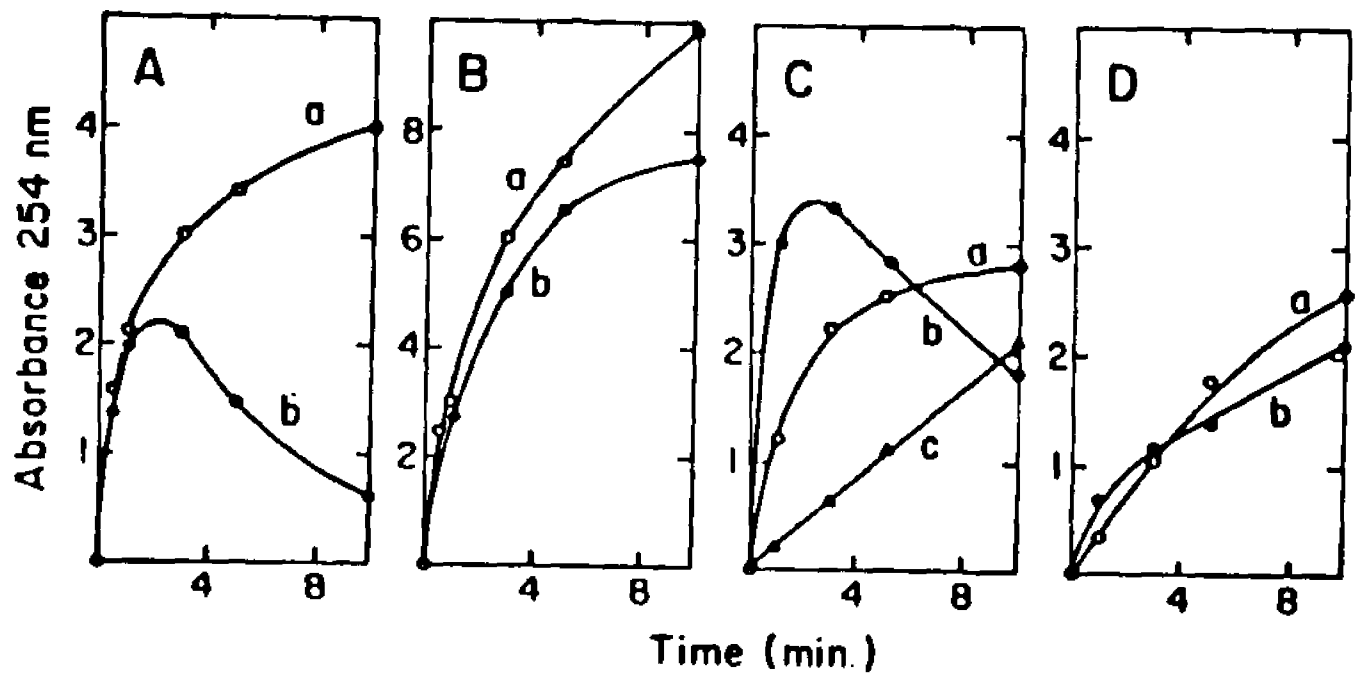

Fig. 15. Rate of appearance of the nucleotides AMP, IMP, and NaMN from incubation mixtures difined in "Materials and Methods" and in Experiments 4 and 5 of Table VI. **a.** Rate of OMP synthesis from an incubation of OPRTase with its substrates in the absence of the complete HGPRTase assay mixture (circles) and in the presence of this mixture (solid circles). **b.** Rate of IMP synthesis from an incubation of HGPRTase with its substrates in the absence of the complete OPRTase assay mixture (circles) and in the presence of this mixture (solid circles). **c.** Rate of OMP synthesis from an incubation of OPRTase with its substrates in the absence of any other enzyme (circles) and in the presence of both the N_aPRTase and HGPRTase assay mixtures (solid circles). Also shown is the rate of NaMN synthesis under these conditions (triangles). **d.** Same as c except that the HGPRTase-catalyzed rate of IMP formation is illustrated (solid circles).

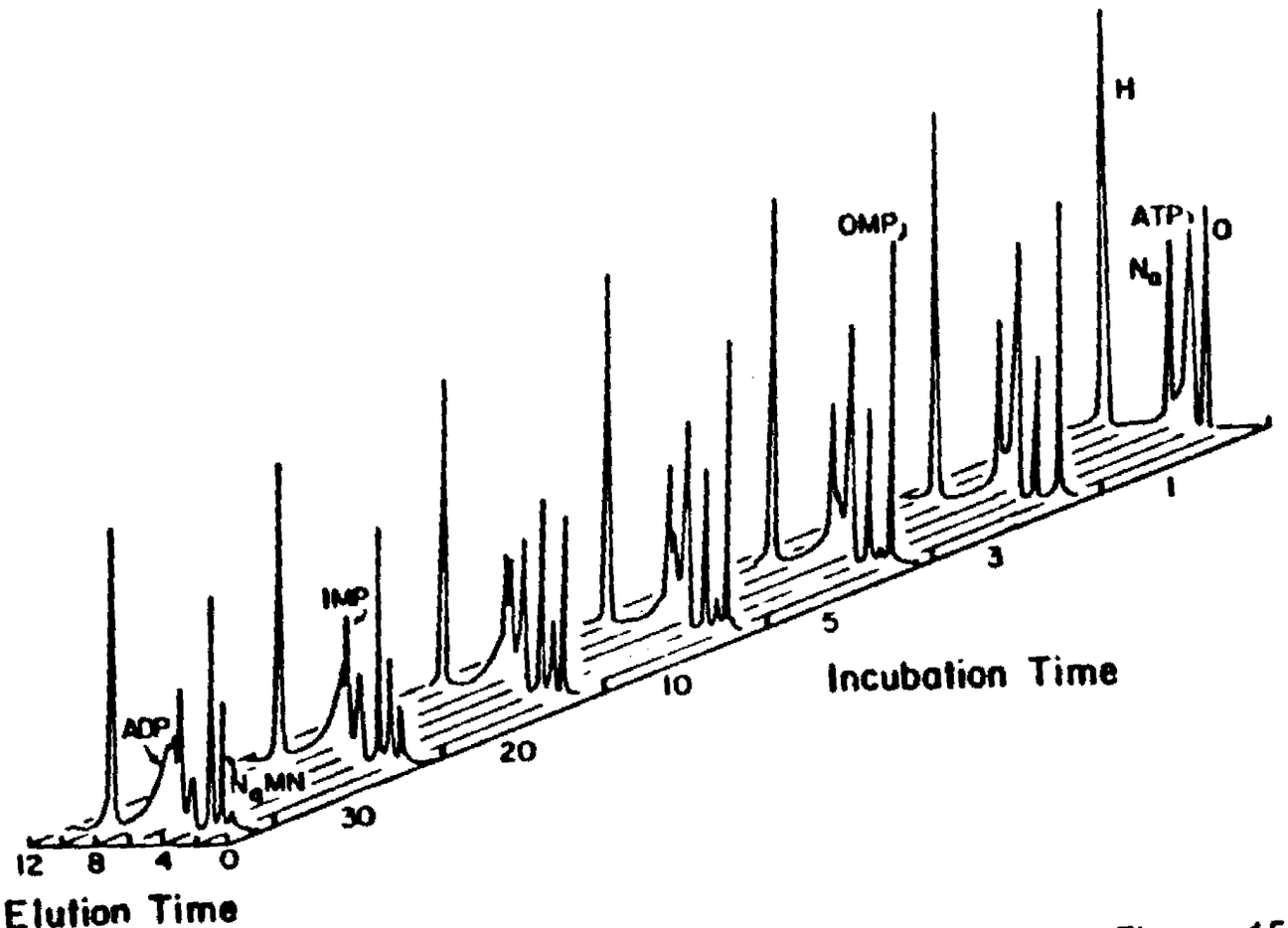

Fig. 16. Elution profiles of the incubation mixtures defined in Figure 15c which illustrates the simultaneous detection of the OPRTase, HGPRTase and N_aPRTase catalysed reactions over a 30 min time period. Elution conditions with a phosphate gradient are as described in "Materials and Methods".

strong at moderate guanine concentrations (50-200 μM), it was further investigated at pH 7.5. Figure 17 shows the effect of increasing concentrations of guanine on the initial velocity of the enzyme at verious PRPP concentrations. As can be seen in Figure 18 this is a classical case of dead end second substrate inhibition as described by Segel (135). Other more complex inhibition effects by guanine were observed at other pH values, but in most cases the normal course taken was to determine the range of guanine concentration that gave linear double reciprocal plots, which in some cases was practically impossible (see below and "Discussion")

pH dependence of [Mg-PRPP], Mg_2PRPP] and [PRPP]

According to the solutions obtained for the equilibrium and balance equations (Table III) for the magnesium-PRPP complexes (see "Materials and Methods"), the major PRPP species present in solutions containing $MgCl_2$ show a very complex pH dependence as can be seen in Figures 19 through 21, yet between the different species a linear relationship is maintained over the whole range of pH studied, at the high magnesium concentration and low range of PRPP concentrations employed in the experimental conditions (see Figures 22-24). This linearity allowed for the simplification of the rate equation developed for the kinetic mechanism proposed for the enzyme (see below and "Discussion").

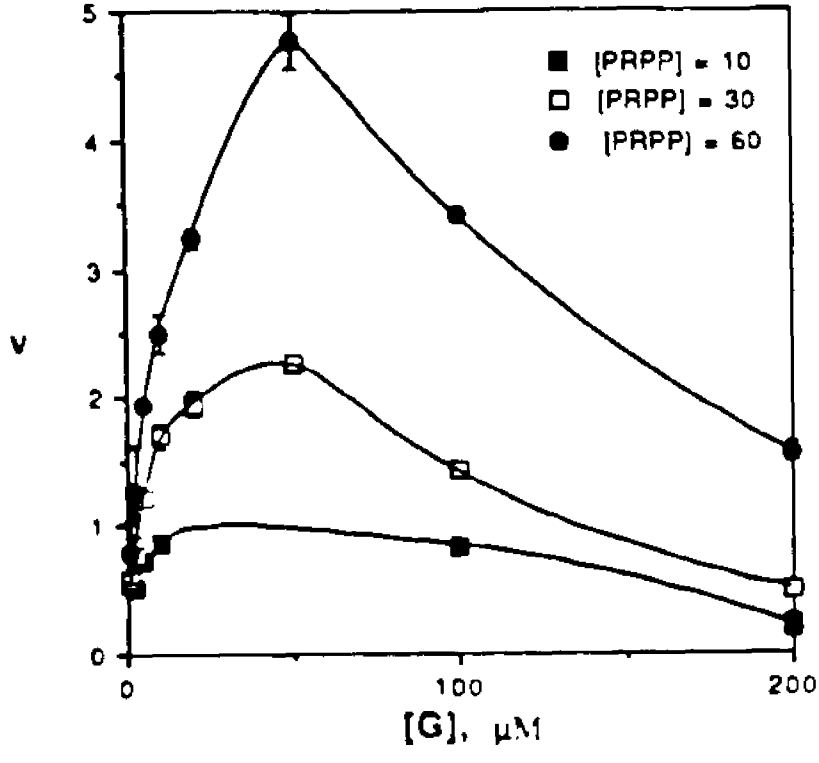

Fig. 17. Effect of guanine on the initial velocity of HGPRTase at variuos PRPP concentrations, at pH 7.5. The units of the reaction rate (V) are expressed in hundrieths of absobance units at 257.5 nm per min, the same units are used in all other experiments unless otherwise epecified. The conditions for this experiment are defined in "Materials and Methods".

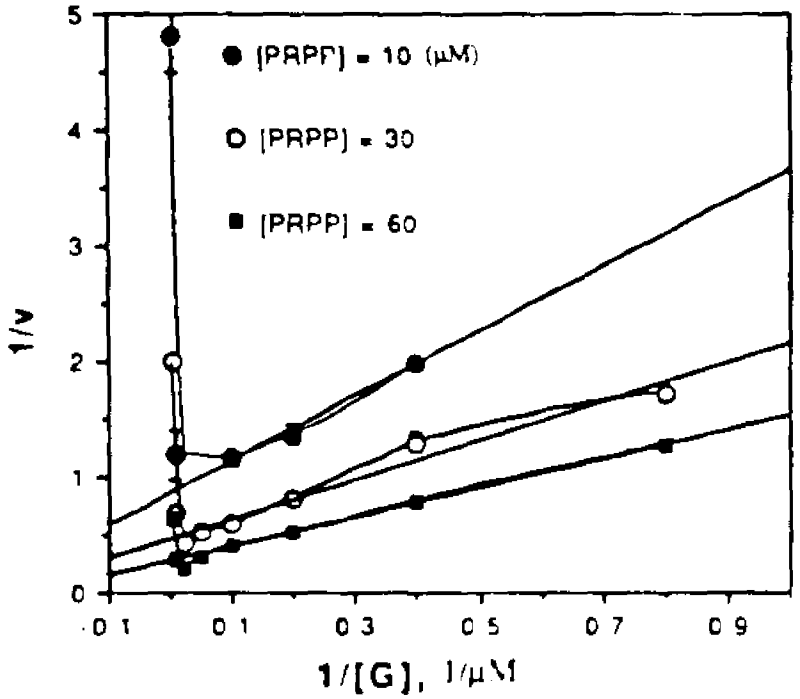

Fig. 18. Kinetics of the HGPRTase inhibition by its second substrate (guanine) at pH 7.5. The experimental conditions are defined in "Materials and Methods".

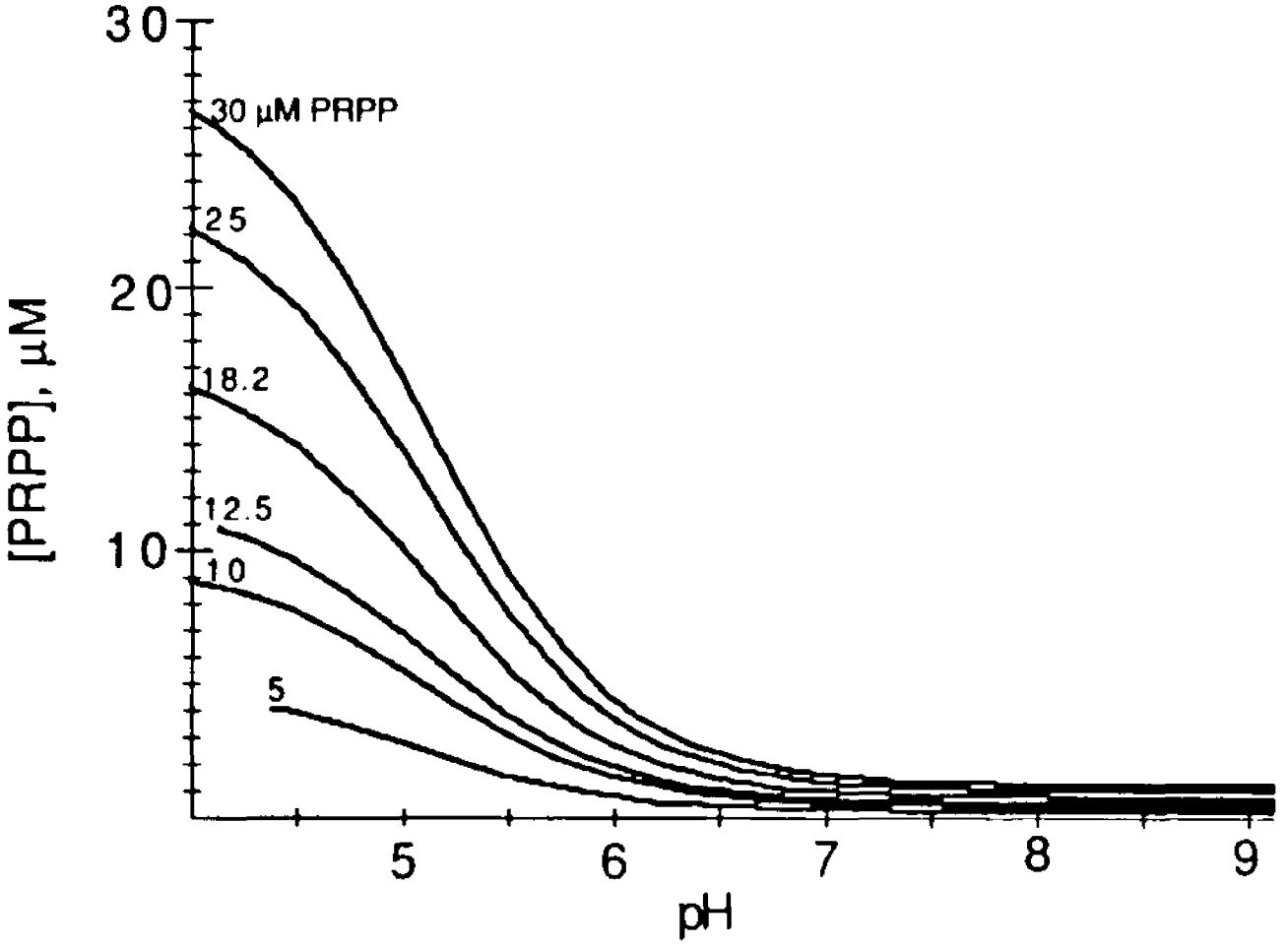

Fig. 19. pH dependence of the uncomplexed PRPP at variuos total concentrations of PRPP (5-30 µM) and 10 mM $MgCl_2$. This graph was obtained with the procedure described in "Materials and Methods".

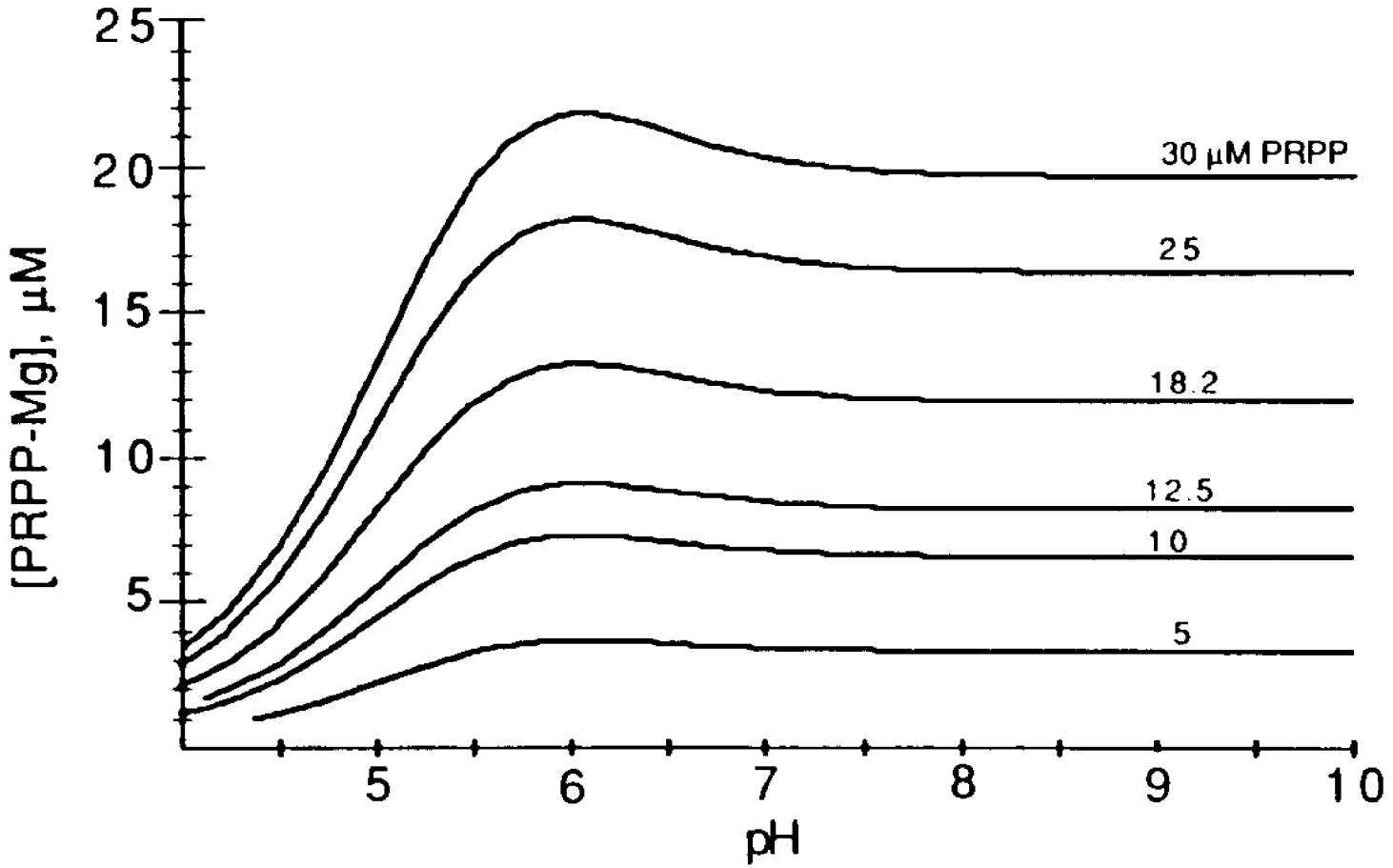

Fig. 20a. pH dependence of the mono magnesium PRPP complex at different total concentrations of PRPP (5-30 µM) and 10 mM $MgCl_2$. This graph was obtained with the procedure described in "Materials and Methods".

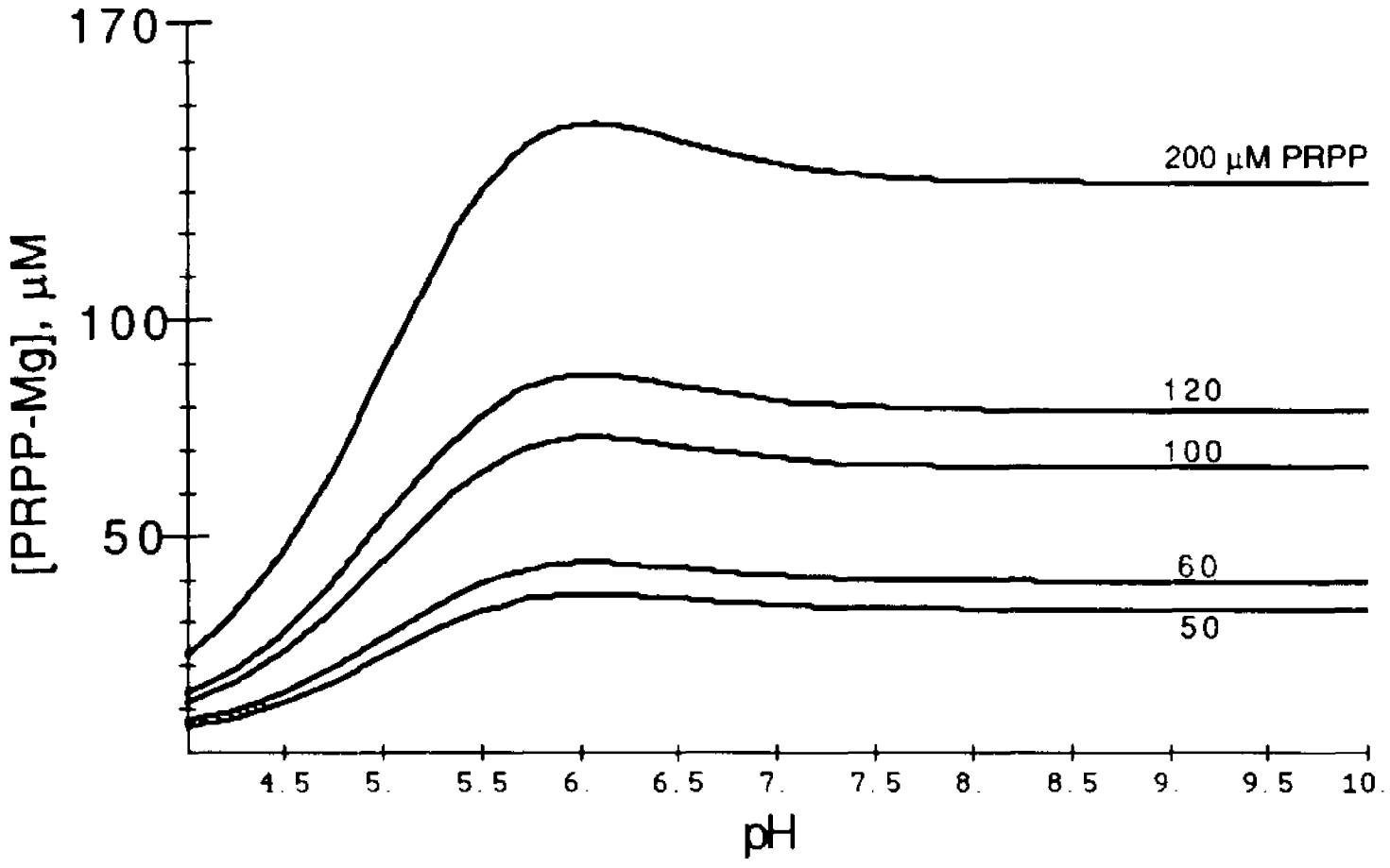

Fig. 20b. pH dependence of the mono magnesium PRPP complex at different total concentrations of PRPP (50-200 µM) and 10 mM $MgCl_2$. Obtained with the procedure described in "Materials and Methods".

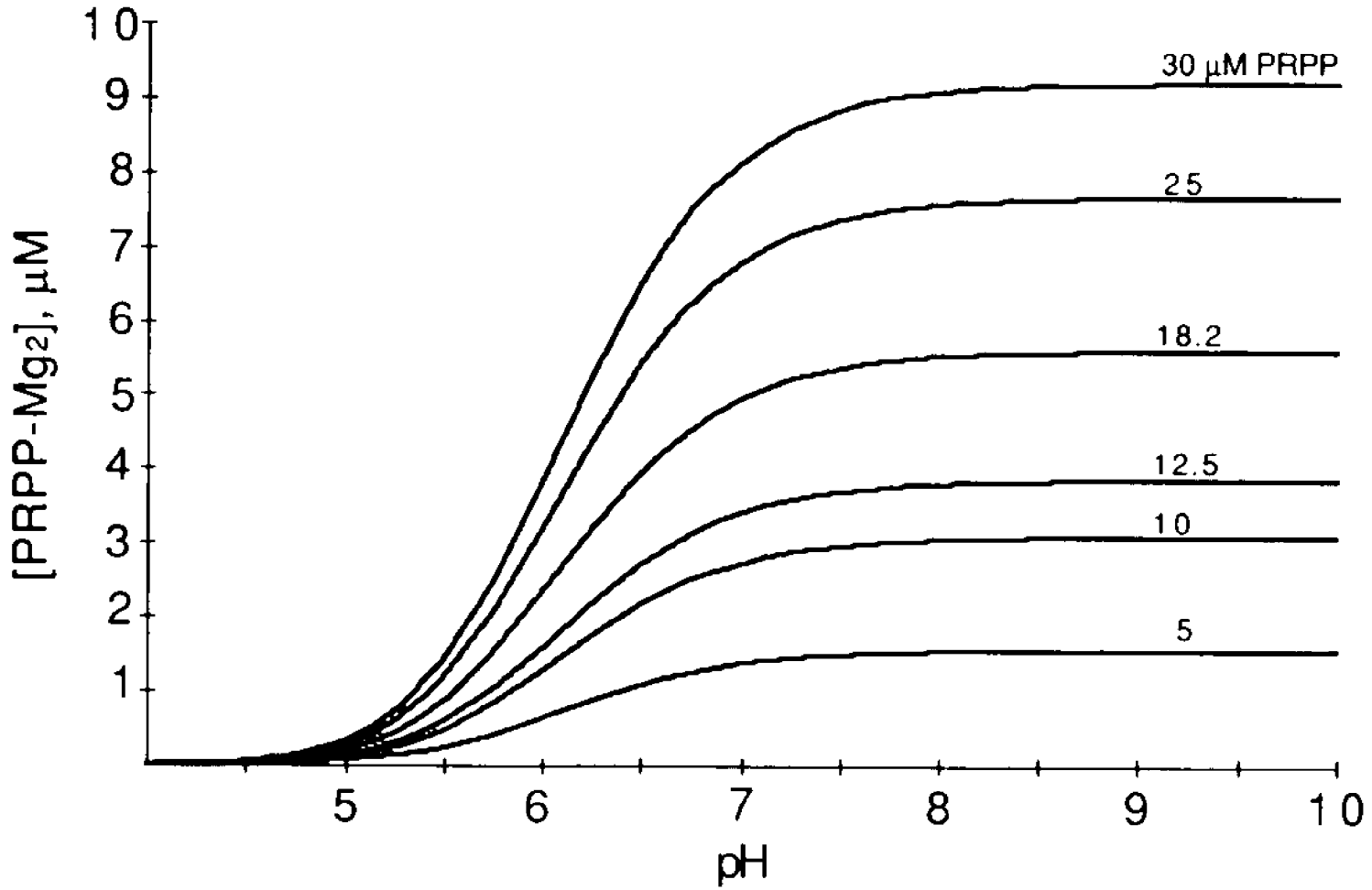

Fig. 21a. pH dependence of the dimagnesium PRPP complex at varoius PRPP concentrations (5-30 µM) and 10 mM $MgCl_2$ Obtained with the procedure described in "Materials and Methods".

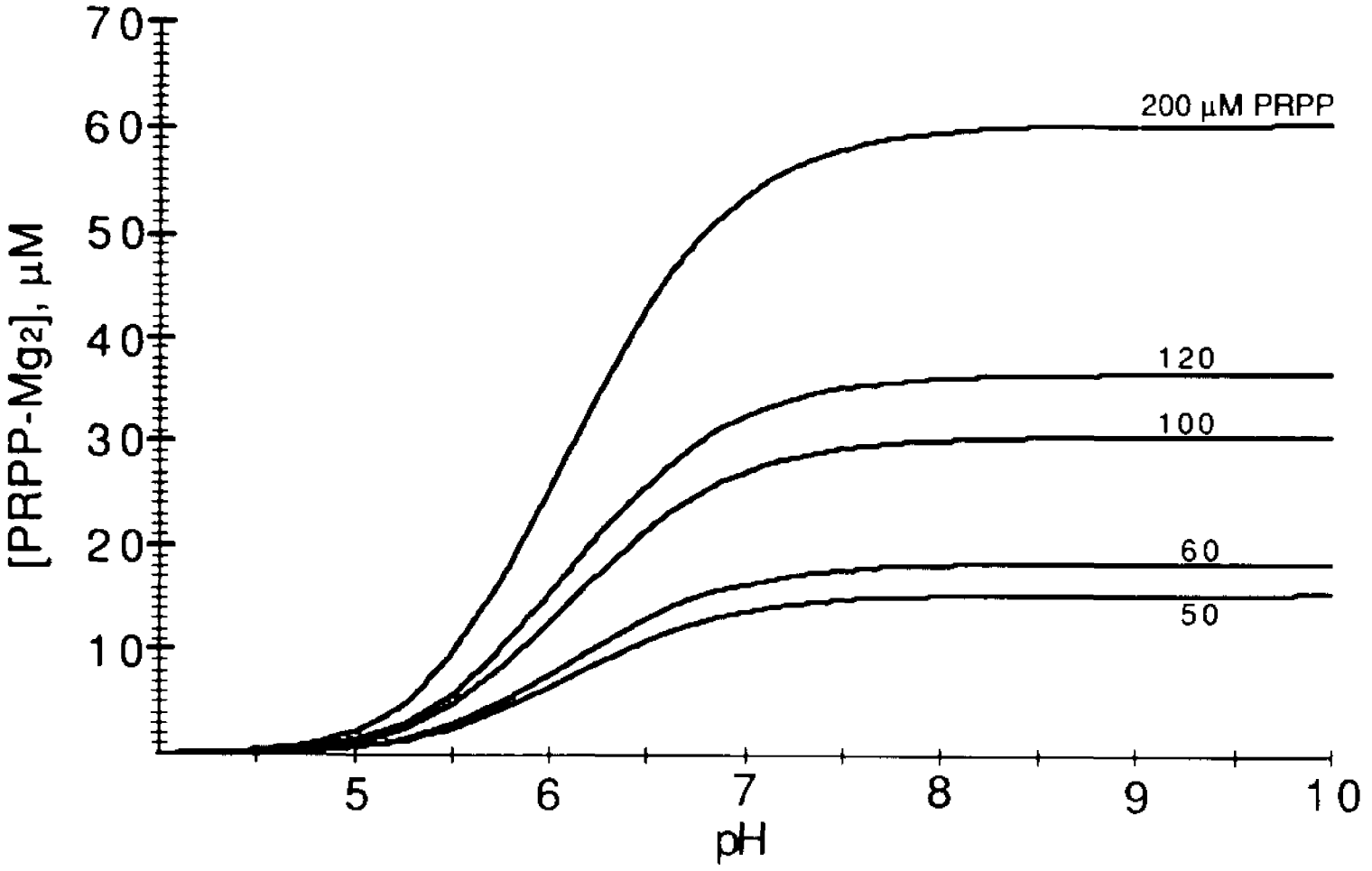

Fig. 21b. pH dependence of the dimagnesium PRPP complex at various total concentration of PRPP (50-200 µM) and 10 mM $MgCl_2$. Obtained with the procedure described in "Materials and Methods".

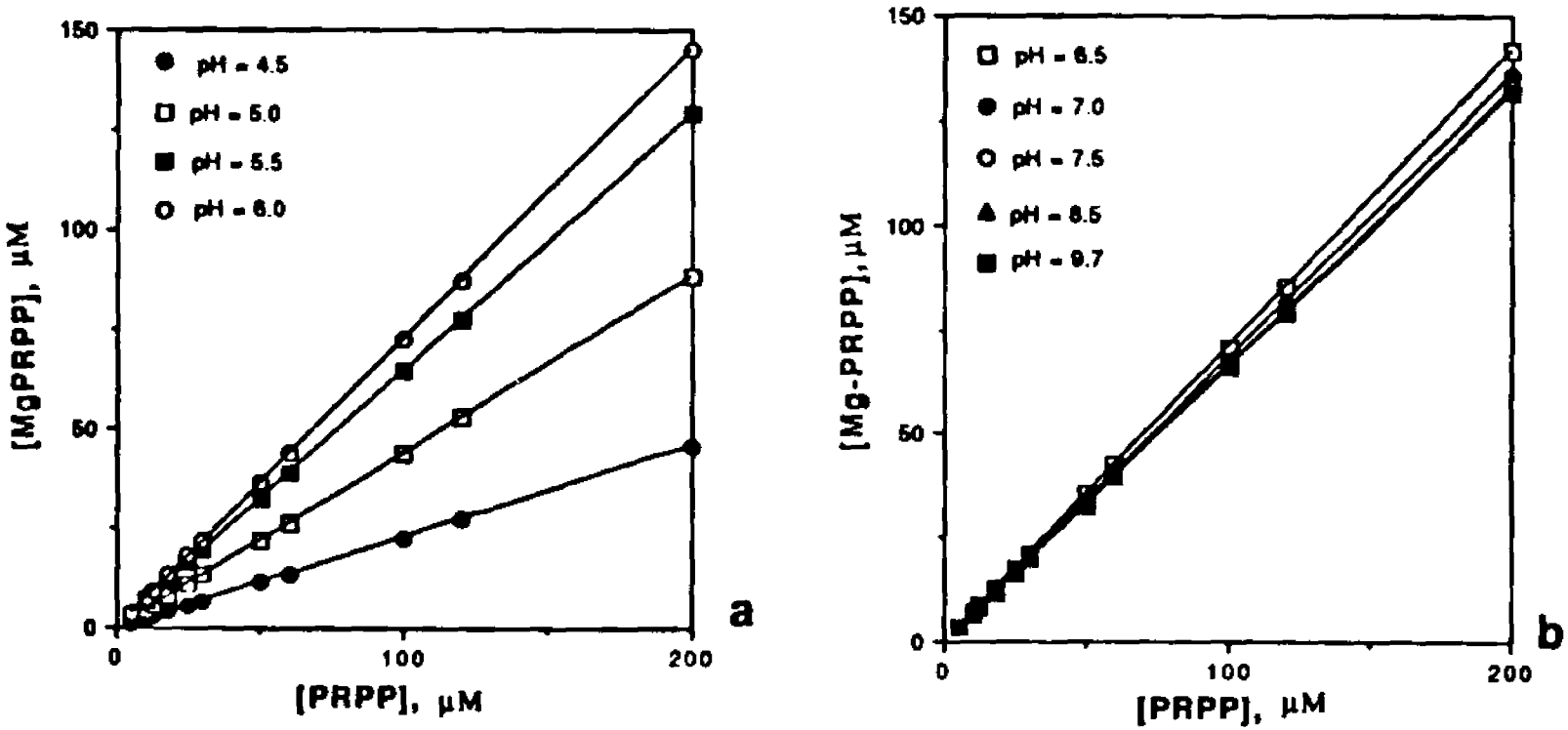

Fig. 22. Dependence of the concentration of Mg-PRPP on the total concentration of PRPP present in solution, $[PRPP]_t$. $[MgCl_2]$ in all cases was 10 mM. The data in this figure was generated following the procedure indicated in "Materials and Methods".

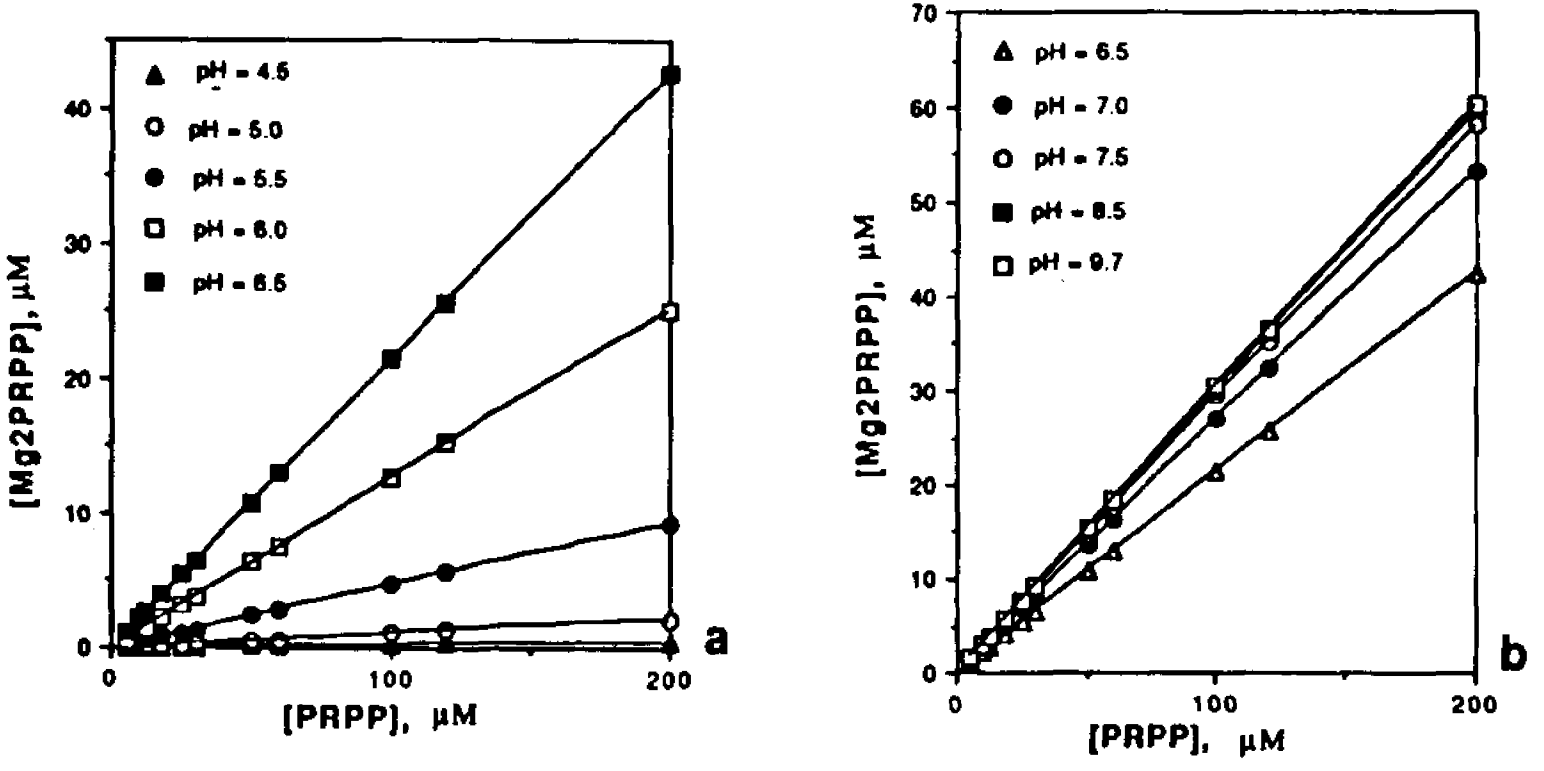

Fig. 23. Dependence of the concentration of Mg_2-PRPP on the total concentration of PRPP present in solution, $[PRPP]_t$. Generated with the procedure described in "Materials and Methods".

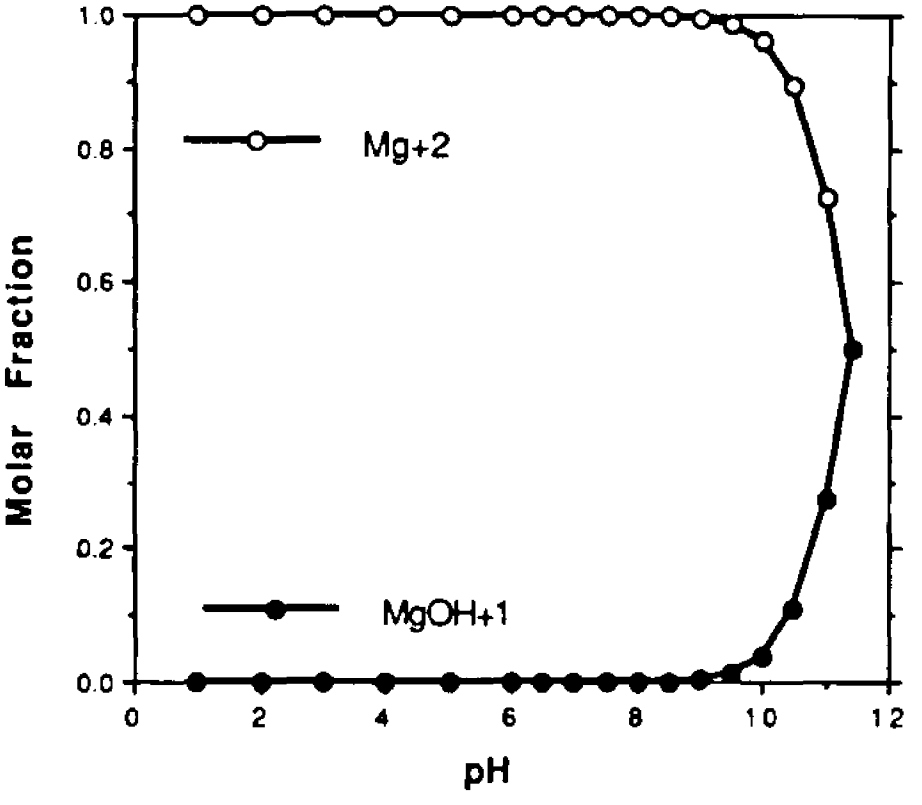

Fig. 24.- Fraction of magnesium present as Mg+2 and as MgOH+1 at various pH values. Generated from the equilibrium equation for Mg+2 + OH-1 <==> MgOH+1. The equilibium constant for this reaction is $3.8 \times 10^{2}\ M^{-1}$. Mg+2, open circles. MgOH+1, solid circles.

pH study

The kinetics of HGPRTase were investigated in the pH range 4.5-9.7 with intervals of 0.5 pH units. The study was confined to the ranges of guanine concentration that gave the more apparent linearity in the double reciprocal plots (1/v vs 1/[t-7]). Previous works have shown that HGPRTase follows an ordered Bi-Bi mechanism with a magnesium-PRPP complex as first substrate (84,89,90), but apparently strange kinetic behavior of the enzyme has led to controversies as to what is the actual mechanism (36,80,85,94).

Second substrate inhibition was observed at all pH values. The data from pH 7.5 was used to further investigate the kinetics of this inhibition. In order to avoid any masking of the kinetics of the enzymatic catalysis, the kinetic study was carried out taking into account the actual concentrations of all the species possibly involved as substrates in the catalytic process, as well as the equilibrium between them in solution (see above). This is justified because if the variation of the concentrations of the substrate complexes with pH is not taken into account (and instead the total concentration of PRPP is taken as substrate), these variations will show in the rate of the catalyzed reaction and may be confused with an effect of pH on the catalytic process.

As a starting point for the treatment of the kinetic data, the ordered Bi-Bi mechanism was taken as valid because of the strong evidence in its favor (89), but taking into account the observed

second substrate inhibition pattern (see above), the plotting scheme recommended by Segel (135) was investigated at all pH values studied. Two separate sets of plots were developed, one for Mg_2-PRPP and other for Mg-PRPP (Figures 25-40). As can be seen comparing part a with part d in Figure 25, the kinetic behaviors of both complexes at pH 8.5 seem identical, the same similarity was observed at pH 7.5 (see Figure 27 a and d), pH 7.0 (see Figure 29 a and d), pH 6.5 (see Figure 31 a and d), pH 6.0 (Figure 33 a and d) and pH 5.0 (Figure 35 a and d). But at pH values 5.0 (Figure 37 a and d) and 4.5 (Figure 39 a and d) a deviation from linearity is observed when the velocity is plotted against [Mg_2-PRPP], but not when plotted against [Mg-PRPP] (see Figures 37b and 39b). The similarity in kinetic behavior observed at pH values 5.5-8.5 is an indication that both magnesium-PRPP complexes are apparent substrates of the enzyme, which is expected because these two complexes are in equilibrium (in solution) and their concentrations are linearly related at every pH studied (in the range of concentrations of total PRPP studied at [$MgCl_2$] = 10 mM), as observed in Figure 41 and Figures 22 and 23. The deviations observed for Mg_2-PRPP at low pH values is probably due to kinetic factors (see "Discussion"). However, the kinetic mechanism can be better studied using the concentration of Mg-PRPP as the varying parameter. Its concentration is higher than Mg_2-PRPP at all pH values (see Figures 19-21). In fact the concentration of Mg_2-PRPP is practically zero at pH values below 5.0 (see Figure 21).

When the data is plotted according to the scheme for the ordered Bi-Bi with second substrate inhibition mechanism (135), a very interesting phenomenon is observed. At high (8.5-7.5) pH values (see Figures 25-28) and low (5.0-4.5) pH values (see Figures 37-40) the system seems to correlate well with this scheme. As predicted by this scheme, the double reciprocal plots of the initial velocities against the concentration of the first substrate as well as against the concentration of the second substrate are both linear (at low B range) crossing over each other at a point to the left of the zero of the abscissa (Figure 25a and 26a, pH 8.5, and Figure 27a and 28a, pH 7.5), giving linear replots of the y intercepts and slopes (Figures 25 b and c, and 26 b and c, pH 8.5, Figures 27 b and c, and 28 b and c, pH 7.5) (135). At intermediate pH values (7.0-5.5) a deviation is apparent, being strongest at pH 6.0 (see Figures 33 and 34). In these cases some of the lines in the double reciprocal plots cross over at the right of the zero and not at a single point (see Figure 33a), while the replots of the slopes(1/B) are not linear (see Figure 34c). These experiments were repeated many times and were all reproducible. Other ranges of substrate concentration were tried and the effects were always observed, indicating that the phenomenon was not due to high substrate A or high substrate B effects, which is also supported by the linearity observed in the double reciprocal plots of 1/v vs 1/[B] (see Figure 34a). As discussed below (see "Discussion"), this indicates that even though there is an ordered mechanism involved in the catalysis, a more complex process is taking place, which is made apparent when the assay conditions are such that neither

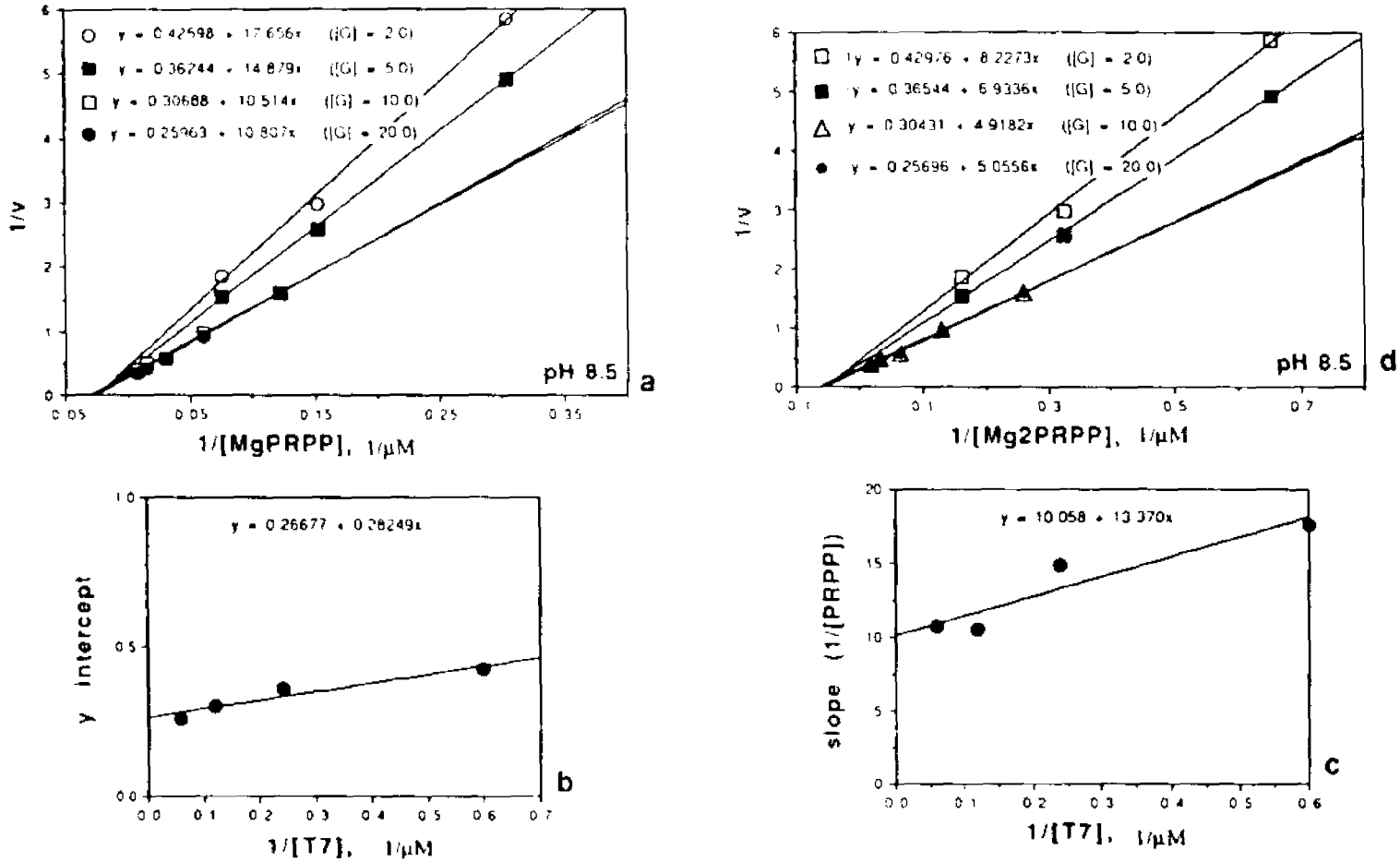

Fig. 25. Double reciprocal plots of the initial velocity of HGPRTase against the first substrate's concentration at various guanine concentrations and pH 8.5. **a**. These plots with Mg-PRPP as first substrate. **b**. Replot of the y intercepts of "**a**" against the reciprocal of the concentration of T-7. **c**. Replot of the slopes of "**a**" against the reciprocal of the concentration of T-7. **d**. These plots with Mg_2-PRPP as first substrate. The reaction rate (v) is defined as in Figure 17. The concentration of the different substrates was determined as indicated in "Materials and Methods". Each point represents the average of at least three data points (as indicated in "Materials and Methods"). Error bars indicate standard deviations (when not indicated standard deviation was less than the default minimum). The line fitting equations were obtained with the polinomial fitting (first order) of Criket Graph from Macintonsh. The experimental conditions are described in "Materials and Methods".

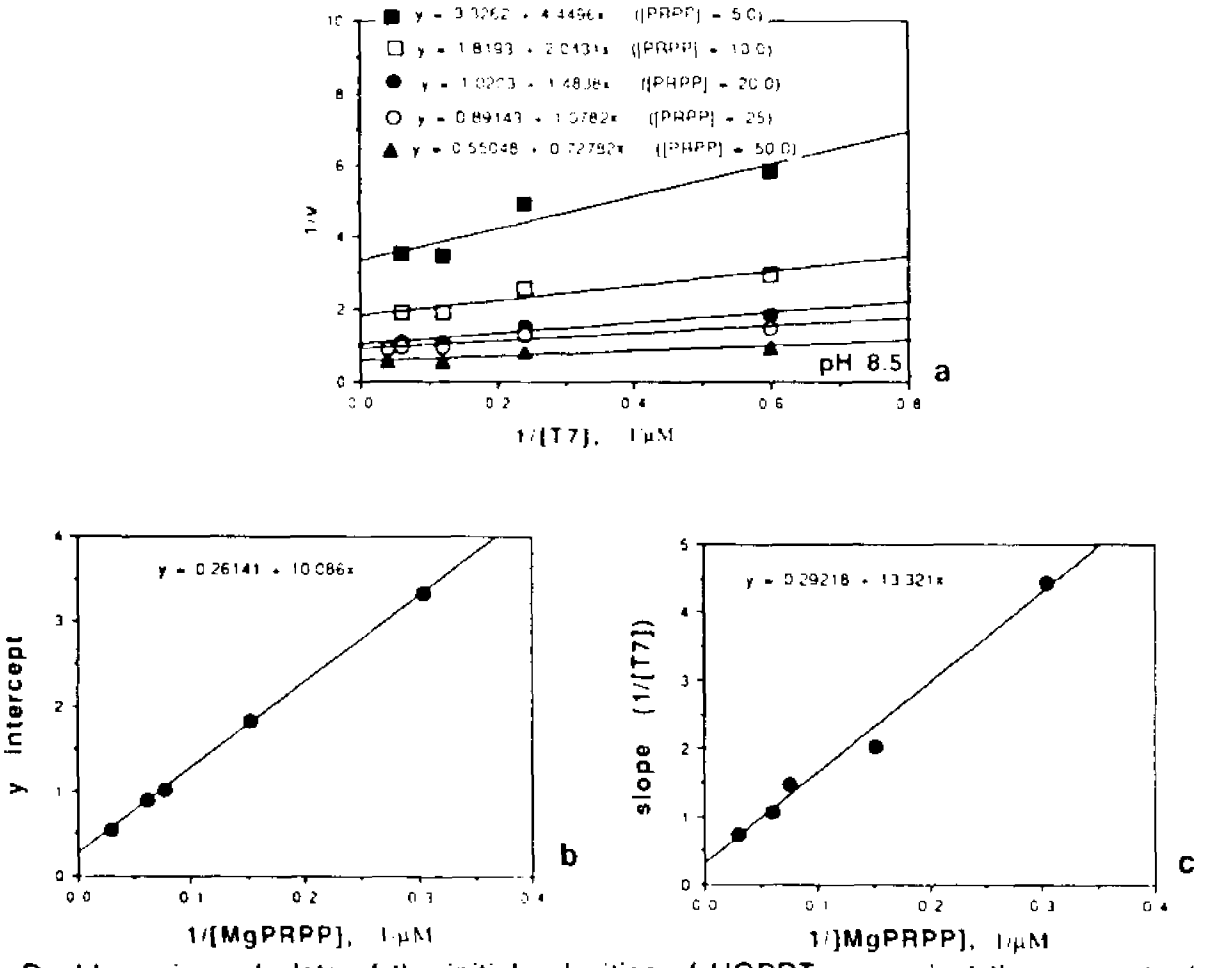

Fig. 26. Double reciprocal plots of the initial velocities of HGPRTase against the concentration of T-7 at various PRPP concentrations and pH 8.5 (**a**). **b**. Replot of the y intercepts of "**a**" against the reciprocal of the concentration of Mg-PRPP. **c**. Replot of the slopes of "**a**" against the reciprocal of the concentration of Mg-PRPP. The reaction rate (**v**) is defined as in Figure 17. The concentration of the different substrates was determined as indicated in "Materials and Methods". Each point represents the average of at least three data points (as indicated in "Materials and Methods"). Error bars indicate standard deviations (when not indicated standard deviation was less than the default minimum). The line fitting equations were obtained with the polinomial fitting (first order) of Criket Graph from Macintonsh. The experimental conditions are described in "Materials and Methods".

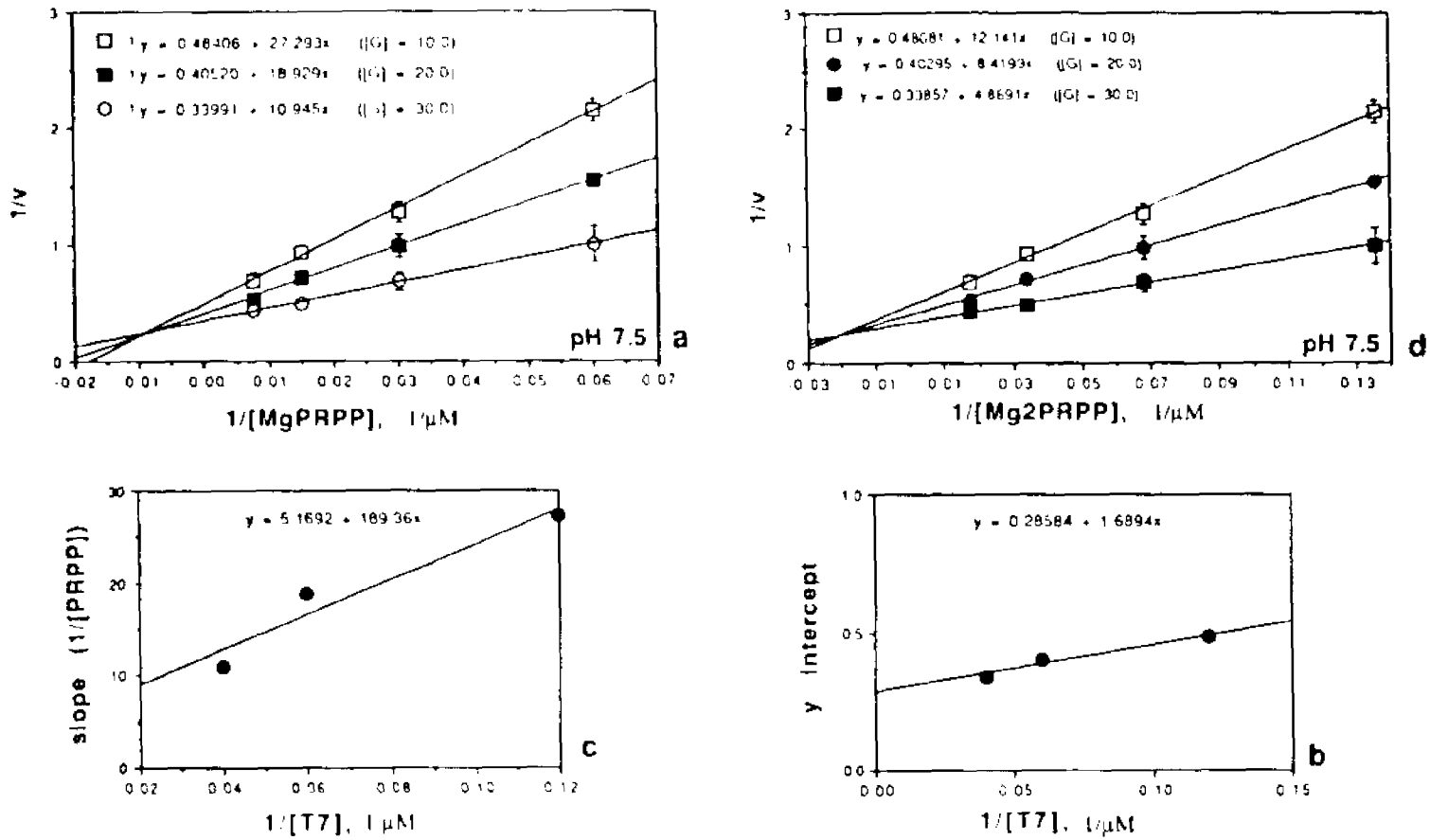

Fig. 27. Double reciprocal plots of the initial velocity of HGPRTase against the first substrate's concentration at various guanine concentrations and pH 7.5. **a**. These plots with Mg-PRPP as first substrate. **b**. Replot of the y intercepts of "**a**" against the reciprocal of the concentration of T-7. **c**. Replot of the slopes of "**a**" against the reciprocal of the concentration of T-7. **d**. These plots with Mg_2 PRPP as first substrate. The reaction rate (**v**) is defined as in Figure 17. The concentration of the different substrates was determined as indicated in "Materials and Methods". Each point represents the average of at least three data points (as indicated in "Materials and Methods"). Error bars indicate standard deviations (when not indicated standard deviation was less than the default minimum). The line fitting equations were obtained with the polinomial fitting (first order) of Cricket Graph from Macintonsh. The experimental conditions are described in "Materials and Methods".

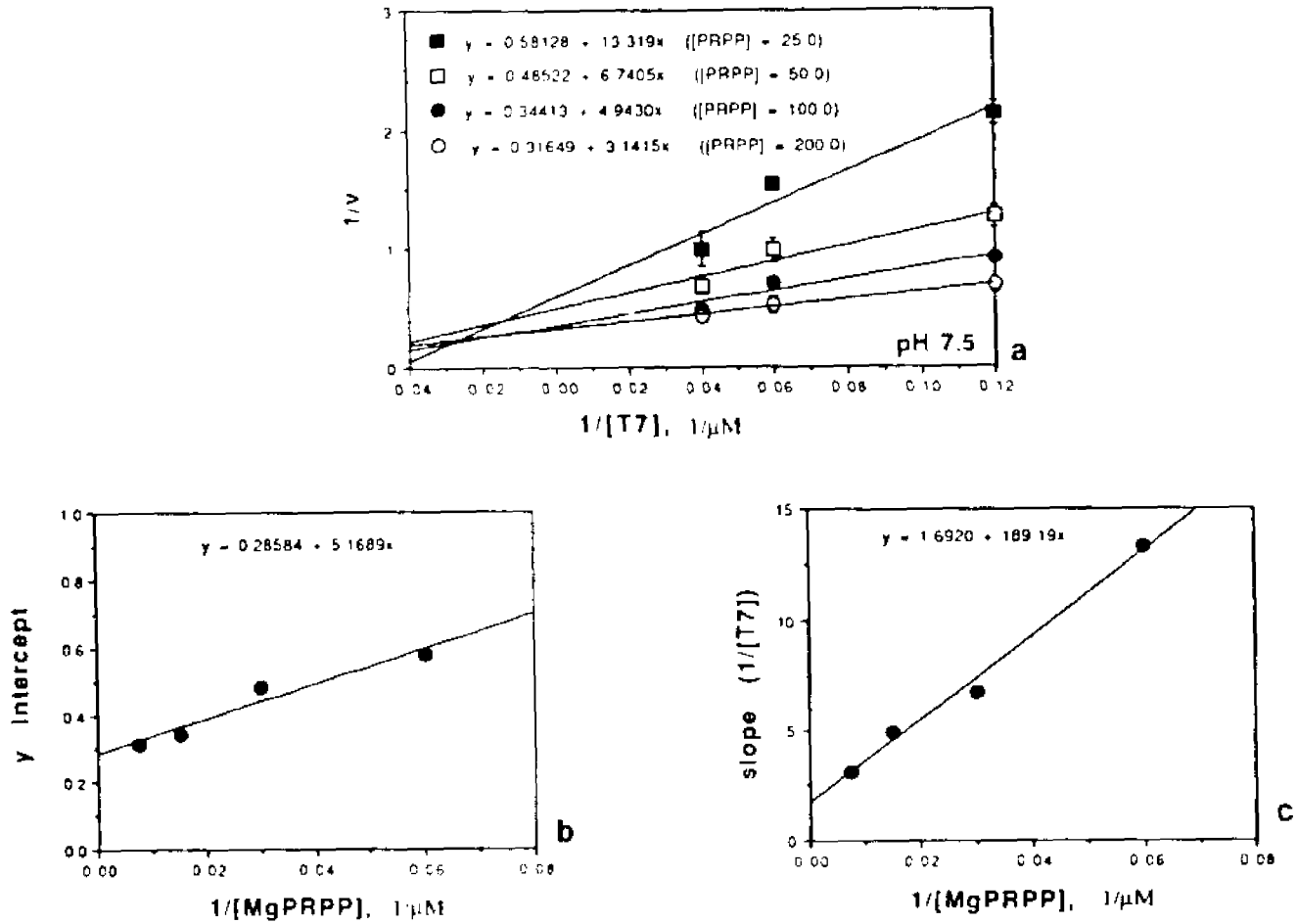

Fig. 28. Double reciprocal plots of the initial velocities of HGPRTase against the concentration of T-7 at various PRPP concentrations and pH 7.5 (**a**). **b**. Replot of the y intercepts of "**a**" against the reciprocal of the concentration of Mg-PRPP. **c**. Replot of the slopes of "**a**" against the reciprocal of the concentration of Mg-PRPP. The reaction rate (**v**) is defined as in Figure 17. The concentration of the different substrates was determined as indicated in "Materials and Methods". Each point represents the average of at least three data points (as indicated in "Materials and Methods"). Error bars indicate standard deviations (when not indicated standard deviation was less than the default minimum). The line fitting equations were obtained with the polinomial fitting (first order) of Criket Graph from Macintonsh. The experimental conditions are described in "Materials and Methods".

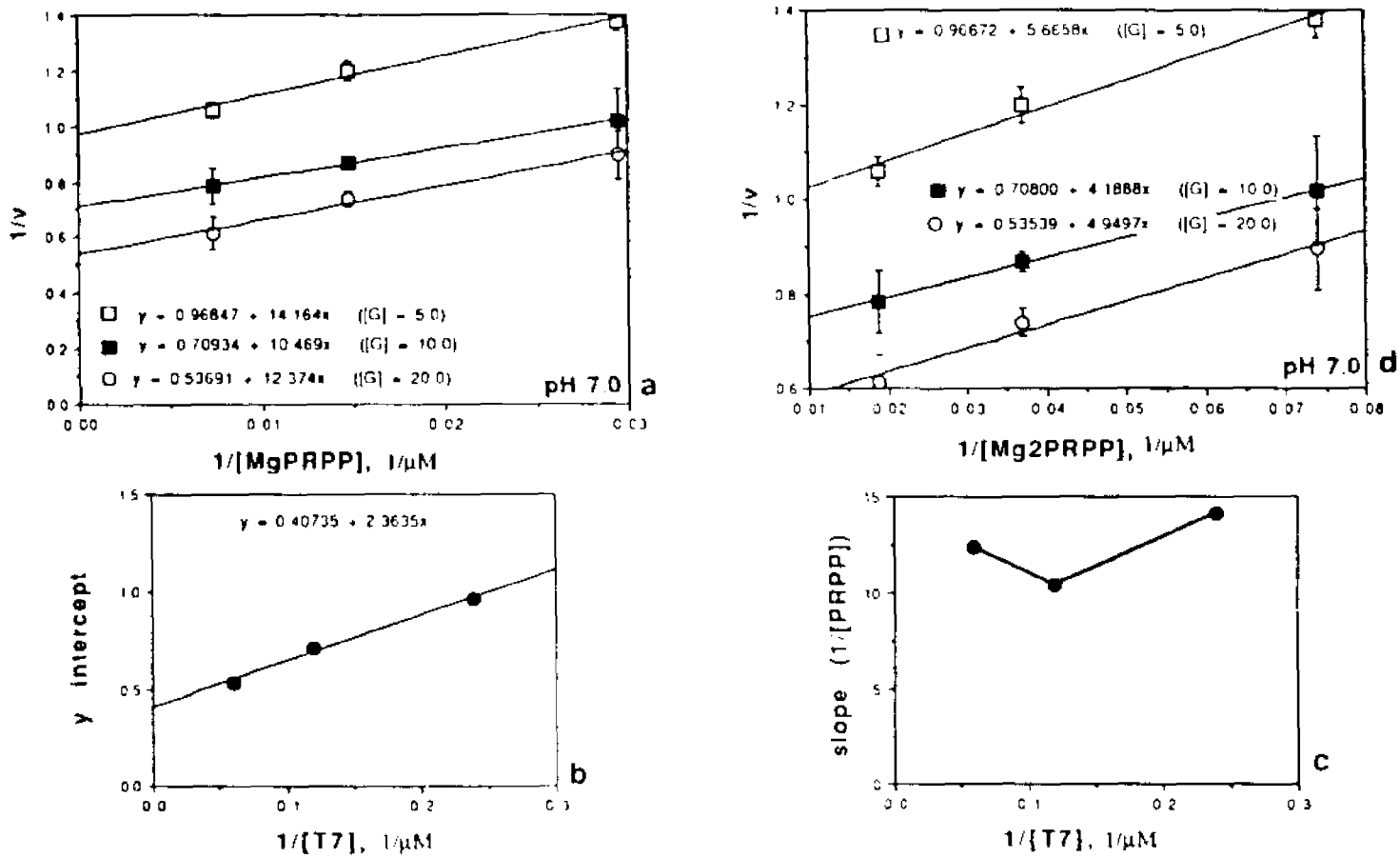

Fig. 29. Double reciprocal plots of the initial velocity of HGPRTase against the first substrate's concentration at various guanine concentrations and pH 7.0. **a**. These plots with Mg-PRPP as first substrate. **b**. Replot of the y intercepts of "**a**" against the reciprocal of the concentration of T-7. **c**. Replot of the slopes of "**a**" against the reciprocal of the concentration of T-7. **d**. These plots with Mg_2-PRPP as first substrate. The reaction rate (v) is defined as in Figure 17. The concentration of the different substrates was determined as indicated in "Materials and Methods". Each point represents the average of at least three data points (as indicated in "Materials and Methods"). Error bars indicate standard deviations (when not indicated standard deviation was less than the default minimum). The line fitting equations were obtained with the polinomial fitting (first order) of Cricket Graph from Macintonsh. The experimental conditions are described in "Materials and Methods".

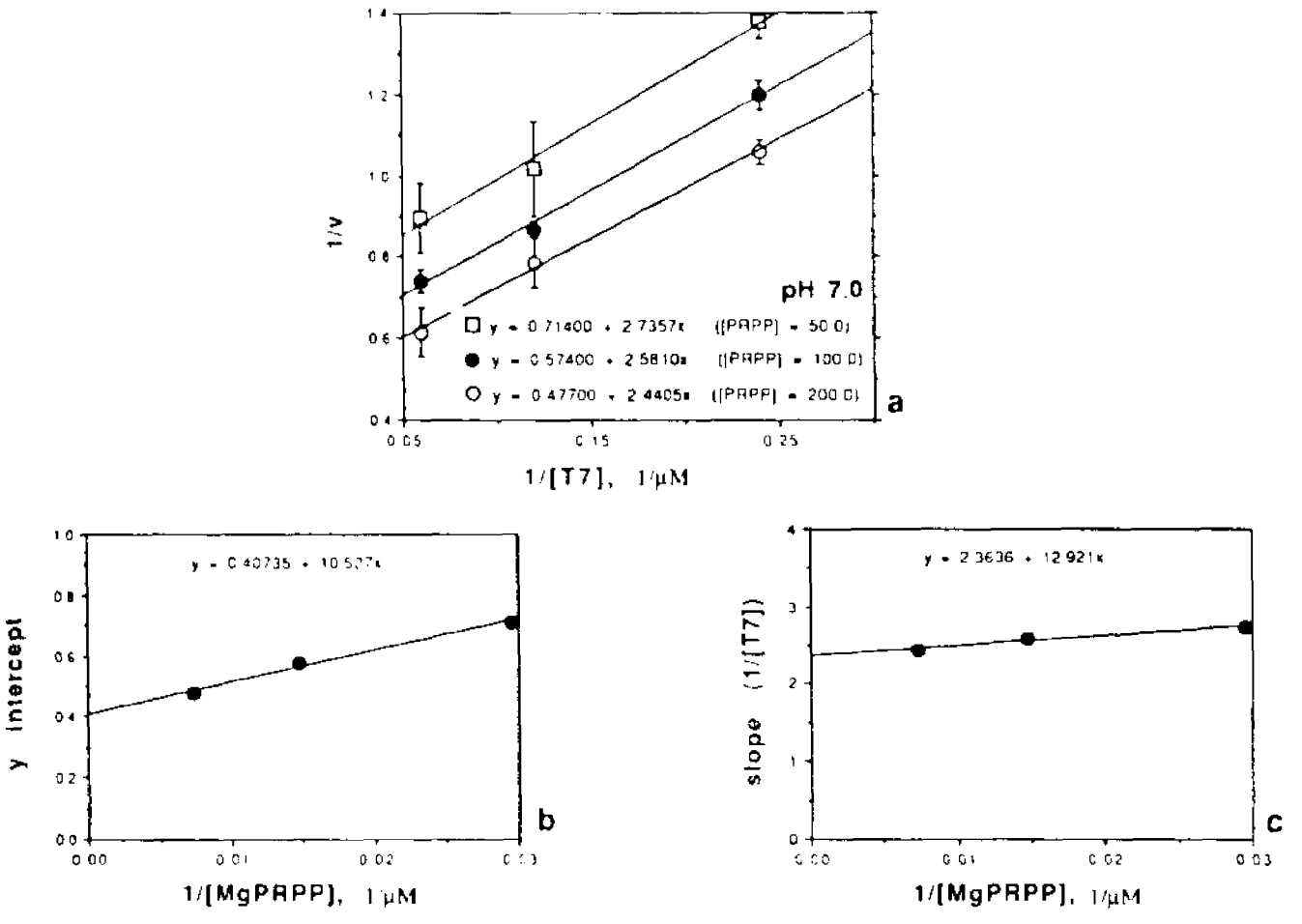

Fig. 30. Double reciprocal plots of the initial velocities of HGPRTase against the concentration of T-7 at various PRPP concentrations and pH 7.0 (**a**). **b**. Replot of the y intercepts of "**a**" against the reciprocal of the concentration of Mg-PRPP. **c**. Replot of the slopes of "**a**" against the reciprocal of the concentration of Mg-PRPP. The reaction rate (**v**) is defined as in Figure 17. The concentration of the different substrates was determined as indicated in "Materials and Methods". Each point represents the average of at least three data points (as indicated in "Materials and Methods"). Error bars indicate standard deviations (when not indicated standard deviation was less than the default minimum). The line fitting equations were obtained with the polinomial fitting (first order) of Criket Graph from Macintonsh. The experimental conditions are described in "Materials and Methods".

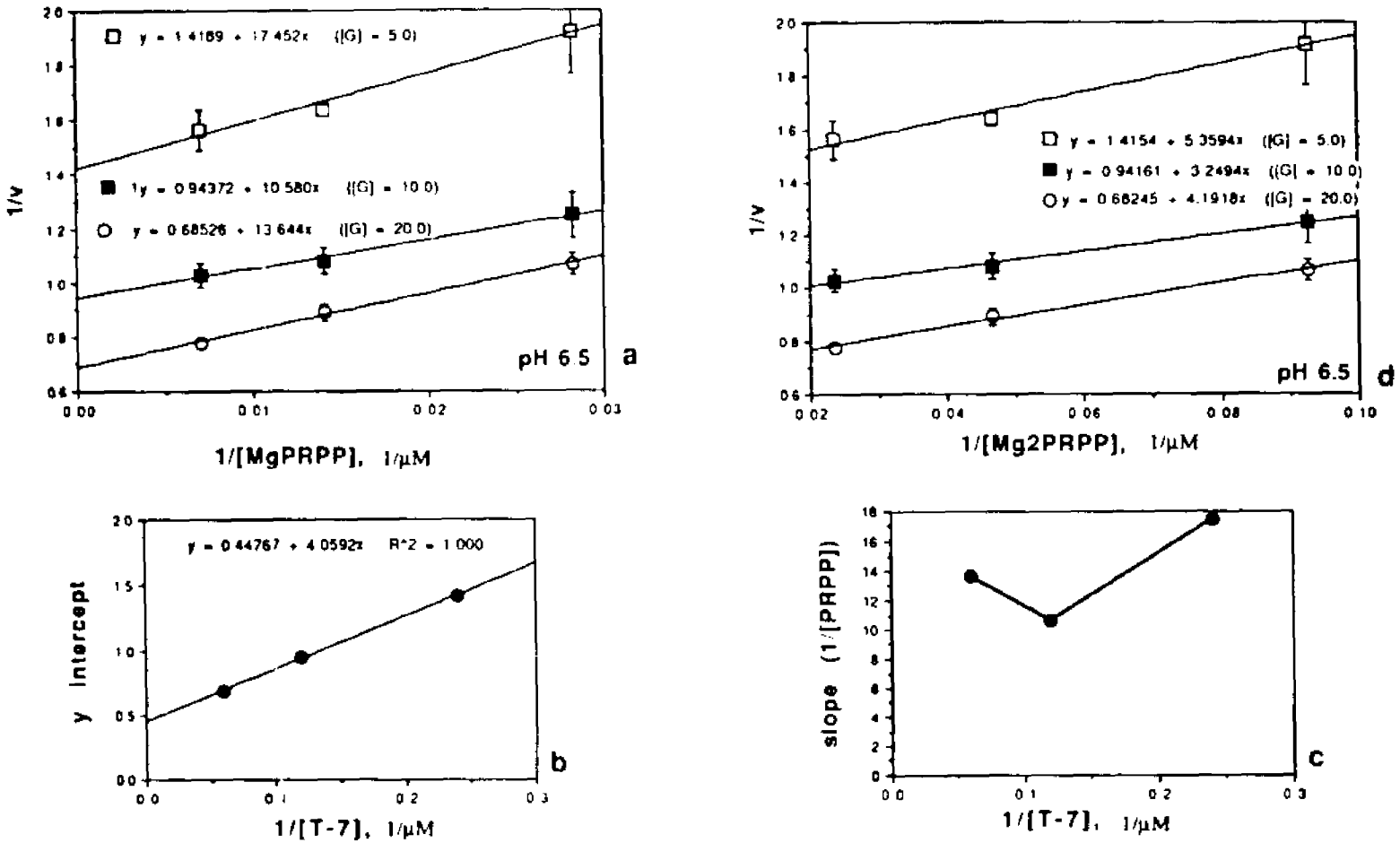

Fig. 31. Double reciprocal plots of the initial velocity of HGPRTase against the first substrate's concentration at various guanine concentrations and pH 6.5. **a**. These plots with Mg-PRPP as first substrate. **b**. Replot of the y intercepts of "**a**" against the reciprocal of the concentration of T-7. **c**. Replot of the slopes of "**a**" against the reciprocal of the concentration of T-7. **d**. These plots with Mg_2-PRPP as first substrate. The reaction rate (v) is defined as in Figure 17. The concentration of the different substrates was determined as indicated in "Materials and Methods". Each point represents the average of at least three data points (as indicated in "Materials and Methods"). Error bars indicate standard deviations (when not indicated standard deviation was less than the default minimum). The line fitting equations were obtained with the polinomial fitting (first order) of Criket Graph from Macintonsh. The experimental conditions are described in "Materials and Methods".

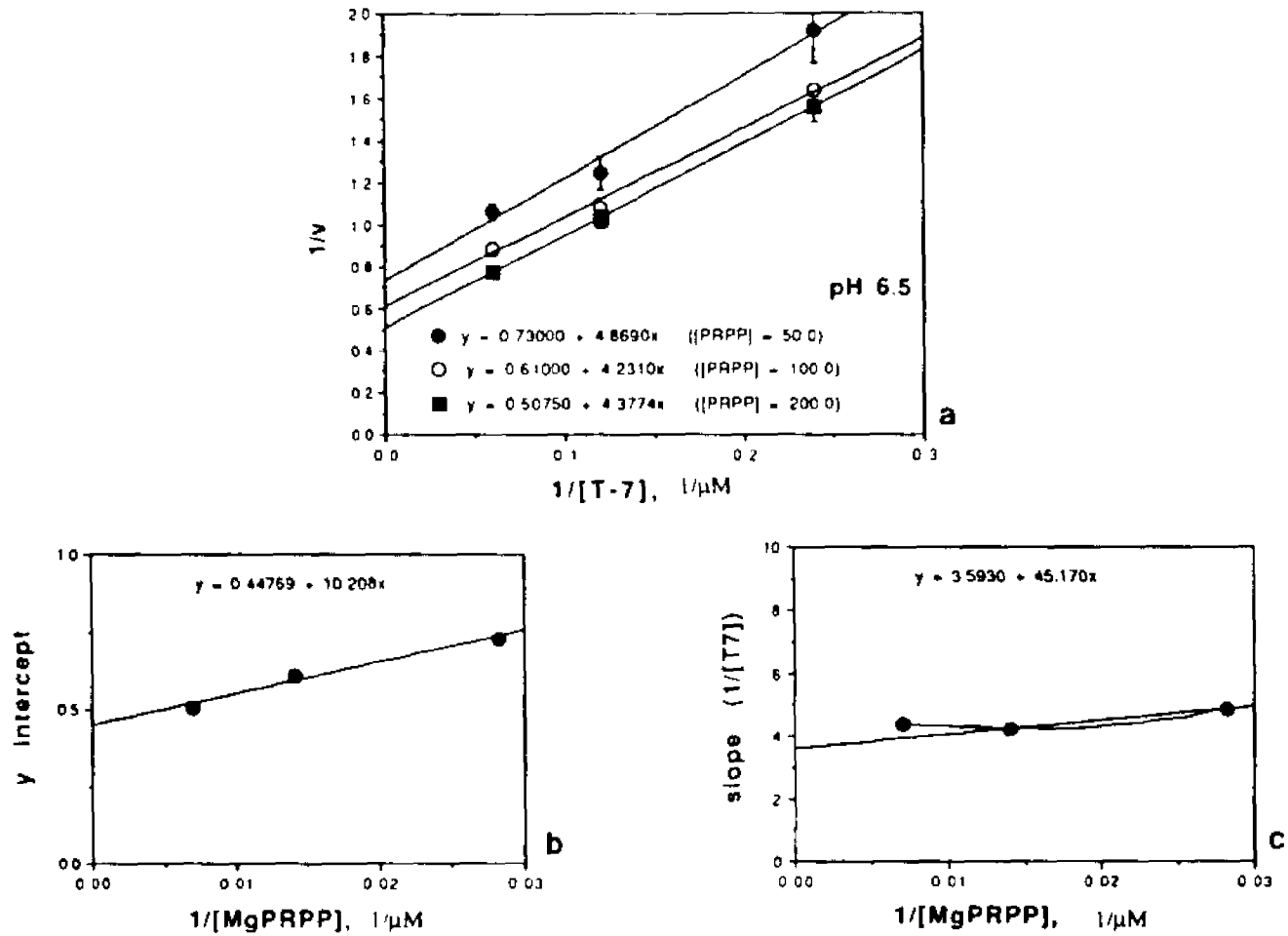

Fig. 32. Double reciprocal plots of the initial velocities of HGPRTase against the concentration of T-7 at various PRPP concentrations and pH 6.5 (**a**). **b**. Replot of the y intercepts of "**a**" against the reciprocal of the concentration of Mg-PRPP. **c**. Replot of the slopes of "**a**" against the reciprocal of the concentration of Mg-PRPP. The reaction rate (**v**) is defined as in Figure 17. The concentration of the different substrates was determined as indicated in "Materials and Methods". Each point represents the average of at least three data points (as indicated in "Materials and Methods"). Error bars indicate standard deviations (when not indicated standard deviation was less than the default minimum). The line fitting equations were obtained with the polinomial fitting (first order) of Criket Graph from Macintonsh. The experimental conditions are described in "Materials and Methods".

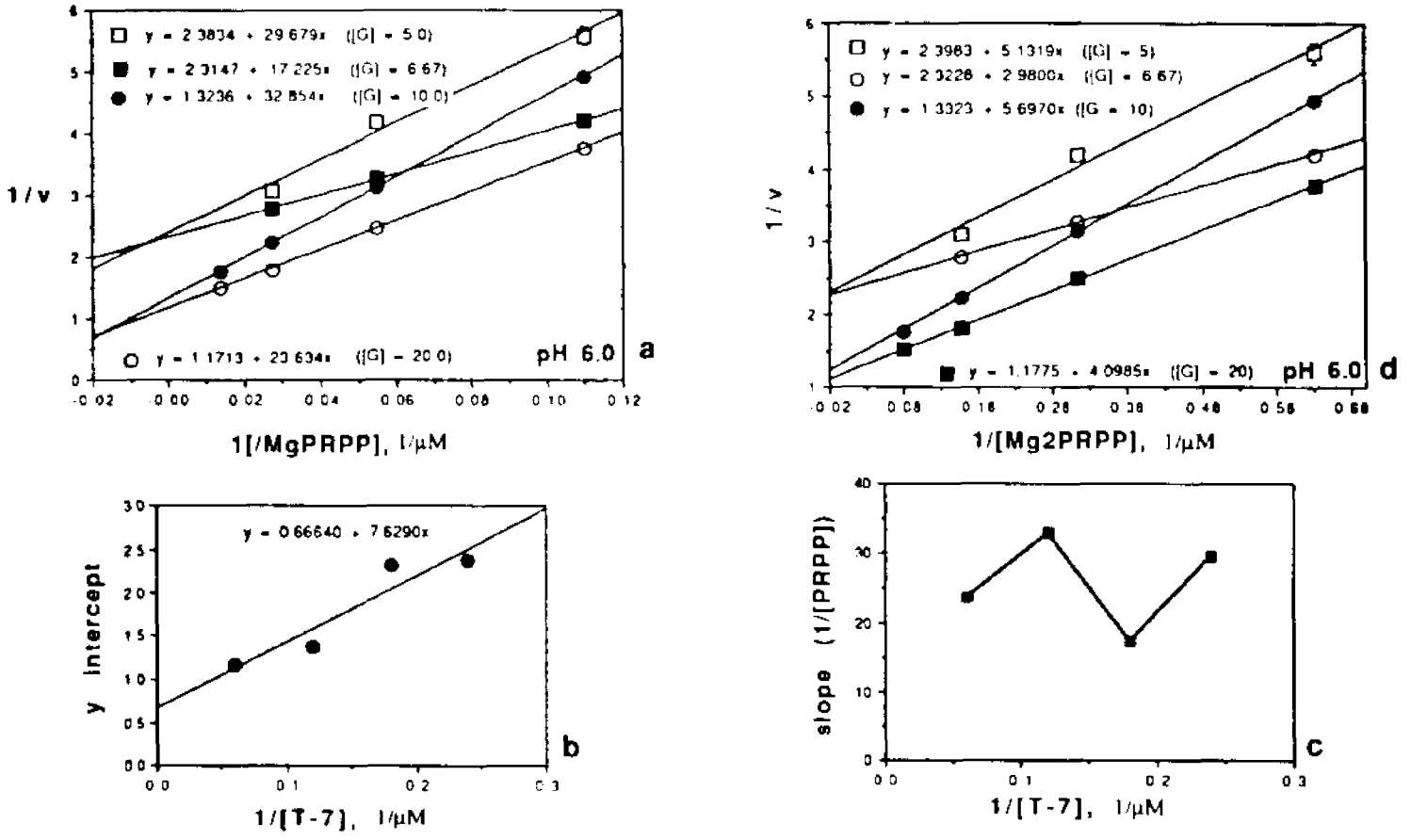

Fig. 33. Double reciprocal plots of the initial velocity of HGPRTase against the first substrate's concentration at various guanine concentrations and pH 6.0. **a**. These plots with Mg-PRPP as first substrate. **b**. Replot of the y intercepts of "**a**" against the reciprocal of the concentration of T-7. **c**. Replot of the slopes of "**a**" against the reciprocal of the concentration of T-7. **d**. These plots with Mg_2-PRPP as first substrate. The reaction rate (v) is defined as in Figure 17. The concentration of the different substrates was determined as indicated in "Materials and Methods". Each point represents the average of at least three data points (as indicated in "Materials and Methods"). Error bars indicate standard deviations (when not indicated standard deviation was less than the default minimum). The line fitting equations were obtained with the polinomial fitting (first order) of Criket Graph from Macintonsh. The experimental conditions are described in "Materials and Methods".

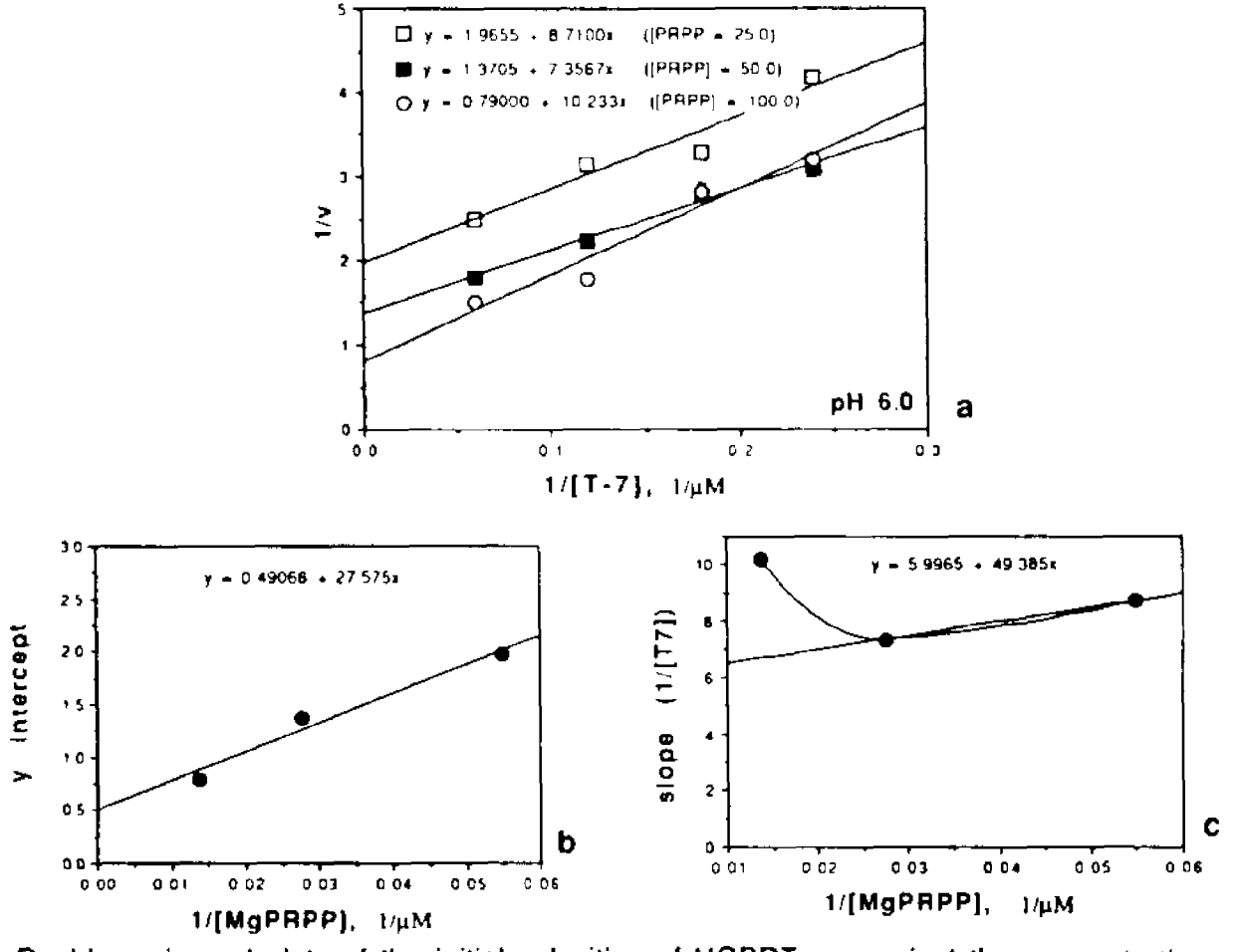

Fig. 34. Double reciprocal plots of the initial velocities of HGPRTase against the concentration of T-7 at various PRPP concentrations and pH 6.0 (a). **b**. Replot of the y intercepts of "a" against the reciprocal of the concentration of Mg-PRPP. **c**. Replot of the slopes of "a" against the reciprocal of the concentration of Mg-PRPP. The reaction rate (v) is defined as in Figure 17. The concentration of the different substrates was determined as indicated in "Materials and Methods". Each point represents the average of at least three data points (as indicated in "Materials and Methods"). Error bars indicate standard deviations (when not indicated standard deviation was less than the default minimum). The line fitting equations were obtained with the polinomial fitting (first order) of Cricket Graph from Macintonsh. The experimental conditions are described in "Materials and Methods".

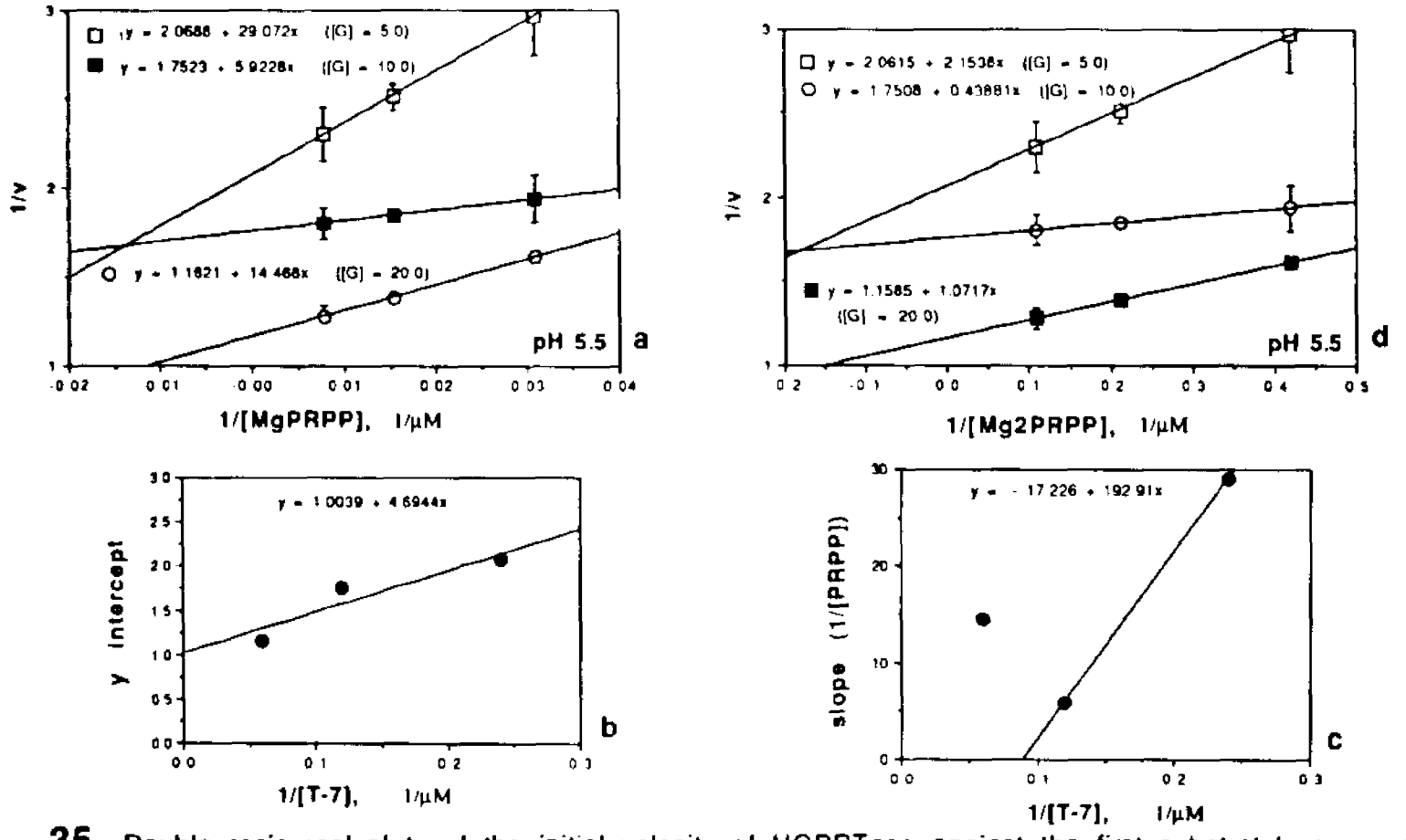

Fig. 35. Double reciprocal plots of the initial velocity of HGPRTase against the first substrate's concentration at various guanine concentrations and pH 5.5. **a**. These plots with Mg-PRPP as first substrate. **b**. Replot of the y intercepts of "**a**" against the reciprocal of the concentration of T-7. **c**. Replot of the slopes of "**a**" against the reciprocal of the concentration of T-7. **d**. These plots with Mg_2-PRPP as first substrate. The reaction rate (v) is defined as in Figure 17. The concentration of the different substrates was determined as indicated in "Materials and Methods". Each point represents the average of at least three data points (as indicated in "Materials and Methods"). Error bars indicate standard deviations (when not indicated standard deviation was less than the default minimum). The line fitting equations were obtained with the polinomial fitting (first order) of Criket Graph from Macintonsh. The experimental conditions are described in "Materials and Methods".

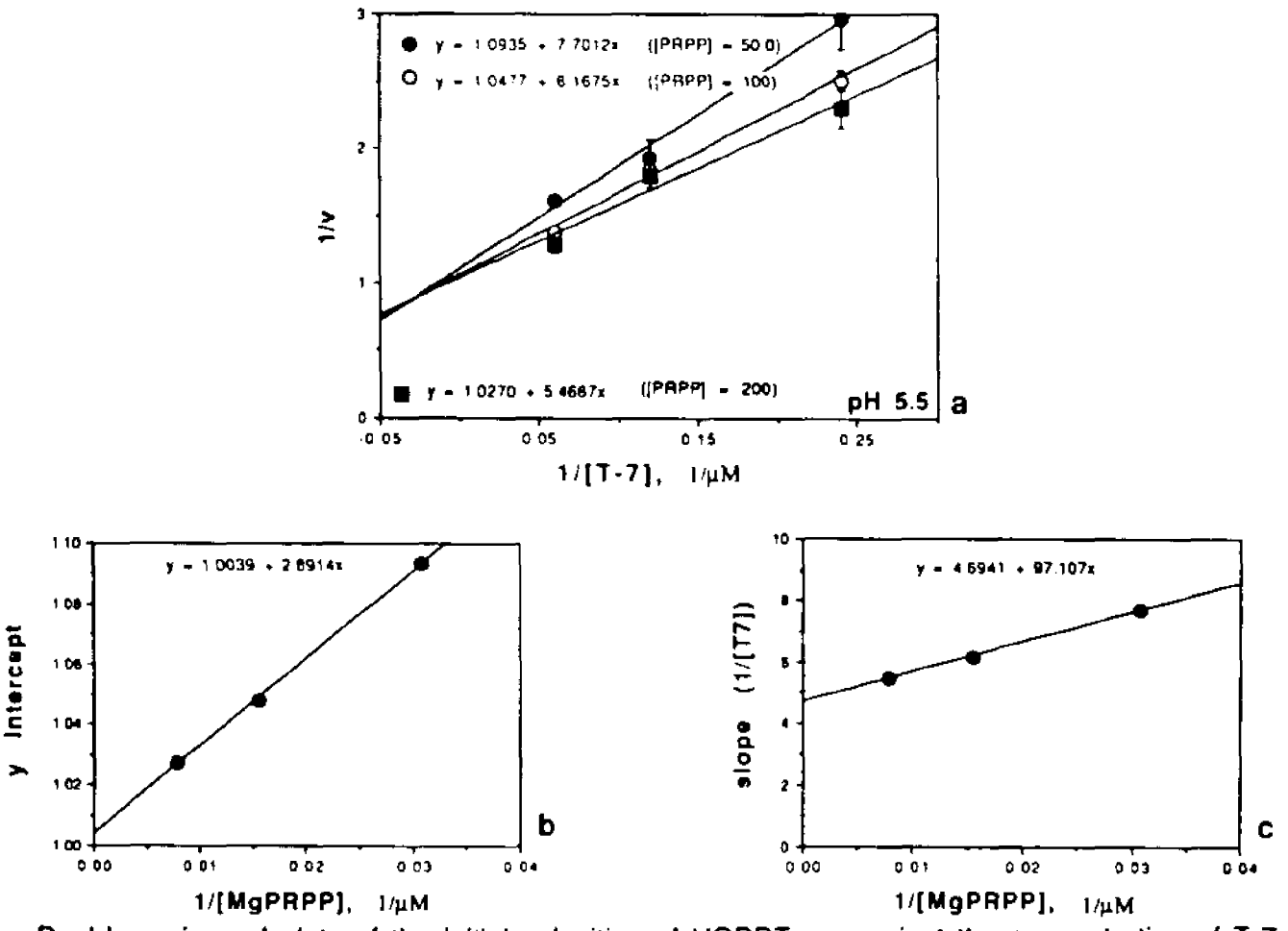

Fig. 36. Double reciprocal plots of the initial velocities of HGPRTase against the concentration of T-7 at various PRPP concentrations and pH 5.5 (**a**). **b**. Replot of the y intercepts of "**a**" against the reciprocal of the concentration of Mg-PRPP. **c**. Replot of the slopes of "**a**" against the reciprocal of the concentration of Mg-PRPP. The reaction rate (**v**) is defined as in Figure 17. The concentration of the different substrates was determined as indicated in "Materials and Methods". Each point represents the average of at least three data points (as indicated in "Materials and Methods"). Error bars indicate standard deviations (when not indicated standard deviation was less than the default minimum). The line fitting equations were obtained with the polinomial fitting (first order) of Criket Graph from Macintonsh. The experimental conditions are described in "Materials and Methods".

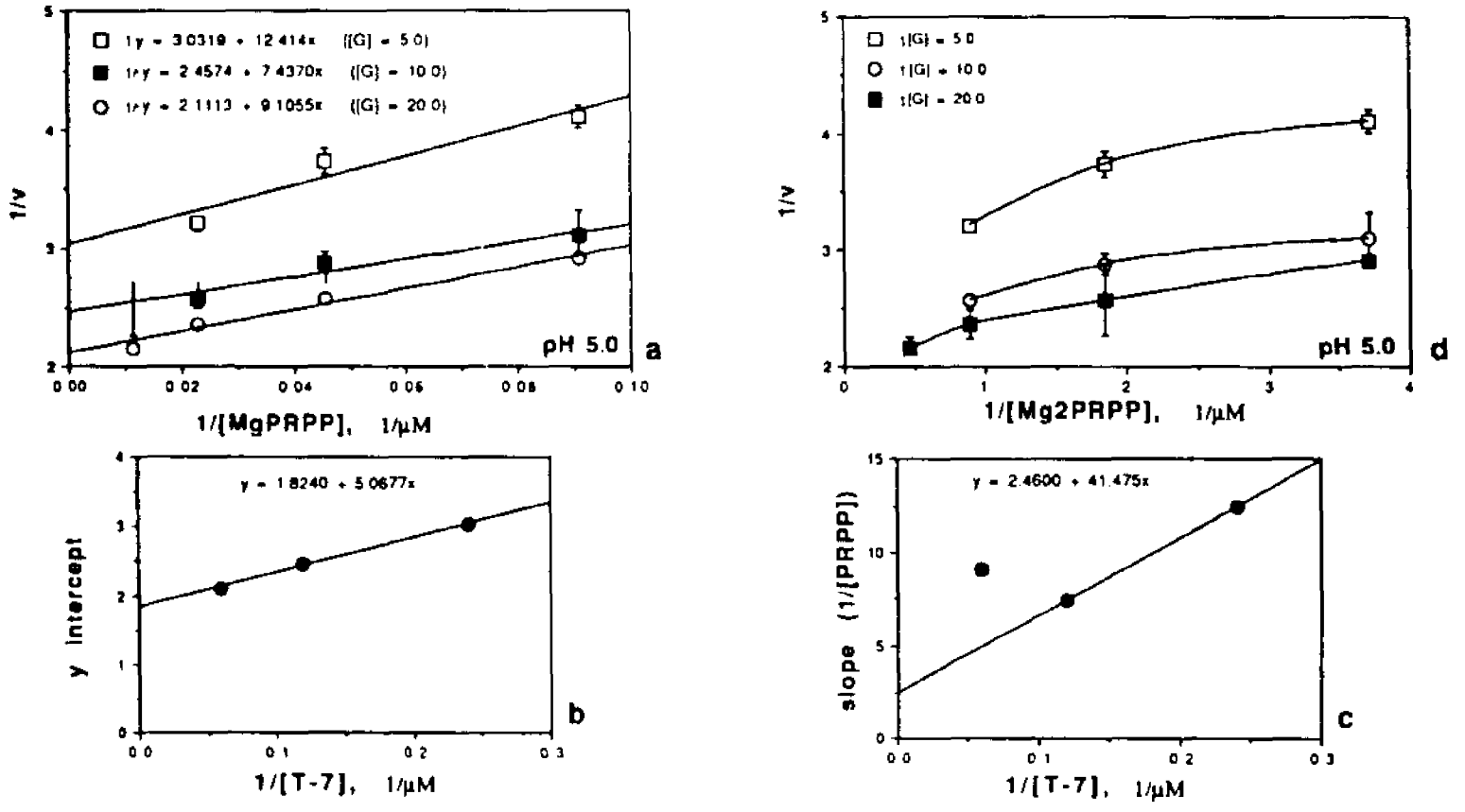

Fig. 37. Double reciprocal plots of the initial velocity of HGPRTase against the first substrate's concentration at various guanine concentrations and pH 5.0. **a**. These plots with Mg-PRPP as first substrate. **b**. Replot of the y intercepts of "**a**" against the reciprocal of the concentration of T-7. **c**. Replot of the slopes of "**a**" against the reciprocal of the concentration of T-7. **d**. These plots with Mg_2-PRPP as first substrate. The reaction rate (v) is defined as in Figure 17. The concentration of the different substrates was determined as indicated in "Materials and Methods". Each point represents the average of at least three data points (as indicated in "Materials and Methods"). Error bars indicate standard deviations (when not indicated standard deviation was less than the default minimum). The line fitting equations were obtained with the polinomial fitting (first order) of Criket Graph from Macintonsh. The experimental conditions are described in "Materials and Methods".

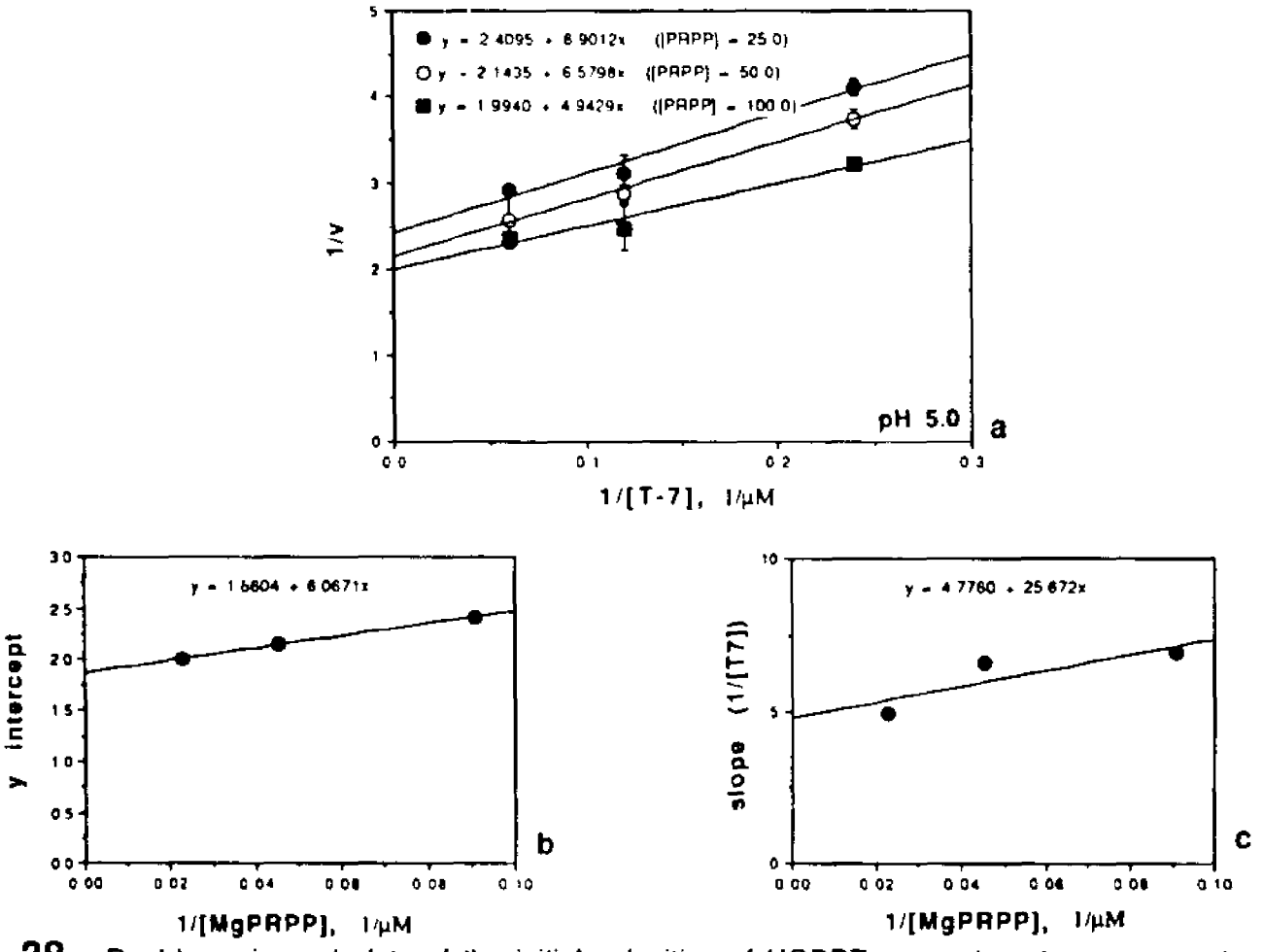

Fig. 38. Double reciprocal plots of the initial velocities of HGPRTase against the concentration of T-7 at various PRPP concentrations and pH 5.0 (**a**). **b**. Replot of the y intercepts of "**a**" against the reciprocal of the concentration of Mg-PRPP. **c**. Replot of the slopes of "**a**" against the reciprocal of the concentration of Mg-PRPP. The reaction rate (**v**) is defined as in Figure 17. The concentration of the different substrates was determined as indicated in "Materials and Methods". Each point represents the average of at least three data points (as indicated in "Materials and Methods"). Error bars indicate standard deviations (when not indicated standard deviation was less than the default minimum). The line fitting equations were obtained with the polinomial fitting (first order) of Criket Graph from Macintonsh. The experimental conditions are described in "Materials and Methods".

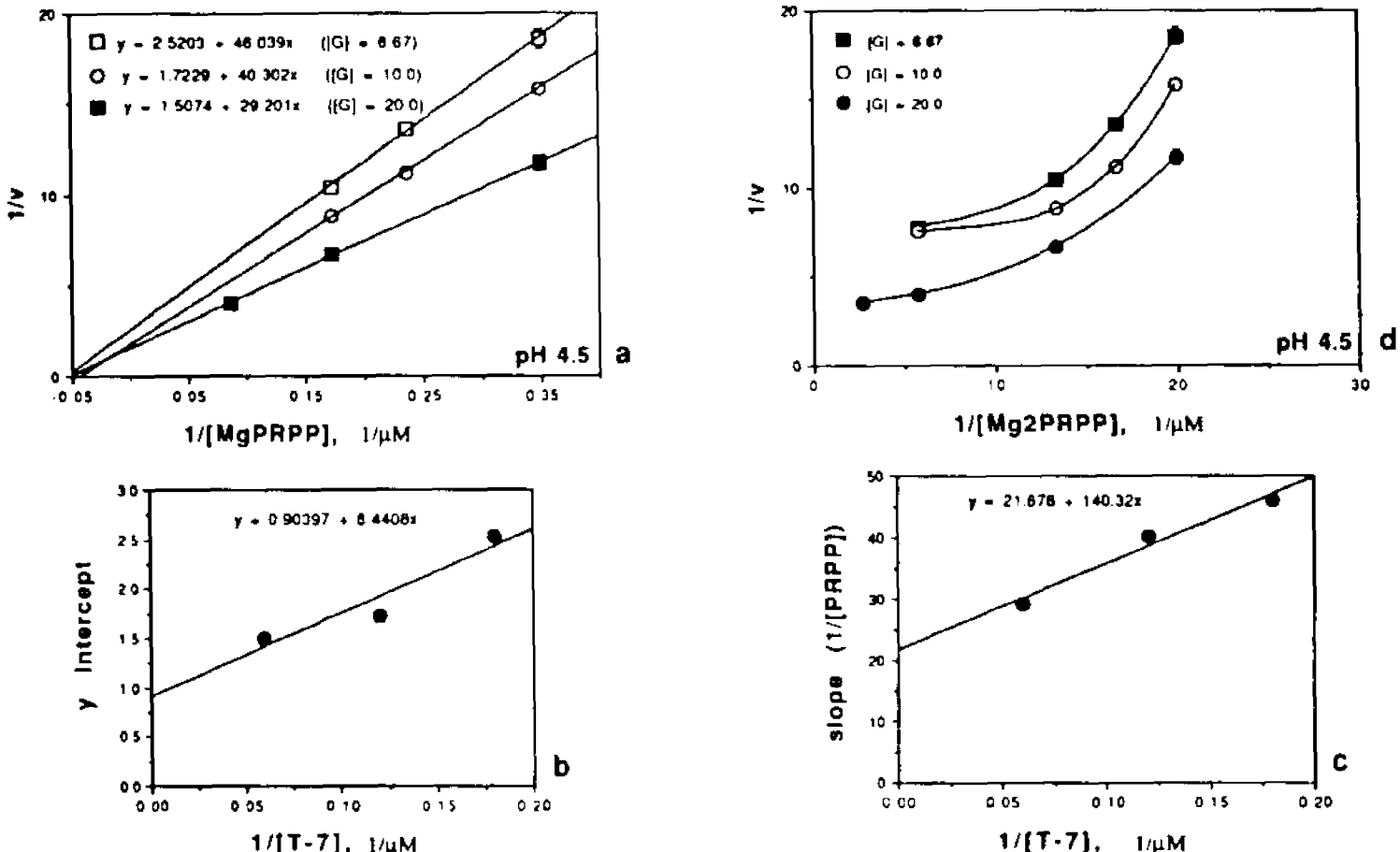

Fig. 39. Double reciprocal plots of the initial velocity of HGPRTase against the first substrate's concentration at various guanine concentrations and pH 4.5. **a**. These plots with Mg-PRPP as first substrate. **b**. Replot of the y intercepts of "**a**" against the reciprocal of the concentration of T-7. **c**. Replot of the slopes of "**a**" against the reciprocal of the concentration of T-7. **d**. These plots with Mg_2-PRPP as first substrate. The reaction rate (v) is defined as in Figure 17. The concentration of the different substrates was determined as indicated in "Materials and Methods". Each point represents the average of at least three data points (as indicated in "Materials and Methods"). Error bars indicate standard deviations (when not indicated standard deviation was less than the default minimum). The line fitting equations were obtained with the polinomial fitting (first order) of Criket Graph from Macintonsh. The experimental conditions are described in "Materials and Methods".

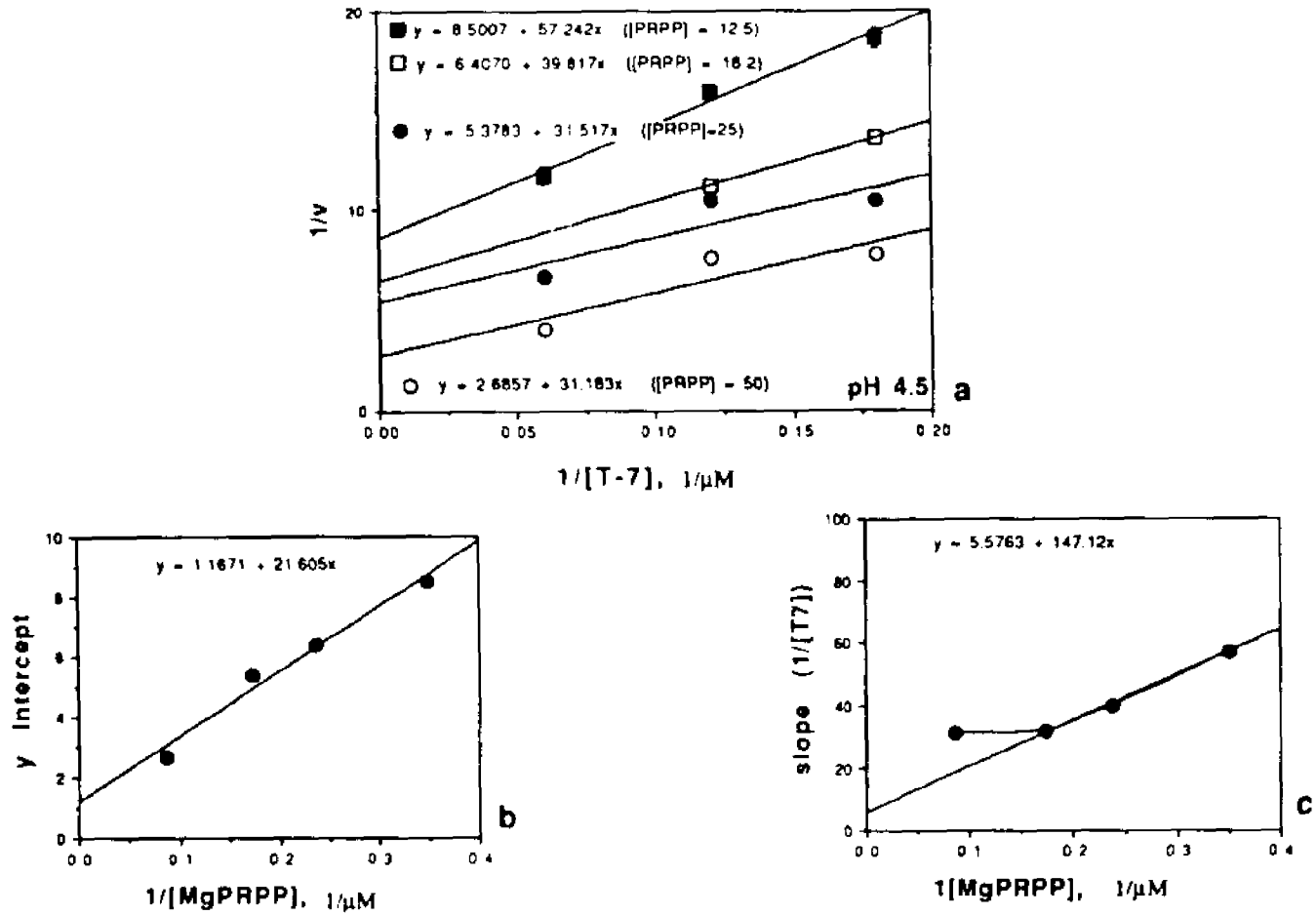

Fig. 40. Double reciprocal plots of the initial velocities of HGPRTase against the concentration of T-7 at various PRPP concentrations and pH 5.0 (**a**). **b**. Replot of the y intercepts of "a" against the reciprocal of the concentration of Mg-PRPP. **c**. Replot of the slopes of "a" against the reciprocal of the concentration of Mg-PRPP. The reaction rate (**v**) is defined as in Figure 17. The concentration of the different substrates was determined as indicated in "Materials and Methods". Each point represents the average of at least three data points (as indicated in "Materials and Methods"). Error bars indicate standard deviations (when not indicated standard deviation was less than the default minimum). The line fitting equations were obtained with the polinomial fitting (first order) of Criket Graph from Macintonsh. The experimental conditions are described in "Materials and Methods".

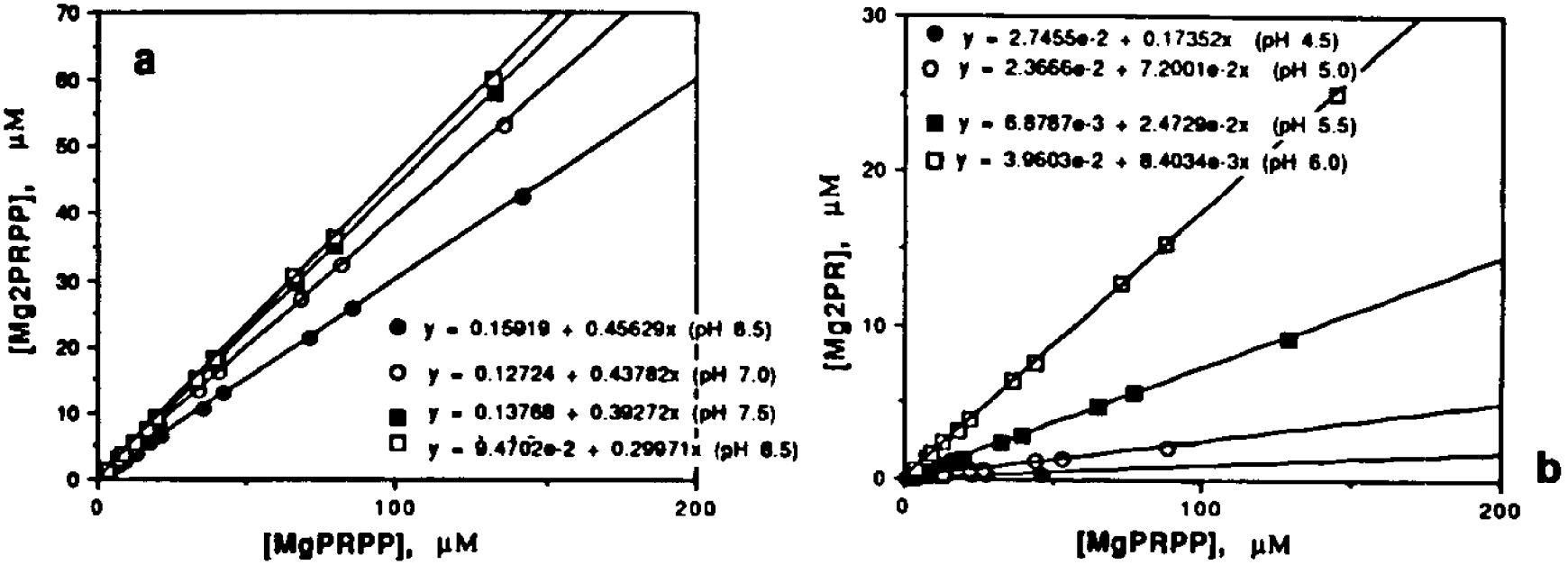

Fig. 41. Relationship between the equilibrium concentrations of Mg-PRPP and Mg_2-PRPP at various pH values. **a**. This relationship for pH range 8.5-6.5. **b**. This relationship for pH range 6.0-4.5. Obtained with the procedure described in "Materials and Methods"

TABLE VII

Kinetic Parameters of HGPRTase Evaluated at Various pH Values, Assuming an Ordered Bi-Bi with Second Substrate Inhibition Mechanism* Using Guanine as Second Substrate

pH	Vmax +	KmA #	KmB#	Kia#	Ki#
4.5	1.106	18.63	9.34	16.62	29.0
7.5	3.50	16.56	5.91	112.1	432.4
8.5	3.75	35.1	1.06	47.3	19.1

* Only those pH values at which this mechanism was apparent were evaluated.

+ Vmax as well as all velocity values in this study have units of hundreths of absorbance units at 257.5/min.

μM.

of the possible paths for the reaction is the preferred one.

Only the kinetic data corresponding to pH 4.5, 7.5 and 8.5 were suitable for calculations based on the second substrate inhibition ordered Bi-Bi scheme (low [B]). These parameters were calculated as an illustration and to obtain approximate values of those parameters at extreme pH values. These calculations were made taking Mg-PRPP as first substrate and T-7 as the second substrate, while both T-7 and T-9 were assumed inhibitors (see Table VII). Any interpretation drawn from the apparent variations of these parameters with varying pH is bound to be erroneous due to the fact that the simplification of the scheme does not take into account the many factors involved in the process (see "Discussion").

Alternate Substrates And Inhibitors

Enzyme Stability

The crude extract of HGPRTase showed no apparent loss of activity when treated for 5 min at 50°C, 60°C and 70°C, but a significant loss was observed at 80°C. The purified enzyme was very stable at room temperature showing no apparent loss of activity over 12 hr. Figure 42 shows these observations for 1 hr.

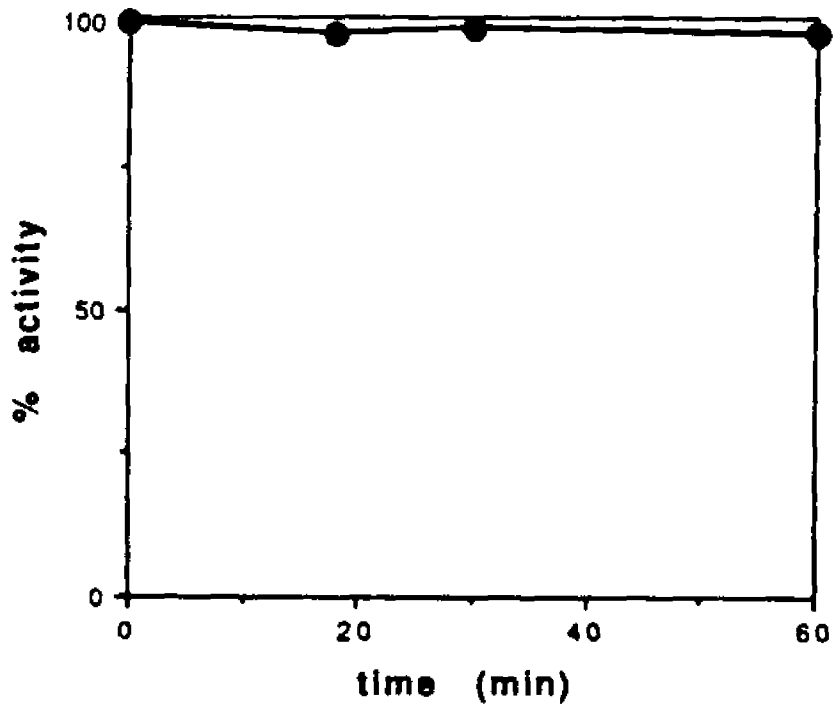

Fig. 42. Temperature stability of HGPRTase. The activity was tested at room temperature (28°C) for at least 12 hrs. Only one hour is shown in this experiment. The activity was defined as hundreths of absorbance units at 257.5 *nm* per min. The concentration of PRPP and guanine employed were 1 mM and 100 µM respectively. The experimental conditions are described in "Materials and Methods".

Mercuric Ion Inhibition

As can be seen in Table VIII the preliminary study of the inhibition of HGPRTase by Hg^{+2} indicated that the effect is quite strong. The enzyme was modified, losing up to 94% of its activity, although a kinetic inhibition effect was also apparent (compare the two control experiments in Table VIII). It was also evident that the inactivation is partially reversed by the presence of mercaptoethanol. This was observed both with the direct incubation of the reaction mixture with mercaptoethanol (see Table VIII) as well as when the mixture was dialysed against mercaptoethanol, in this case up to 66% of the original activity was recovered after two hours of dialysis (see Figure 43b). The time-dependence of the inactivation with Hg^{+2} shows two phases, a fast phase that lasts about 5 min and a slow one that is made appparent after 10 min of incubation (see Figure 43a). When the kinetics of inactivation was investigated further the inactivation shows a first order kinetics with varying [Hg^{+2}] (see Figure 43c).

Fosfomycin Study

The antibiotic fosfomycin has been used to irreversibly inhibit the enzyme p-enolpyruvate-UDP-GlcNac-3-O-enolpyruvyltransferase (pyruvyltransferase) (132,133). Later, Kahan and Cassidy (134) showed that this inhibition was due to the chemical modification of a specific cysteine residue of the enzyme by fosfomycin. Since an irreversible inhibition of HGPRTase activity by Hg^{+2} has been observed, a cysteine residue might be involved in the activity of the enzyme, thus making fosfomycin a

TABLE VIII

Effect of Mercuric Ion on HGPRTase Activity

Treatment *		% Activity
1.	Control	100
2.	50 mM $HgCl_2$, 30 min ($[Hg^{+2}]$ = 0.1mM in assay)	6.2
3.	Control + $HgCl_2$ (0.1 mM) in assay	82
4.	Treatment 2 followed by 0.06 mM ME** (10 min)	29
5.	Treatment 4 after 1 hr	37
6.	Treatment 4 after 2 hr	40

* The assay procedures and conditions are described in "Materials and Methods".

** Mercaptoethanol

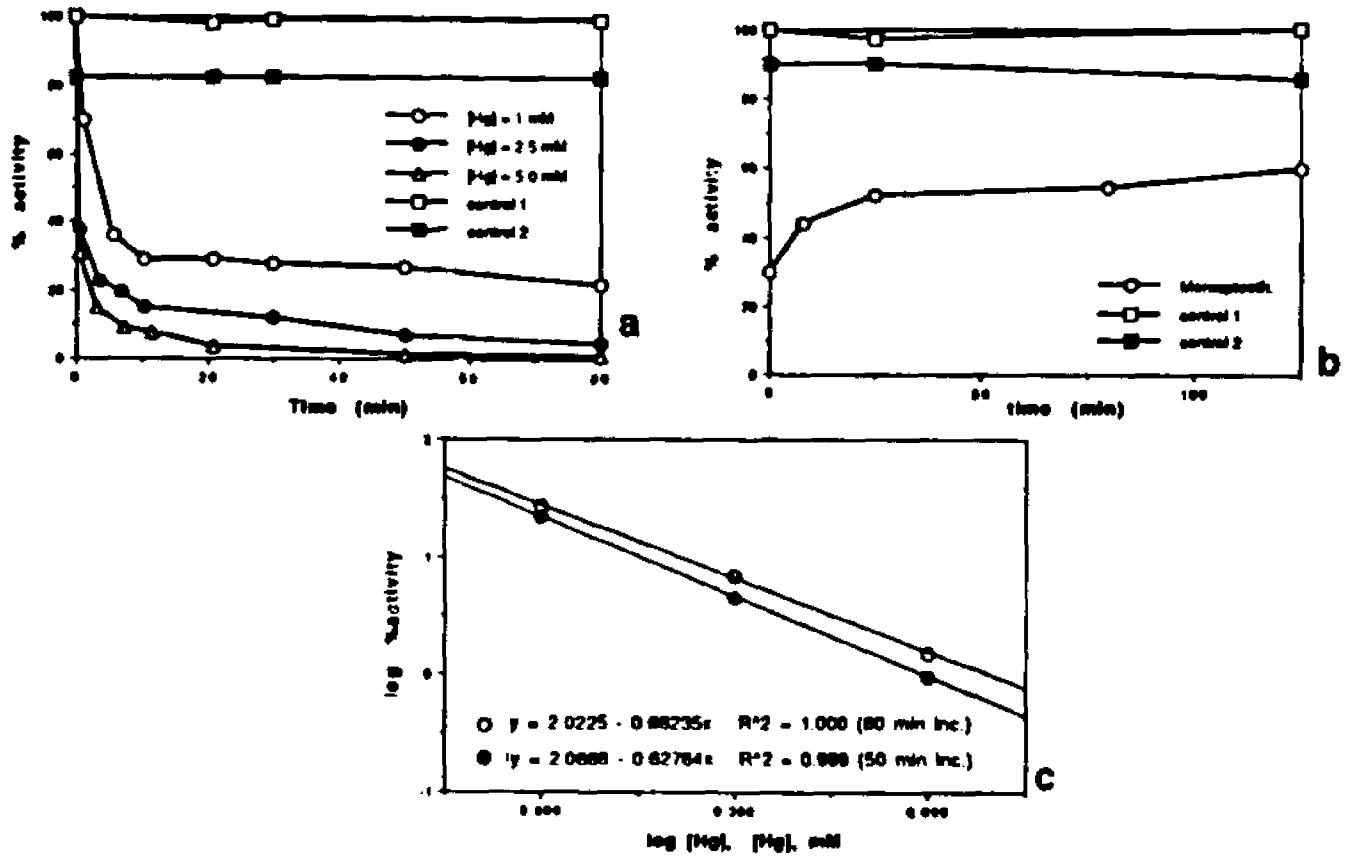

Fig. 43. Effect of mercuric ion on the activity of HGPRTase. a. Time dependence of the inactivation of HGPRTase by various concentrations of Hg^{+2}. b. Recovery of the activity of mercury-inactivated HGPRTase after dialysis against a solution of mercaptoethanol. c. Logarithmic plot of the % remaining activity against mercury concentration at two different moments of the inactivation reaction. Circles, after 50 min inactivation. Solid circles, after 80 min inactivation. The activity is defined as hundrieths of absorbance units per min. Line fitting was done as in Figure 25. Experimental conditions are described in "Materials and Methods".

candidate for chemical modification studies of HGPRTase. However, as shown in Figure 44, fosfomycin caused no apparent inhibition on the enzyme.

Alternate Substrate/Xanthine-Analog Inhibition Study

Of the alternate substrates tested only xanthine proved to be a substrate for HGPRTase, although with very slow turnover as compared to guanine (Figure 45). Adenine, caffeine and 3-methylxanthine showed no apparent product formation over a period of 12 hr in the conditions employed in this experiment (Figures 45b, 45d and 45e).

The inhibitory effect of these bases on HGPRTase was also investigated. Figure 46 shows the effect of xanthine, 3-methylxanthine and caffeine, respectively, on the double-reciprocal plot of HGPRTase against guanine. Interestingly, the inhibition seems to be of mixed characteristics for all of them. This effect was investigated further for caffeine at low (200 μM) and high (1000 μM) PRPP concentration, covering two ranges of caffeine concentration (see Figure 47). As can be seen in Figure 46c and 47a, at a high PRPP concentration (Figure 46c) the inhibition by caffeine has a noncompetitive character (although mixed), while at low PRPP concentration (Figure 47a) the inhibition is clearly uncompetitive. If the caffeine concentration is raised (Figure 47b), the noncompetitive characteristic reappears.

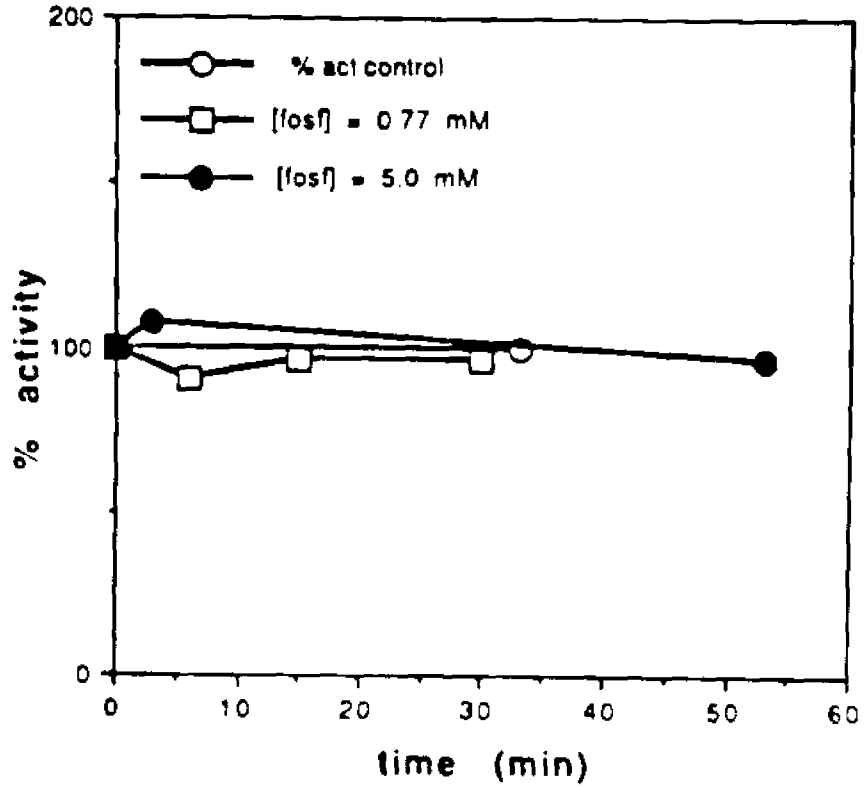

Fig. 44. Effects of fosfomycin on the activity of HGPRTase. The activity is defined hundrieths of absorbance units per min. The experimental conditions are described in "Materials and Methods.

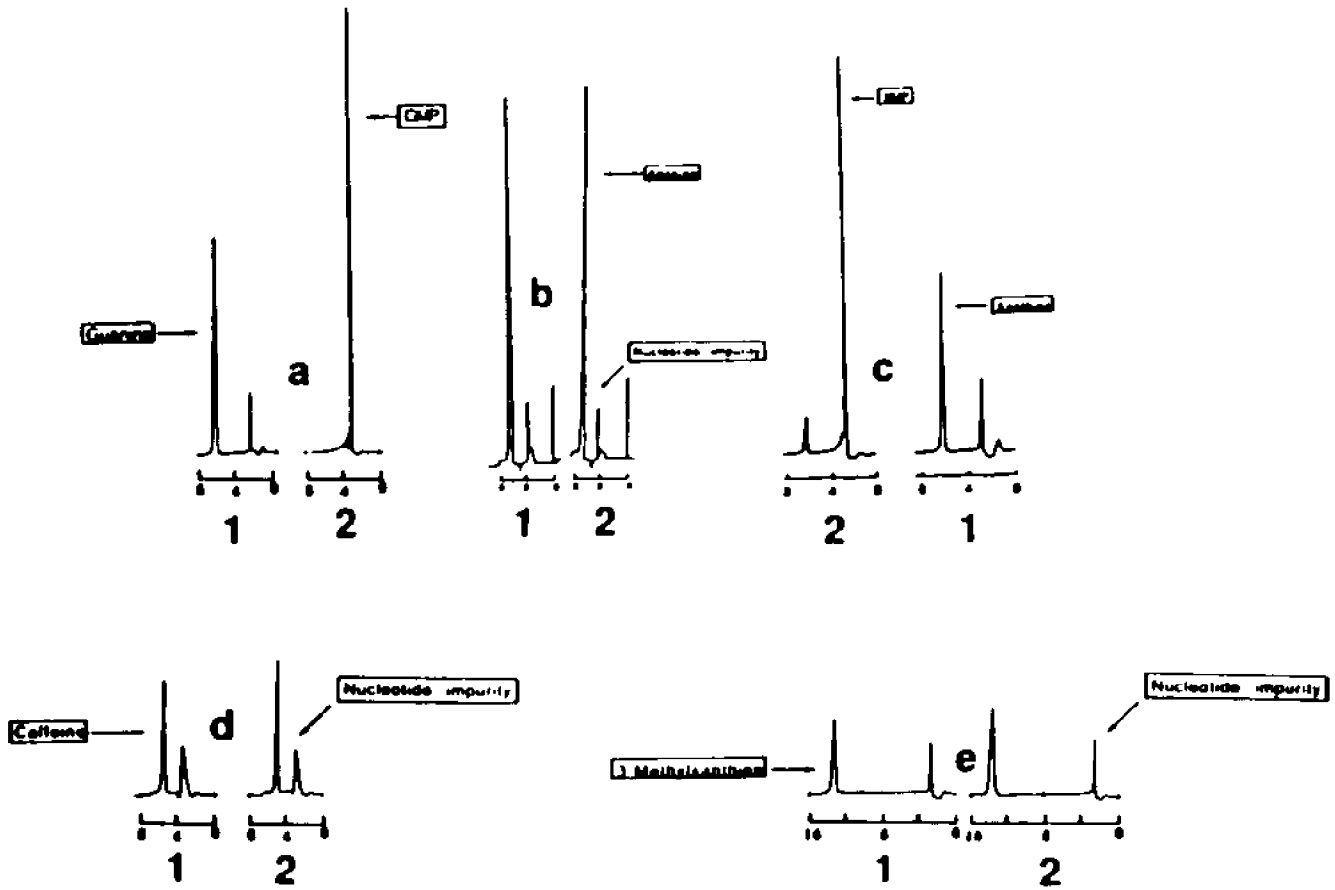

Fig. 45. HPLC elution profile of the HGPRTase assay solution containing different purine derivatives as second substrate. **a**. Guanine as second substrate. **b**. Adenine as second substrate. **c**. Xanthine as second substrate. **d**. Caffeine as second substrate. **e**. 3-Methyl-xanthine as second substrate. The 1 ml reaction mixture was composed of 50 mM Tris-HCl (pH 7.5), 10mM $MgCl_2$,1 mM PRPP, 100 µM of the appropriate second substrate and HGPRTase (activity = 0.1 mM guanine utilized/min). The reaction mixture was incubated for 12 hours at room temperature and then 10 µl was injected onto a reverse phase column and eluted using 10% methanol/water. The elution rate was 1 ml/min. The control (same reaction mixture in the absence of the enzyme) is indicated with 1, and the 12-hour incubation aliquot with 2. Vertical = Absorbance at 254. Horizontal = Elution time (min). The experimental procedure is described in "Materials and Methods".

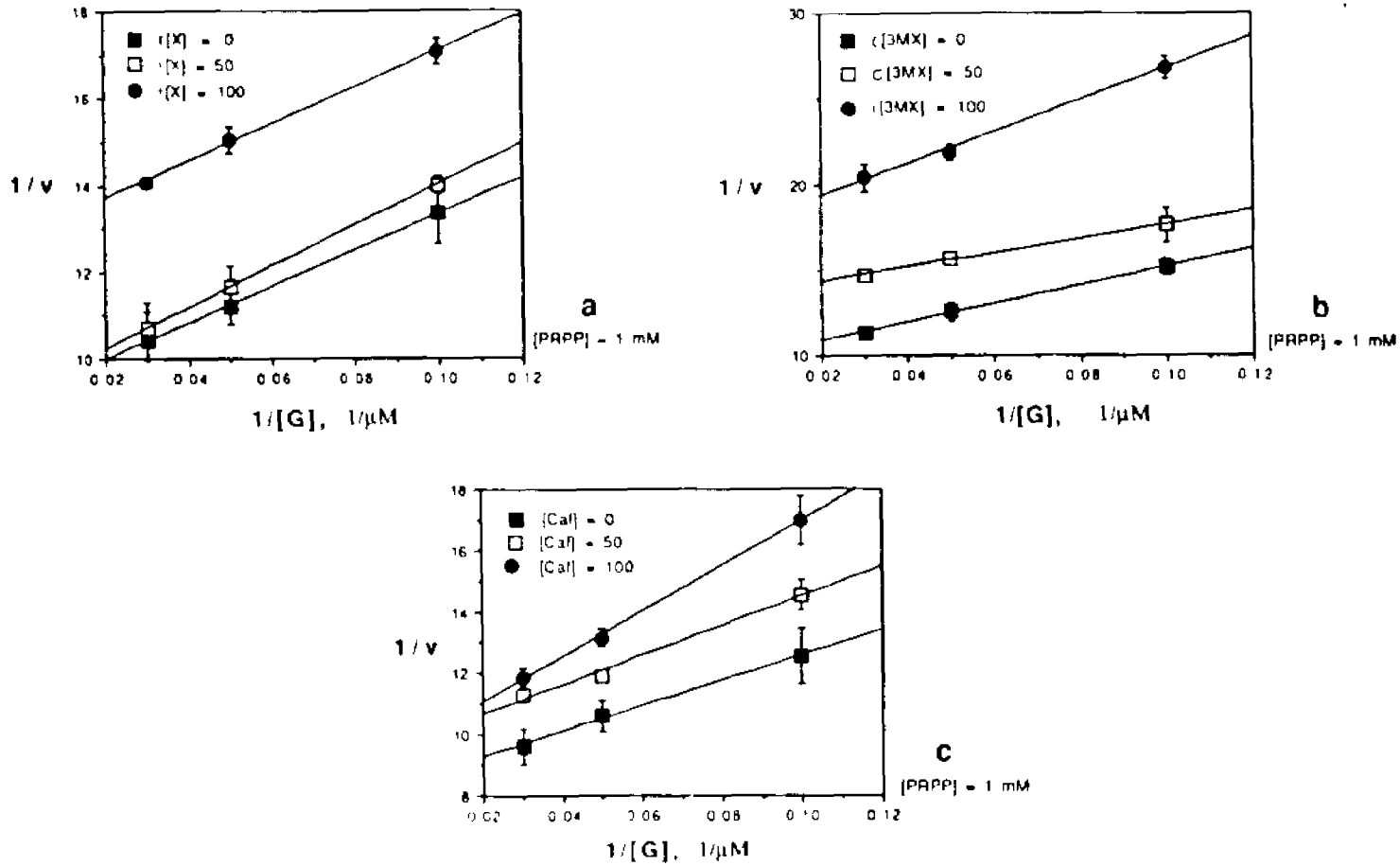

Fig. 46. Double reciprocal plots of the initial velocity of HGPRTase against guanine concentration at pH 7.5 and [PRPP] 1 mM, in the presence of different methylated xanthine derivatives. **a**. These plots in the presence of various concentrations of Xanthine. **b**. These plots in the presence of various concentrations of 3-methyl-xanthine. **c**. These plots in the prsence of various concentrations of caffeine. Velocities are defined as Hundrieths of absorbance units per min. All concentrations reffer to μM. The experimental conditions are described in "Materials and Methods".

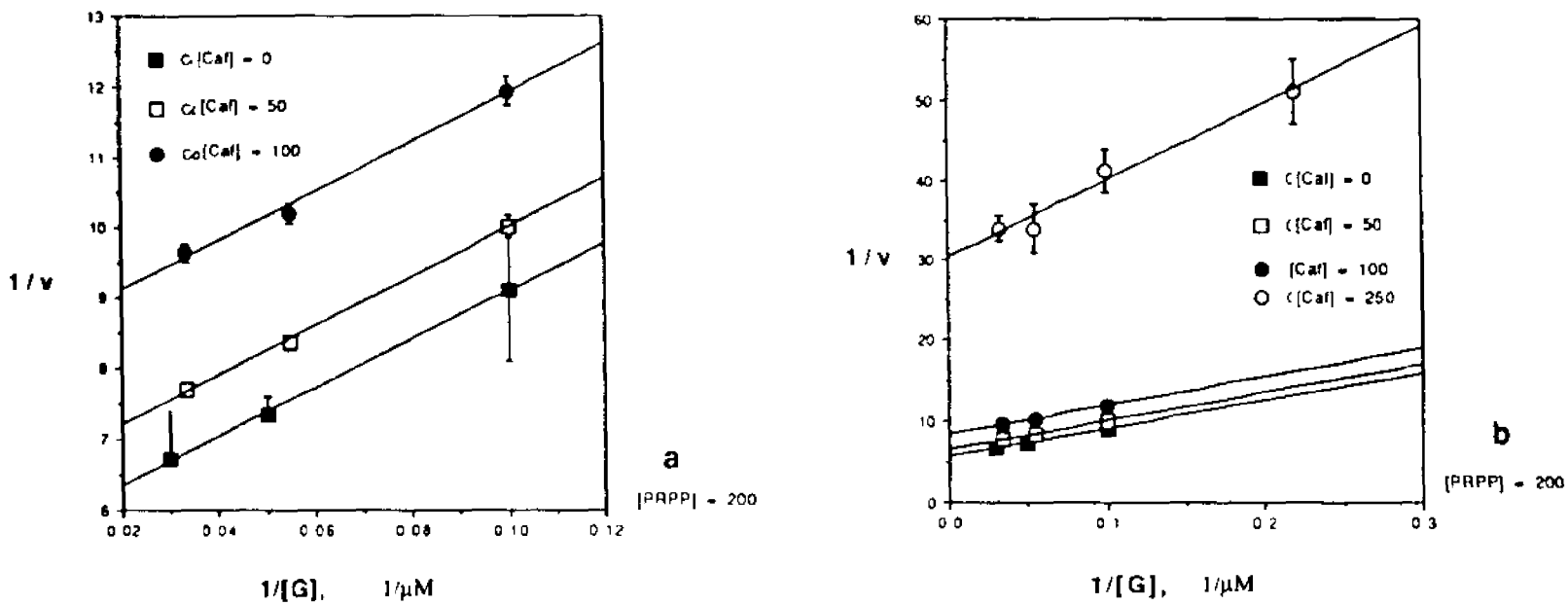

Fig. 47. Variation of caffeine inhibition pattern against HGPRTase at two different caffeine concentration ranges at pH 7.5 and [PRPP] = 200 μM. **a.** Double reciprocal plots of the initial velocity against guanine concentration at [caf] range 0-100 μM. **b.** The same as "**a**" at [caf] range 0-250 μM. Comparison of "**a**" and "**b**" with Figure 46c shows the variation of the inhibition pattern when [PRPP] is varied. Velocities are defined as hundrieths of absorbance units per min.

Discussion

On the Salt-Burst Procedure

The salt-burst elution HPLC procedure takes advantage of the dynamics of a rapid nonequilibrium desorption of macromolecules when suddenly exposed to a higher ionic strength medium. As is well known, the distribution of surface charge and the shape of protein molecules depends on the pH of the medium. Protein molecules have a high capacity for hydrogen bonding, which is highly affected by the pH and the ionic strength of the medium. Thus if a suspension containing several different proteins is bound to the surface of an ion exchange bed, a sudden increase of the ionic strentgh of the liquid phase will start the process of detachment of a group of those proteins (which proteins will detach at that particular ionic strentgh and pH depends on the factors mentioned above), even though (if this ionic strength is maintained for a suffiently long time) all the proteins of this group will eventually come to equilibrium between the bed and the solution, every one of these proteins will have different dynamics of detachment and consequently a different rate of achieving equilibrium (these dynamics depend on the pI, size and shape of the protein molecule). Thus if the ionic strength perturbance timing could be controlled this would introduce a great advantage for separating these proteins utilizing this phenemenon. This is what has been achieved by using the FPLC gradient controller system combined with fast-flow low back pressure ion exchange media. This phenomenon can be observed in Figure 13. When the salt

perturbance is maintained for a long time (Figure 13a) the protein and the activity profiles of the activity peak (eluted with the salt step gradient) are out of phase indicating that the dynamics of detachment of the active protein is different from that of the bulk of the proteins eluting in that peak, while if the salt perturbance is arrested at a time when most of the active protein has eluted (Figure 13b), the two profiles coincide and the undetached proteins can be transferred to the next peak.

The salt-burst elution procedure offers several advantages over other chromatographic methods employed to isolate enzymes. These advantages can best be described by comparing the new procedure with the one it replaces in the HGPRTase scheme, hydroxyapatite (HA) chromatography (Table IVb).

The older method, HA chromatography, had numerous drawbacks. A linear elution through fragile hydroxyapatite currently employs highly concentrated protein samples which curtail the rate of the column flow and develop high back pressures, consequently producing long retention time of the protein to be purified. This normally makes the protein in the effluent to be diluted by more than 50-fold in a high salt medium. The breakdown of the matrix also contributes to lower flow rates and the regeneration of such a column requires several days. It has been denoted that most of the protein samples, including HGPRTase, that have been eluted through hydroxylapatite lose total activity because of their dilution in a high salt environment and because

significant amounts of protein are retained irreversibly on the column (see Table IVb). Because of these conditions, the degree of purification (calculated from the heat treatment suspension) of HGPRTase was determined to be 5-fold with an overall yield of 7%, only 14% of the activity loaded is recovered (see Table IVb) (89). Furthermore, it is usually difficult to generate reproducible elution profiles using hydroxylapatite columns and large amounts of elution buffer solution are required. It was for these reasons that the salt-burst procedure was designed to replace hydroxyapatite in the HGPRTase purification scheme.

In contrast, the salt-burst procedure is fast, reproducible and has a high yield. The speed with which large quantities of protein extract can be purified is exceptional. The HGPRTase isolation (from 10 lb of yeast) takes only four days once both the TSK and affinity columns have been prepared. Virtually no loss of activity was observed (the total activity recovered appeared to be higher than the amount injected, probably due to the effects of inhibitors present in the crude extract), in contrast with 14% of the activity recovered with the hydroxyapatite procedure (see Table IVb), an average of 130% of the activity is recovered when the burst procedure is employed (Table IV). The procedure (when automated with the programs written in this laboratory for the Pharmacia instrument, as listed in Table I) was highly reproducible. The regeneration of the TSK column is also automated and can be accomplished in 3 hr for a 250 ml matrix. The high level of purification achieved with the salt-burst procedure (19 fold,

with 50 min total time requirement for a 10 ml injection of saturated protein suspension) increases the lifetime of the GMP-Sepharose affinity column used in the final step of the procedure by producing an enzyme solution with few impurities that might otherwise irreversibly bind to and reduce the binding capacity of the affinity column (When the hydroxyapatite effluent was used, the affinity column could be used a maximum of three times, while with the salt-burst effluent the affinity column had been used several times and it still retained its binding capacity). Finally, the total volume of buffer solution is minimized. Each burst procedure utilizes a volume of elution buffer equal to 1-3 times the column's void volume (depending on the amount of protein injected) and the activity in the effluent will only be diluted 3-5 fold, with respect to the starting material, thus highly concentrated active fractions are collected.

Because of the general basis of the phenomenon on which this procedure is based, it seems reasonable to conclude that it is applicable to the purification of any macromolecules with ionic functional groups and not only to proteins.

On the Multiple Enzymes Competition for PRPP

Assay procedures which characterize the allocation of phosphoribosyltransferase substrates between more than one enzymatic reaction have been presented. With this protocol the HPLC procedure demonstrates its power in simultaneously following several reactions. This study provides a closer analysis

of the dynamic interaction between different enzymes with a common substrate. A very interesting observation was the differential nature of the behavior of ATP-driven enzymatic reactions as compared to kinetically driven ones. When a sudden change of the common substrate pool is produced even though the kinetically driven paths may take advantage of the initial surge, in the long run, the ATP-driven paths take over, overcoming and reversing the other reactions as can be seen in Figure 15. More details of this phenomenon have been published (8). The apparent dynamics of the equilibrium driven competition for the common substrate (as shown in Figure 15) cannot be used infer any metabolic effect because the enzyme and substrate concentrations used do not necessarily reflect the actual metabolic condition *in vivo*.

On the Kinetics and pH Study

It is clearly visible from the kinetic plots at different pH values that HGPRTase seems to change its kinetic mechanism in going from a high to a low pH. At high and low pH values ($pH \geq 7.5$ and $pH = 4.5$), the enzyme appears to follow an ordered bi-bi mechanism with a dead-end second substrate inhibition. But at intermediate pH values ($5.0 \leq pH \leq 7.0$), the enzyme shows kinetic patterns that vary and are difficult to interpret. Variable patterns were also observed when the total concentration of PRPP was used as first substrate (not shown). The effect of varying concentrations of effective substrates was discarded because, in the case of PRPP, the actual concentrations of its magnesium

complexes were calculated from the corresponding equilibrium constants and total PRPP concentrations at each pH studied. Guanine is poorly soluble in water and could possibly precipitate and introduce the observed effects, but the concentrations of guanine employed were very low (micromolar range) and no precipitation was observed during any spectrophotometric assay. Another interesting effect was observed at pH values below 5.5. When Mg_2-PRPP is used as first substrate in the kinetic plot (Figure 37d and 39d), the double reciprocal plot deviates from linearity. This effect may be due either to an artifact introduced during the evaluation of the concentration of Mg_2-PRPP, because at this pH range the concentration of this complex is practically zero (see Figure 21), which makes it difficult to evaluate it with sufficiently high accuracy, or to a kinetic effect when varying the total concentration of PRPP. This kinetic effect could only be observed if the concentrations of Mg-PRPP and Mg_2-PRPP were not linearly related, or if they bind the enzyme with different affinities and modes, as if two different alternate first substrates were always present in the reaction mixture (see below). Another possible explanation is that one of them is an inhibitor of the active form of the enzyme.

As has been already discussed HGPRTase has a variety of possible substrates, stemming from the different PRPP species present in solution as well as the different tautomeric forms of guanine present in appreciable concentrations. Although these different forms of possible substrates are readily interconverted

in solution, some may bind the enzyme forming dead-end inhibitory complexes or altering the catalytic route of the enzyme.

This strange kinetic behavior has lead other authors to propose combined kinetic mechanisms for HGPRTase. A ping-pong plus sequential mechanism (84) and an ordered binding followed by a random release of products (85, 91) have been proposed. A metal activation study was conducted to explain some of the irregularities of the kinetics of HGPRTase (37-b), but the study was done at a fixed pH. This metal activation study shows that Mg-PRPP is the preferred substrate for the enzyme, but another study conducted to correlate initial velocities with the concentration of Mg-PRPP and Mg_2-PRPP, in an attempt to determine which is the actual first substrate, concluded that Mg_2-PRPP is the preferred one (80).

As indicated in "Results", it is not possible to determine which of the two magnesium-PRPP complexes is the preferred first substrate by a simple inspection of the kinetic pattern. The best approach would be to analyze the data using a scheme which takes all possibillities into account, and determine experimentally the values of the kinetic constants corresponding to the proposed scheme.

Since strong evidence exists in favour of an ordered bi-bi mechanism for HGPRTase in which a magnesium-PRPP complex binds first (84,89,90), any combination of kinetic mechanisms is to

be discarded. It seems more appropriate to assume that more than one route for the sequential mechanism exists, depending on the availability of the appropriate substrates and the ratio of apo to metal-bound enzyme. These two conditions depend on pH. For the first substrate this dependence has been determined in this work. In contrast the two main forms of the the second substrate have a ratio which is independent of pH (97). For the pH-dependence of the equilibrium apoenzyme/metal-bound enzyme no accurate data is available (37-b).

Another observation that must be taken into account is the dead-end inhibition by guanine blocking the binding of the PRPP complex substrate. This inhibition is strongest at higher pH values, suggesting that guanine binds to a form of the enzyme that is favored at higher pH values. At high pH values the enzyme has been shown to be practically all bound to Mg^{+2} (37-b). Thus it may be concluded that guanine binds this form of the enzyme to form the dead-end complex. An indicaion that the dead-end HGPRTase guanine complex is formed only with the metal-bound enzyme is that no binding of guanine was observerd in flow dialysis experiments in the absence of magnesium (89).

A mechanism that takes into account all these considerations is shown in the scheme in Figure 48. The concentrations of many of the reactants shown in this scheme depend on pH (E, EM, M_2A, and MA). At low pH values more of the enzyme is present as apoenzyme, E, (37-b), but its appropiate

substrate (Mg_2-PRPP or M_2A in the scheme in Figure 48) is lower at this pH range (practically zero at pH 4.5, see Figure 21). Thus for this route to be viable the apoenzyme ought to have a greater affinity for M_2A than EM (the metal-bound enzyme) has for MA (Mg-PRPP). At high pH values most of the enzyme is present as EM, while MA and M_2A are both at high concentrations (Figures 20 and 21). Thus at these pH values the route through MA would be preferred and a stronger inhibition by the second substrate ($B_t = B_1 + B_2$, in the scheme B is the second substrate) would be observed. After the first substrate-enzyme complex (M_2AE) has been formed, the enzyme may take two possible routes (through B_1, T-7, or through B_2, T-9), these two routes may differ both in the affinity of M_2AE for B_1 and B_2 (k_4/k_{-4} and k_{-5}/k_5) or in catalysis (k_6/k_{-6} and k_{-7}/k_7), one of the two routes will be preferred (the one corresponding to T-7, as discussed in the Introduction), if k_{-7}/k_7 is close to zero, AM_2EB_2 becomes another dead-end complex.

At a pH value in which the concentration of the apoenzyme (E) is not negligible and M_2A is at sufficiently high concentration (pH above 4.5 and below 7.0), when the second substrate dead-end inhibition of EM is sufficiently high, the route through M_2A becomes the preferred one, and by increasing the concentration of guanine ($B_1 + B_2$), after the reaction rate hits a minimum (due to the formation of BEM), the rate may start to rise up because the route through M_2A will be driven by higher concentrations of B_1 and B_2. This behavior can be seen at pH 6 in Figure 33.

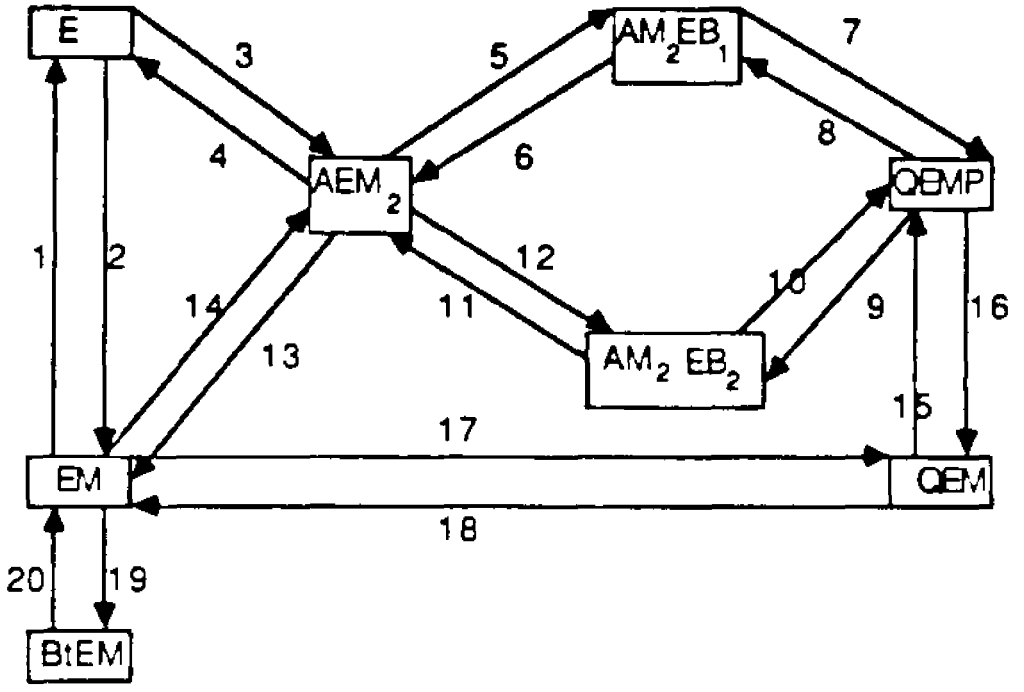

Fig. 48. General scheme for the kinetic mechanism of HGPRTase. **E**, the apoenzyme. **M**, appropriate divalent metal ion. **EM**, the metal-bound enzyme. **A**, the uncomplexed form of the first substrate. **MA**, the monometal complex of the first substrate. **M_2A**, the dimetal complex of the first substrate. **AEM_2**, the first substrate-enzyme complex. **B_1**, the T-7 tautomeric form of the second substrate (guanine). **B_2**, the T-9 tautomeric form of the second substrate. **$B_t = B_1 + B_2$** **B_tEM**, dead end complex of the metal-bound enzyme with the second substrate. **AM_2EB_1** and **AM_2EB_2**, ternary complexes of the enzyme with T-7 and T-9 respectively. **P**, First product released (Mg-PPi). **Q**, second product released (GMP). {1} = k_1, {2} = $k_{-1}[M]$, {3} = $k_2[M_2A]$, {4} = k_{-2}, {5} = $k_4[B_1]$, {6} = k_{-4}, {7} = k_6, {8} = k_{-6}, {9} = k_7, {10} = k_{-7}, {11} = k_5, {12} = $k_{-5}[B_2]$, {13} = k_3, {14} = $k_{-3}[MA]$, {15} = $k_{-8}[P]$, {16} = k_8, {17} = $k_{-9}[Q]$, {18} = k_9, {19} = k_{10}, {20} = k_{-10}.

Interestingly, intracellular pH in humans ranges from 7.0 in the brain to 7.25 in the liver (138), which is in the range in which HGPRTase begins to show a mixed kinetic mechanism. Furthermore, in humans Mg+2 concentration is in the mM range in the cytosol of most tissues, ranging from 8.0 mM in the brain and 10 mM in nonosseus tissues to 3 mM in red blood cells (139,140), while in serum it is in the order of 1 mM (of which 55% exists as free ion, 32% is protein bound and the rest complexed to organic phosphates) (141). These data suggest that the physiologic conditions in which HGPRTase is found in humans is very close to the experimental conditions used for our experiments at pH 7.0 and 7.5. In normal individuals purine levels are in the μM range (136,142), below the inhibitory concentrations found for that pH range, which indicates that enzyme regulation through purine inhibition is not relevant in normal conditions.

On Alternate Substrate and Inhibitors

The mixed character of the inhibition of HGPRTase by different oxypurines (against guanine) is an indication that oxypurines not only compete for the same form of the enzyme that guanine binds (M_2AE), but also the form of the enzyme that binds the first substrate (ME). This is illustrated for caffeine in Figure 47. The higher the concentration of the inhibitor the more apparent the inhibition characteristics that indicates the binding of the inhibitor to the free enzyme (ME). This fact, taken together with the observed dead-end second substrate inhibition suggests a

general pattern in HGPRTase: it is inhibited by moderate concentrations of oxypurines.

These HGPRTase characteristics may have metabolic implications, since HGPRTase is a salvage enzyme and a high level of oxypurines in the cytoplasm may be a signal of cell lysis. Theinhibition of the enzyme in that case may serve the purpose of saving energy by shutting off the consumption of PRPP. This is a condition that may be present during hybernation or sporulation in yeast, as may also be the case for bacteria when these are under starving conditions, at which time PRPP becomes limiting as a way of saving energy (4). This phenomenon is probably also present in mammals, since it would avoid the consumption of the common pool of PRPP (shared by neighbor population of cells) by a dying cell entering the lytic stage. Dietary gout may be a side effect of this energy saving metabolic regulation.

HGPRTase from other sources has been reported to be inactivated by sulhydryl and free amino modifying agents (83, 84). The observed inactivation by the mercuric ion with a partial reversibility induced by incubation with mercaptoethanol, suggests that this may be the case in the yeast HGPRTase. But the enzyme was unaffected by the cysteine-modifying reagent fosfomycin, which, being small in size (a substituted three-member ring), is probably not hindered in its way to the binding site of PRPP, which suggests that the mercuric ion inhibition was due to the binding of a cysteine residue of limited access.

In conclusion, many problems have plagued the works published on HGPRTase kinetics, from the technique to detect and follow the reaction (see "Materials and Methods") to the poor assessment of the actual substrates and the kinetic mechanism. Without knowing which are the actual substrates and the role they play in the kinetic regulation of the enzyme's activity, little could be understood of its actual catalytic mechanism. Since HGPRTase is involved in two important diseases, it is imperative that the nuances and details of its kinetic and catalytic mechanisms be studied. This study clarifies many aspects of the confusion existing, although the results point to the need for more research.

Conclusions

I.- The salt-burst procedure has a series of advantages over other elution procedures in ion exchange chromatography.

1) It permits rapid and significant purification of globular proteins.

2) It is easily established and reproducible.

3) It produces a minimum loss of activity and high yield of recovery and purification in a single step.

4) With this technique an average of 23-fold purification was achived in a single step for HGPRTase. Complete recovery of the initial activity was observed.

II.- The pH study of HGPRTase has shown the following with regard to the enzyme mechanism:

1) Guanine (the second substrate) inhibits the enzyme forming a dead-end binary complex.

2) This inhibition is stronger at high pH values. At pH 8.5 the inhibition was observed after a guanine concentration of 20 μM, while at pH 7.5 it was observed after 50 μM. When an

ordered bi-bi with second substrate inhibition mechanism was assumed to estimate the k_i values of this inhibition, the values obtained (pH 4.5, k_i = 29 μM. pH 7.5, k_i = 432.4 μM. pH 8.5, k_i = 19.1) seem to disagree with the observations, especially the value obtained for pH 7.5. This anomaly confirms that HGPRTase kinetic mechanism is not simple ordered bi-bi.

3) HGPRTase seems to change its kinetic mechanism in going from high to low pH.

4) At low and high pH values (4.5 and 8.5, respectively) the mechanism seems to conform to an ordered bi-bi system with a dead-end second substrate inhibition.

5) At intermediate pH values (7.0-5.5) the enzyme shows patterns that cannot be recognized as a simple mechanism. This pattern is most apparent at pH 6.0.

6) The behavior of the enzyme could be a consequence of the combination of several factors, of which the most outstanding are:

a) The variation of the concentration of the different PRPP species with pH.

b) The variation of the ratio of apo-enzyme to metal-bound enzyme (E/ME) with pH, and the possibility of these two different forms of HGPRTase have different affinities for the different forms of PRPP.

7) The fact that the apparent V_{max} of the enzyme does not decrease at high pH is an indication that the amino acid involved in the activity must be deprotonated for catalysis to occur.

III.- These studies have also shown:

8) Guanine, hypoxanthine and xanthine are the only purine substrates for HGPRTase, guanine being the preferred one.

9) Xanthine, 3-methylxanthine and caffeine are inhibitors of the enzyme.

10) The facts that (1) most purine derivatives inhibit HGPRTase, (2) while only three of them can be substrates, and that (3) guanine inhibits the enzyme at relatively low concentrations, all point to the importance of dietary control not only for persons with gout or Lesch-Nyhan syndrom, but in general to avoid high levels of uric acid production. Normal HGPRTase could still be inhibited by high levels of dietary purines, thus inducing uric acid accumulation.

References

1.- W.D.L. Musik, CRC Crit. Rev. Biochem. **11**, 1(1981).

2.- J.B. Wyngaarden, W.N. Kelley, Gout, in Metabolic Basis of Inherited Diseases, part VI, p.889, J.B. Stanbury, J.B. Wyngaarden and D.S. Fredrickson(editors), 3rd edit., Mc Graw-Hill Book Company, N.Y., 1972.

3.- W.N. Kelley, J.B. Wyngaarden, The Lesch-Nyhan Syndrome, in Metabolic Basis of Inherited Diseases, part VI, p.969, J.B. Stanbury, J.B. Wyngaarden and D.S. Fredrickson(editors), 3rd edit., Mc Graw-Hill Book Company, N.Y., 1972.

4.- A.S. Bagnara, L.R. Finch, Eur. J. Biochem **36**, 422(1973).

5.- A.S. Bagnara, L.R. Finch, Eur. J. Biochem. **41**,421(1974).

6.- D.C. McFarland, C.N. Coon, Proc. Soc. Exp. Biol. Med. **174**, 407(1983).

7.- G. Vitkauskas, E.S. Canellakis, Exper. Cell Res. **152**, 541(1984).

8.- D.L. Sloan, L.Z. Ali, D. Aybar-Batista, C. Yan, S.L. Hess, J. Chromat. **316**, 43(1984).

9.- M.A. Becker, M.J. Losman, A.L. Rosenberg, I. Mehlman, D.J. Levinson, E.W. Holmes, Arth. and Rheum. **29**, 880(1986).

10.- M.A. Becker, M.J. Losman, J. Wilson, A. Simmonds, Biochem. Biophys. Acta **882**, 168(1986).

11.- J.M. Wilson, W.N. Kelley, J. Clin. Invest. **71**,1331(1983).

12.- G. Rijksen, G.E.J. Staal, M.J.M. Van der Vlist, F.A. Beemer, J. Troost, W. Gutenson, J.P.R.M. Van Laarhoven, C.H.M.M. de Bruyn, Hum. Gen. **57**, 39(1981).

13.- M. Cassidy, M.C. Gregory, E.H. Harley, SA Med. J. **57**, 948(1980).

14.- J.E. Seegmiller, F.M. Rosenbloom, W.N. Kelley, Science **155**, 1682(1967).

15.- L.H. Smith, C.M. Huguley, J.A. Bain, in Metabolic Basis of Inherited Diseases, part VI, p.1003, J.B. Stanbury, J.B. Wyngaarden and D.S. Fredrickson(editors), 3rd edit., Mc Graw-Hill Book Company, N.Y., 1972.

16.- T.E. Worthy, W. Grobner, W.N. Kelley, Proc. Natl. Acad. Sci. USA **71**, 3031(1974).

17.- F. Delbarre, C. Ausher, B. Amor, A. de Gery, P. Cartier, M. Hamet, Biomedicine **21**, 82(1974).

18.- J.E. Seegmiller, Adv. Hum. Gen. **6**, 75(1976).

19.- P. Boer, B. Lipstein, A. de Vries, D. Sperling, Biochim. Biophys. Acta **432**, 10(1976).

20.- K.J. Van Ackar, H.A. Simmonds, C. Potter, S.J. Cameron, N Eng. J. Med. **297**, 127(1977).

21.- A.C. Foster, W.O. Whetsell Jr., E.D. Bird, R. Schwarcz, Brain Res. **336**, 207(1985).

22.- W.H. Meyer, J.A. Houghton, P.J. Lutz, P.J. Houghton, Cancer Res. **46**, 4896(1986).

23.- D.W. Melton, D.S. Konecki, D.H. Ledbetter, J.F. Hejtmancik, C.T. Caskey, Proc. Natl. Acad. Sci. USA **78**, 6977(1981).

24.- J.M. Wilson, A.B. Young, W.N. Kelley, N. Eng. J. Med. **309**, 900(1983).

25.- W.N. Kelley, F.M. Rosenbloom, J.F. Henderson, J.E. Seegmiller, Proc. Natl. Acad. Sci. USA **57**, 1735(1967).

26.- R.L. Nussbaum, W.E. Crowder, W.L. Nyhan, C.T. Caskey, Proc. Natl. Acad. Sci. USA **80**, 4035(1983).

27.- A.C. Chinalt, C.T. Caskey, Prog. Nuc. Acid Res. Mol. Biol. **31**, 295(1984).

28.- C.T. Caskey, G.D. Kruh, Cell **16**, 1(1979).

29.- S.M. Aldritt, C.C. Wang, J. Biol. Chem. **261**, 8528(1986).

30.- H.F. Dovey, J.H. McKerrow, S.M. Aldritt, C.C. Wang, J. Biol. Chem. **261**, 944(1986).

31.- J. Hochstad, Hypoxanthine PRT`ase and Guanine from enteric bacteria, in Methods in Enzymology, vol. LI, p.549, P.A. Hoffee, and M.E. Jones (editors), Academic Press, N.Y., 1978.

32.- R.L. Miller, G.A. Ramsey, T.A. Krenitsky, G.B. Elion, Biochemistry **11**, 4723(1972).

33.- J. Brennand, A.C. Chinault, D.S. Konecki, D.W. Melton, C.T. Caskey, Proc. Natl. Acad. Sci. USA **79**, 1950(1982).

34.- D.S. Konecki, J. Brennand, J.C. Fuscoe, C.T. Caskey, A.C. Chinault, Nucl. Acids Res. **10**, 6763(1982).

35.- R. Schmidt, H. Wiegand, U. Reichert, Eur. J. Biochem. **93**, 355(1979).

36.- L.Z. Ali, D.L. Sloan, Biochemistry **22**, 3419(1983).

37.- D.L. Sloan, L.Z. Ali, D. Picou, A. Joseph, Jr., in Purine Metabolism in Man IV, Part B, C.H.M. de Bruyn, H.A. Simmonds and M.M. Muller (editors), Plenum Publising Corporation, 1984.

37b.- L.Z. Ali, D.L. Sloan, J. Inorg. Biochem. **28**, 407(1986).

38.- D.B. Syed, R.S. Straus, D.L. Sloan, Biochemistry **26**, 1051(1987).

39.- M. Nagy, A.M. Ribet, Eur. J. Biochem. **77**, 77(1977).

40.- V.A. Paulus, R.G. Ingals, B. Vasquez, A.L. Breber, J. Biol. Chem. **255**, 2377(1980).

41.- J.M. Wilson, B.W. Baugher, L. Landa, W.N. Kelley, J. Biol. Chem. **256**, 10306(1981).

42.- J.M. Wilson, G.E. Tarr, W.C. Mahoney, W.N. Kelley, J. Biol. Chem. **257**, 10978(1982).

43.- P. Argos, M. Hanei, J.M. Wilson, W.N. Kelley, J. Biol. Chem. **258**, 6450(1983).

44.- A.L. Elder, G.G. Johnson, Biochem. Gen. **21**, 227(1983).

45.- G.W. Smithers, W.J. O'Sullivan, Biochem. Med. **32**, 106(1984).

46.- D.J. Jolly, H. Okayama, P. Berg, A.C. Esty, D. Filpula, P. Bohlen, G.G. Johnson, J.E. Shively, T. Hunkapillar, T. Friedman, Proc. Natl. Acad. Sci. USA **80**, 477(1983).

47.- G.G. Johnson, A.L. Ramage, J.W. Littlefield, H.H. Kazazian, Jr., Biochemistry **21**, 960(1982).

48.- G.G. Johnson, S.A. Nash, Biochem. Gen. **21**, 213(1983).

49.- W.J. Arnold, W.N. Kelley, J. Biol. Chem. **246**, 7398(1971).

50.- H. Muensch, A. Yoshida, Eur. J. Biochem. **76**, 107(1977).

51.- A.S. Olsen, G. Milman, Biochemistry **16,** 2501(1977).

52.- J.A. Holden, W.N. Kelley, J. Biol. Chem. **253**, 4459(1978).

53.- K. Ikeda, H. Suzuki, S. Nakagawa, Int. J. Biochem. **18**, 555(1986).

54.- W.N. Kelley, F.M. Rosenbloom, J.F. Henderson, J.E. Seegmiller, Proc. Natl. Acad. Sci. USA **57**, 1735(1967).

55.- I. Willers, S. Singh, H.W. Goedde, Enzyme **32**, 241(1984).

56.- J.M. Wilson, B.W. Baugher, P.M. Mattes, P.E. Daddona, W.N. Kelley, J. Clin. Inv. **69**, 706(1982).

57.- J.M. Wilson, G.E. Tarr, W.M. Kelley, Proc. Natl. Acad. Sci. USA **80**, 870(1983).

58.- T. Page, B. Bakay, E. Nissinen, W.L. Nyhan, J. Inher. Metab. Dis. **4**, 203(1981).

59.- G.G. Johnson, L.R. Eisenberg, B.R. Migeon, Science **203**, 174(1979).

60.- W.J. Arnold, W.N. Kelley, Studies in the Electrophoretic Variants of Human Hypoxanthine-guanine-phosphoribosyltransferase, in C.L. Markert (editor), Isozymes, Vol I, p.213, Academic Press, N.Y., 1975.

61.- V.I. Zannis, L.J. Gudas, D.W. Martin, Jr., Biochem. Gen. **18**, 1(1980).

62.- G.S. Gangas, G. Milman, Science **196**, 1119(1977).

63.- J.M. Wilson, L.E. Landa, R. Kobayashi, W.N. Kelley, J. Biol. Chem. **257**, 14830(1982).

64.- A.B. Robinson, Proc. Natl. Acad. Sci. USA **71**, 885(1974).

65.- C.A. Nelson, P. Handler, J. Biol. Chem. **243**, 5368(1968).

66.- S. Segal, J.B. Wyngaarden, Proc. Soc. Exp. Biol. Mid. **88**, 342(1955).

67.- R. Parker, W. Snedden, R.W.E. Watts, Biochem. j. **116**, 317(1970).

68.- S. Jogersen, H.E. Puolsen, Acta Pharmacol. Toxicol. **11**, 223(1955).

69.- S. Jogersen, Acta Pharmacol. Toxicol. **11**, 265(1955).

70.- A.G. Gilman, Ann. Rev. Biochem. **56**, 615(1987).

71.- P.J. Pfaffinger, J.M. Martin, D.D. Hunter, N.M. Nathanson, B. Hille, Nature 317, 536(1985).

72.- G.E. Breitwieser, G. Zsabo, Nature **317**, 538(1985).

73.- V.A. Florio, P.C. Sternweis, J. Biol. Chem. **260**, 3477(1985).

74.- K. Haga, T. Haga, A. Ichiyama, T. Katada, H. Kurose, M. Ui, Nature **316**, 731(1985).

75.- G.G. Holz IV, S.G. Rane, K. Dunlap, Nature **319**, 670(1986).

76.- H. Itoh, T. Kozada, S. Nagata, S. Nakamura, T. Katada, Proc. Natl. Acad. Sci. USA **83**, 3776(1986).

77.- P.C. Sternweis, J.D. Robishaw, J. Biol. Chem. **259**, 13806(1984).

78.- E.J. Neer, J.M. Lok, L.G. Wolf, J. Biol. Chem. **259**, 14222(1984).

79.- T. Katada, M. Dinuma, M. Ui, J. Biol. Chem. **261**, 8182(1986).

80.- C. Salerno, A. Giacomello, J. Biol. Chem. **256**, 367(1981).

81.- T.A. Krenitsky, R. Rapaioannou, G.B. Elion, J. Biol. Chem. **244**, 1263(1969).

82.- R.E. Thompson, E.L.F. Li, H. Olinspivey, J.P. Chandler, A.J. Katz, J.R. Appleman, Bioorg. Chem. **9**, 35(1978).

83.- Y. Natsumeda, M. Yoshino, K. Tsushima, Biochim. Biophys. Acta **483**, 63(1977).

84.- T.A. Krenitsky, R. Rapaioannou, J. Biol. Chem. **244**, 1271(1969)

85.- A. Giacomello, C. Salermo, J. Biol. Chem. **253**, 6038(1978).

86.- W. Gutensohn, H. Jahn, Hoppe-Seyler`s Z. Physiol. Chem. **358**, 939(1977).

87.- L.A. Johnson, R.B. Gordon, B.T. Emmerson, Proc. Aust. Biochem. Soc. **11**, 27(1978).

88.- W. Goutensohn, M. Huber, Hoppe-Seyler`s Z. Physiol. Chem. **356**, 431(1975).

89.- L.Z. Ali, D.L. Sloan, J. Biol. Chem. **257**, 1149(1982).

90.- J.F. Henderson, L.W. Brox, W.N. Kelley, F.M. Rosenbloom, J.F. Seegmiller, J. Biol. Chem. **243**, 2514(1968).

91.- H. Muensch, A. Yoshida, Eur. J. Biochem. **76**, 107(1977).

92.- C.M. Kong, R.E. Parks, Jr., Molec. Phamacol. **10**, 648(1974).

93.- R.M. Smith, R.A. Alberty, J. Phys. Chem. **60**, 180(1956).

94.- C. Salerno, A. Giacomello, J. Biol. Chem. **254,** 10232(1979).

95.- R.D. Berlin, Arch. Biochem. Biophys. **134**, 120(1969).

96.- D.P. Morton, S.M. Parsons, Arch. Biochem. Biophys. **175**, 677(1976).

97.- R. Shapiro, Prog. Nuc. Acids Res. Molec. Biol. **8**, 73(1968).

98.- A. Albert, D. J. Brown, J. Chem. Soc. P., 400(1954).

99.- R.H. Jensen, N. Davidson, Biopolymers **4,** 17(1966).

100.- G.L. Erichhorn, P. Clark, J. Am. Chem. Soc. **85**, 8020(1963).

101.- R.B. Simpson, J. Am. Chem. Soc. **86**, 2059(1964).

102.- B. Pullman, A. Pullman, Adv. Heterocyc. Chem. **13**, 77(1971).

103.- N.K. Kochetkov, E.I. Budovskii (ed.), Organic Chemistry of Nucleic acids, Part A, 121-182, Plenum Press, 1971.

104.- A.R. Katritzky, J.M. Lagowski, Adv. Hetercyc. Chem. **1**, 312(1963).

105.- B. Hartman, R. Lavery, J. Ramstein, Nuc. Acids Res. **14**, 7083(1986).

106.- S.F. Mason, J. Chem. Soc. P., 5010(1957).

107.- A.T. Miles, F.B. Howard, J. Frazier, Science **142**, 1458(1963).

108.- H.T. Miles, Proc. Natl. Acad. Sci. USA **47**, 791(1961).

109.- R.C. Lord, G.J. Thomas, Spectrochim. Acta **A23**, 2551(1967).

110.- B.C. Pal, C.A. Horton, J. Chem. Soc., 400(1964).

111.- L. Gatlin, J.C. Davis, Jr, J. Am. Chem. Soc. **84**, 4464(1962).

112.- P.O.P. T`so, M.P. Schweizer, D.P. Hollis, Ann. N.Y. Acad. Sci. **158**, 256(1969).

113.- R.V. Wolfenden, J. Mol. Biol. **40**, 307(1969).

114.- R.F. Steward, L.H. Jensen, J. Chem. Phys. **40**, 2071(1964).

115.- S.T. Rao, M. Sundaralingam, J. Am. Chem. Soc. **91**, 1210(1969).

116.- C.E. Bugg, V.T. Thewalt, R.E. Marsh, Biochem. Biophys. Res. Comm. **33**, 430(1968).

117.- N. Olaru, Z. Simon, Rev. Roum. Biochim. **18**, 1(1981).

118.- H.T. Miles, J. Frazier, Biochim. Biophys. Acta **79**, 216(1964).

119.- J.S. Kwiatkowski, Acta Phys. Pol. **34**, 365(1968).

120.- H. Fujita, A. Imamura, Ch. Nagata, Bull. Chem. Soc. Japan **42**, 1467(1969).

121.- L.B. Townsend, R.K. Robins, J. Org. Chem. **27**, 990(1962).

122.- L.B. Townsend, R.K. Robins, J. Am. Chem. Soc. **84**, 3008(1962).

123.- F.B. Howard, H.T. Miles, J. Biol. Chem. **240**, 801(1965).

124.- F.B. Howard, H.T. Miles, Biochem. Biophys. Res. Comm. **15**, 18(1964).

125.- Bio-Rad Protein Assay, Instruction Manual, Bio-Rad chemical division, **LIT-33, 85-0521, 1285.**

126.- L.S. Hanna, S.L. Hess, D.L. Sloan, J. Biol. Chem. **258**, 9745(1983).

127.- J. Victor, L. Greenberg, D.L. Sloan, J. Biol. Chem. **254**, 2647(1979).

128.- L.S. Hanna, D.L. Sloan, Analyt. Biochem. **103**, 230(1980).

129.- J.B. Flaks, Methods Enzymol. **6**, 144(1963).

130.- P. Natalini, S. Ruggieri, I. Santarelli, A. Vita, G. Magni, J. Biol. Chem. **254**, 2558(1979).

131.- A. Kornberg, I. Lieberman and E.S. Sims, J. Biol. Chem. **215**, 417(1955).

132.- B.G. Christensen, N.J. Leanza, T.R. Beattie, A.A. Patchott, B.H. Arison, R.E. Ormond, F.A. Kuehl, Jr., G. Albers-Schonberg, O. Jadetzky, Sciece **166**, 123(1969).

133.- D. Hendlin, E.O. Stapley, M. Jackson, H. Wallick, A.K. Miller, F.J. Wolf, T.W. Miller, L. Chaiet, F.M. Kahan, E.L. Foltz, H.B. Woodruff, J.M. Mata, S. Hernandez, S. Mochales, Science **166**, 122(1969).

134.- P.J. Cassidy, F.M. Kahan, Biochernistry **12**, 1364(1973).

135.- I.H. Segel, Enzyme Kinetics, Behavior and Analysis of Rapid Equilibrium and Steady-State Enzyme Systems, p. 819, John Wiley & Sons(1975).

136.- M. Castro-Gago, S. Lojo, R. del Rio, A. Rodriguez, I. Novo, S. Rodriguez-Segade, Child's Nerv. Syst. **2**, 109(1986).

137.- H. Freiser, Q. Fernando, Ionic Equilibria in Analytical Chemistry, John Wiley & sons, New York, 1963.

138.- R.D. Oberhaensli, P.J. Bore, R.P. Rampling, D. Hilton-Jones, L.J. Hands, G.K. Radda, The Lancet **2**, 8(1986).

139.- W.E.C. Wacker, B.C. Vallee, Min. Metabol. **2A**, 483(1964).

140.- E.I. Ochiai, General Principles of Biochemistry of the Elements, in Biochemistry of the Elements **7** (Frieden Earl, Ed.), 234(1987), Plenum Press, New York.

141.- F. Bronner, Min. Metabol. **2A**, 341(1964).

142.- M.H.N. Tattersall, P. Slowiaczek, A De Fazio, Adv. Exper. Med. Biol. **165A**, 301(1984).

143.- R.B. Gordon, L. Thomson, B.T. Emmerson, Adv. Exper. Med. Biol. **41A**, 291(1974).

144.- I.A. Fox, W.N. Keley, Adv. Exper. Med. Biol. **41B**, 471(1974).

145.- M.M. Müller, G. Falkner, Adv. Exp. Med. Biol. **76B**, 131(1977).

146.- C.H.M.M. de Bruyn, T.L. Olei, Adv. Exp. Med. Biol. **76B**, 139(1977).

147.- J.A. McDonald, W.N. Kelley, Adv. Exp. Med. Biol. **41A**, 167(1974).